COMPUTER SIMULATION STUDY TO INVESTIGATE THE PERFORMANCE OF A WINDOW TYPE AIR-CONDITIONING UNIT THAT USES THE REFRIGERANT R-407C INSTEAD OF R-22.

By

Abed Alrzaq Sleman Alshqirate

Supervisor

Dr. Mohammed A. Al-sa'ad, Prof.

This Thesis was Submitted in Partial Fulfillment of the Requirements for the Master's Degree of Science in Mechanical Engineering

Faculty of Graduate Studies
The University of Jordan

November, 2003

This Thesis (Computer Simulation Study to Investigate the Performance of a Window Type Air-Conditioning Unit that Uses the Refrigerant R-407c Instead of R-22) was successfully defended and approved on 12th, November 2003.

Examination Committee	**Signature**
Dr. Mohammed A. Al-sa'ad, Chairman Prof. of Mechanical Engineering.	……
Dr. Mohammed A. Hamdan, Member Prof. of Mechanical Engineering.	……...
Dr. Yousef H. Zurigat, Member Assoc. Prof. of Mechanical Engineering.	……...
Dr. Handri Th. Ammari, Member Prof. of Mechanical Engineering. (Mu'ta University)	…….

DEDICATION

To my great father and mother

To my brothers and sisters

To my family

To all my friends,

I dedicate this work

Abed Alrzaq …..

ACKNOWLEDGMENT

I would like to express my sincere gratitude to my supervisor professor Mohammed Al-sa'ad without his assistance, insights, fruitful advice, generous support and persistence this work would not be completed.

Special thanks to the members of the examination committee

Finally, I would like to express full thanks to my family, for their care, love, support, encouragement and patience.

List of Contents

LIST OF TABLES

LIST OF FIGURES

COMPUTER SIMULATION STUDY TO INVESTIGATE THE PERFORMANCE OF A WINDOW TYPE AIR-CONDITIONING UNIT THAT USES THE REFRIGERANT R-407C INSTEAD OF R-22.

By
Abed Alrzaq Sleman Alshqirate

Supervisor
Dr. Mohammed A. Al-sa'ad, Prof.

ABSTRACT

The present work deals with developing a computer simulation program to study the performance parameters of a window type air-conditioning unit that uses the refrigerant R-407c instead of R-22. This computer simulation study investigates the various performance parameters per one kW of refrigeration capacity such as the mass flow rate, the compressor power consumption, the condenser heat rejection rate, the coefficient of performance and the compressor exit temperature. These performance parameters are obtained for the standard cycle and ideal one with superheating and sub-cooling for various evaporating and condensing temperatures.

Results of the present work indicate that refrigerant R-407c can be used as an alternative refrigerant for R-22 in this type of air conditioning units.

The results of the present work reveal that the mass flow rate of R-407c when it replaces R-22 is increased by 14.3 % for standard cycle. While for ideal cycle it increased by 6.9 %, at T_e = 10 ^oC and T_c = 40 ^oC.

On the other hand, the COP is decreased from 7.9 to 6.4 when R-407c replaces R-22 for standard cycle and from 8.2 to 6.9 for ideal cycle with superheating and sub-cooling at the same conditions.

INTRODUCTION

Air conditioning is accomplished by the application of the principles of mechanical refrigeration into an air recirculation system arranged to absorb heat from the air within a contained space and transfer the heat to the outside of the structure.

Air conditioning and refrigeration systems use refrigerants, which must satisfy many requirements, so it should be non- flammable, non- explosive and posses low toxicity.

Several chlorofluorocarbons (CFCs) and hydrochloroufluorocarbons (HCFCs) are being extensively used as refrigerants for air conditioning and refrigeration purposes. They posses most of the desirable characteristics such as thermal and chemical stability, thermodynamic efficiency, non-flammability and low cost. But due to the influence of the (CFCs) and (HCFCs) on the environment, alternative refrigerants must be found to replace them and posses good thermodynamical and physical properties, high chemical and thermal stability, low toxicity, good miscibility with lubricants, compatibility with materials, less expensive and low flammability with no environmental side effect.

Refrigerant R407c which is a blend of 23 % R32, 25 % R125, and 52 %R134a (all of them are free of chlorine atoms) is a new refrigerant being used, which has a friendly effect on the ozone layer and low effect in the global warming (GWE) compared to the other traditional refrigerants.

1- Thermodynamic properties

The following thermodynamic properties are presented and discussed for use in air conditioning systems:

1.1 Transport properties

Thermal conductivity and viscosity are the main transport properties, which affect performance of any heat exchanger and their installations. What we need is high thermal conductivity and low viscosity of refrigerants to improve the performance of any air conditioning system.

1.2 Critical temperature

It is defined as the temperature at which a gas can not be liquefied however the amount of pressure is applied on it.

In order to achieve low work of the compression, the refrigerant should have high critical temperature. The operating condenser temperature must be kept below the critical temperature.

1.3 Boiling point

Boiling point is the temperature at which the vapor pressure of liquid is equal to the pressure on its surface where the substance state changes from liquid to vapor.

The tendency to have greater efficiency and higher-pressure drop is achieved when using fluids with higher boiling points.

1.4 Freezing point

At freezing point the refrigerant will change its state from liquid to solid which is not preferable because of its affect in compressor operation and normal operating conditions. So refrigerants should have low value of freezing point.

1.5 Pressures

Low condensing pressure and high evaporating pressure is preferable in order to increase the amount of heat extracted, which will improve the coefficient of performance of the refrigerant system.

2- Physical properties

The physical properties of any refrigerant that affect the performance of air conditioning units are as follows:

2.1 Specific heat

In order to increase the refrigeration effect for a given evaporating temperature, the subcooling state of the liquid is required to be increased which will be achieved by using low specific heat of refrigerant liquid.

2.2 Temperature glide

For zeotropic mixtures, the temperature of saturated liquid at a given pressure is the bubble point and the temperature of saturated vapor at a given pressure is called the dew point.

Temperature glide is the difference between the bubble and dew point temperatures. Evaporator glide describes the difference in temperature between the outlet and inlet

due to fractionation. Glide can vary depending on the state of the liquid refrigerant at either end of the evaporator (or condenser). This property will affect the capacity of the heat exchange in the condenser and the evaporator, which require a special design for the main system components.

2.3 Latent heat of vaporization

It is the heat given to or taken from a substance that changes its state without changing its temperature.

The refrigerant should have high value of latent heat of vaporization in order to have high values of refrigeration effect per unit mass of the refrigerant.

3- Chemical properties

The chemical properties of any refrigerants are presented and discussed as follows:

3.1 Miscibility with oil

When the oil has high solubility with the refrigerant, then good heat transfer and a suitable return of oil to the compressor will be achieved.

3.2 Water solubility

Because of the freezing of the water effects, which will lead to component damage, refrigerants should have low water solubility.

3.3 Safety

Safety consideration had to be taken relating to handling and usage of refrigerants.

3.4 Toxicity

The main aspect of toxicity in refrigerants is existence of chlorine atoms that can be measured by chlorine exposure limits. This classification defines the level to which an individual can expose over his working life without ill effects.

These limits are defined by the threshold limit value (TLV), which is defined as the maximum exposure at any given time and the time weighted average (TWA). Refrigerants with no identified toxicity at concentrations greater than 400 ppm based on TLV and TWA are considered class A, while those that show evidence of toxicity at concentration below 400 ppm are class B. most of the refrigerant in present use are of class A.

3.5 Flammability

Safety concerning flammability aspects must be considered for refrigerant during production, distribution, use, recovering, and recycling. The good refrigerant is the non-flammable one.

3.6 Ozone depletion potential

Chlorofluorocarbons (CFCs) and hydrohlorofluorocarbons (HCFCs) compounds have been used for decades in applications ranging from refrigerators, air conditioning, heat pumps and refrigeration systems, to blowing agents in foam thermal insulation and other applications. Due to their atmospheric life times CFCs and HCFCs can migrate to the stratosphere where ultraviolet sunlight decomposes the molecules, releasing chlorine. Chlorine in turns reacts with ozone, reducing stratospheric ozone concentrations.

The stratospheric ozone layer has a protective effect for life on earth in filtering out a portion of the sun's ultraviolet radiation (UV-B). Increased levels of UV-B at the earth's

surface may affect human health (such as causing increased incidence of skin cancer) and may damage plants and cause injury to aquatic and terrestrial life. R407c has zero ozone depletion potential while R22 has low ozone depletion potential.

3.7 Global warming potential

The molecules of CFCs absorb infrared radiation, which may contribute to the warming of the earth; R407C has approximately equal values of global warming potential as that for R22.

Table (1) gives some thermodynamic, physical and chemical properties of R22 and R407c.

Table (1) Thermodynamic, physical and chemical properties of R22 and R407c.

PROPERTY	R22	R407C
Boiling temperature at 1 atm, (° C)	-41	-44
Critical temperature, (° C)	96	87
Heat of vaporization, (kJ/kg)	245.1	233.5
Liquid specific heat at 25 (° C), (kJ/kg. K)	1.24	1.426
Vapor specific heat at 25 (° C), (kJ/kg. K)	0.685	0.83
Temperature glide, (K)	0	7.4
Ozone Depletion Potential, (ODP)	0.05	0
Global Warming Potential, (GWP)	1700	1610
Toxicity, (ppm)	1000	1000

LITERATURE SURVEY

Depletion of the ozone layer, the global warming potential and other destructive effects of the (CFCs), (HCFCs) and halons are the major reasons for the Montreal Protocol of (1987) and the European Community regulations which call for the phasing out of their usage.

Recently, scientists and researchers have been working to find out suitable substitutions for the harmful refrigerants with minimum design changes of the existing units. The most recent researches are discussed below.

The American Society of Mechanical Engineers (1998), studied the five major factors that design engineers must consider in selecting a refrigerant for a particular application. These factors are performance, safety, reliability, environmental acceptability, and simple economics. It was found that the primary criteria in the performance of a refrigeration system are refrigeration capacity and efficiency. One good indicator of a refrigeration capacity is its normal boiling point. The higher the boiling point the lower the fluids refrigeration capacity. On the other hand, fluids with higher boiling points tend to have greater efficiency. One of the advantages of R407c is that its vapor pressure is only slightly higher than that of R22, so it can be used as a retrofit fluid in R22 systems with only a lubricant change. It also has performance comparable to R22 one disadvantage of R407c is its temperature glide, which can be as high as 6 to 7 ˚C at typical system pressures.

Sleiti (2001), studied the performance of two tons split air conditioning unit working on R407c using a developed computer algorithm. The algorithm covered both theoretical and actual vapor- compression cycles. The cycles were studied at different condensing and evaporating temperatures. Performance curves were presented and compared with experimental results. The same trend of coefficient of performance was noticed with an increase in coefficients of performance ranging from (3%) to (18%) for theoretical results. He concluded that refrigerant R407c is a suitable replacement for R22 in air conditioning split unit despite the small reduction in the performance when compared to that of R22.

Pananonda (1998), examined the R407c refrigerant performance in retrofitting the R22 refrigerant. He compared the results calculated based on the theory and the results obtained from the experiment. He concluded that the refrigeration capacities of R407c and R22 refrigerants are very close to each other. However, the power consumption of R407c was less than that for R22 but at a certain level.

Douglass, *et al*. (1991), used a computer model to evaluate the performance of several R22 alternatives for window type air conditioners. They showed that R407c had optimal cost identical to that of R22.

Corr, *et a*l. (1994), investigated two contributing mechanisms to the composition shifts observed when using zeotropic HFC refrigerants in refrigerating and air conditioning applications using both computer modeling and the experimental techniques. The major distinctive features of the model are the inclusion of refrigerant – lubricant interactions

and the effects of composition shifts associated with vapor – liquid volume fraction in zeotropic refrigerants.

German Compressor Manufacturing Company (BITZER) (1998), demonstrated that R407c has similar thermodynamic properties and performance as R22 in air conditioning systems with medium temperature cooling range.

German Compressor Manufacturing Company (BITZER) (1999), showed that R407c is preferred when compared to other available alternatives to R22. They also showed that the distinctive temperature glide requires a special design for the main system components such as evaporator, condenser and expansion valve.

Mongey, *et al.* (1996), examined the performance of potential alternatives to R22 by constructing a refrigeration test facility. The performance of R407c was compared to that of R22. They concluded that the performance of R407c approached that of R22 at higher evaporator temperatures, but reductions in evaporator capacity and COP were found with decreasing evaporator temperature.

Burke, *et al.* (1994), studied the oil behavior of R407c.They found that R407c is miscible with ester- type oil in the temperature range from 80˚C down to –70 ˚C.

Dawood (2001), examined a locally manufactured air-cooled water chiller using R407c as an alternative refrigerant to R22. The experiment was conducted on the same chiller, for both R407c and R22, with some modifications on the case when R407c is being used. The oil being used with R407c refrigerant is polyester oil, which is different from

the oil that used in the case of R22. He concluded that R407c is a suitable alternative for R22. He obtained coefficients of performance up to 5.2 at Te = -3.5 ˚C and Tc = 39 ˚C.

Herz (2003), studied experimentally the performance of window type air conditioning unit using R407c as an alternative refrigerant. He concluded that refrigerant R407c could be used as an alternative refrigerant for R22 in this type of air conditioning units with optimum charge quantity of 900 gram. The COP of R407c and R22 reached a value of 3.6 and 4.2, respectively at Te = 10˚C and Tc = 40 ˚C. This indicates that COP of R407c is less than that of R22 by 14.3 %.

Herz did not compare his experimental results with theoretical one, so to estimate the possible experimental error of Herz (2003), the present work investigates the theoretical values of the various performance parameters of the compression refrigeration cycle. This enables us to obtain the difference between the experimental and theoretical parameters using the same operating conditions.

The Air Conditioning and Refrigeration Institute (1999) carried out experiments on the refrigerants properties and their alternatives of new blends. They studied the chemical behavior of R407c on the global warming and the ozone depletion effects. They found that R407c has small harmful effect on the environment.

The present work uses a computer simulation study to investigate the various performance parameters of window type air conditioning unit. The parameters investigated are mass flow rate, refrigeration capacity, compressor work, COP, heat rejection rate and compressor exit temperature when R22 is replaced by R407c.

REFRIGERATION CYCLE CALCULATIONS

1- General

Thermodynamic properties of the refrigerant R407c are presented in tables and graphs form for many states. These tables and graphs are available for researchers in order to simplify the calculations and usage of this refrigerant. But in order to study the performance of the refrigerant cycle by using computer simulation, these properties should be presented in equation forms.

For saturated properties, these equations are function of pressures, P, or temperatures, T, but for superheated properties these equations are function of pressure and temperature.

Microsoft Excel software and Segma plot software and Minitab software were used to construct the equations of saturated properties, while Matlab software, version 5.3 and Segma plot software were used for superheating properties equations.

1.1 Saturation properties equations for R407c

(a) Saturated vapor temperature

The coefficients of the saturated vapor temperature, T_v , equation are given in table (2). This table shows that the smaller percentage of error is achieved when using third order equation as:

$T_v = A_{01} + A_{11}(P) + A_{21}(P)^2 + A_{31}(P)^3$ (1)

Where T_v in ^oC, P in kPa. The range of applicability is from 70 to 2100 kPa.

Table (2) Coefficients of equation (1)

Coefficients	2_{nd} order	3_{rd} order
A_{01}	- 40.87	- 47.5
A_{11}	0.1103	0.157
A_{21}	$-4.581 * 10^{-5}$	$-1.387 * 10^{-4}$
A_{31}	_	$5.453 * 10^{-8}$
Max. error	4	2

(b) Saturated vapor pressure

The coefficients of the saturated vapor pressure, P_v , equation are given in table (3). This table shows that the smaller percentage of error is achieved when using third order equation as:

$P_v = A_{02} + A_{12}(T) + A_{22}(T)^2 + A_{32}(T)^3$ (2)

Where P_v in kPa, T in ^oC. The range of applicability is from - 50 ^oC to 50 ^oC.

Table (3) Coefficients of equation (2)

Coefficients	2_{nd} order	3_{rd} order
A_{02}	451.9	451.9
A_{12}	16.32	15.81
A_{22}	0.215	0.215
A_{32}	_	$1.3 * 10^{-3}$
Max. error	3.3	0.8

(c) Saturated liquid pressure

The coefficients of the saturated liquid pressure, P_l , equation are given in table (4). This table shows that the smaller percentage of error is achieved when using third order equation as:

$$P_l = A_{03} + A_{13}(T) + A_{23}(T)^2 + A_{33}(T)^3 \qquad (3)$$

Where P_l in kPa, T in ^oC. The range of applicability is from - 50 ^oC to 50 ^oC.

Table (4) Coefficients of equation (3)

Coefficients	2_{nd} order	3_{rd} order
A_{03}	560.2	560.2
A_{13}	18.65	18.19
A_{23}	0.2247	0.2247
A_{33}	_	$1.179 * 10^{-3}$
Max. error	3.1	1.2

(d) Saturated vapor enthalpy

The coefficients of the saturated vapor enthalpy, h_g , equation are given in table (5). This table shows that the smaller percentage of error is achieved when using third order equation as:

$$h_g = A_{04} + A_{14}(P) + A_{24}(P)^2 + A_{34}(P)^3 \qquad (4)$$

Where h_g in kJ/kg, P in kPa. The range of applicability is from 70 to 2100 kPa.

Table (5) Coefficients of equation (4)

Coefficients	2_{nd} order	3_{rd} order
A_{04}	389.5	384.9
A_{14}	0.06801	0.1001
A_{24}	$-3.205 * 10^{-5}$	$-9.579 * 10^{-5}$
A_{34}	_	$3.742 * 10^{-8}$
Max. error	-5	-2.6

(e) Saturated liquid enthalpy

The coefficients of the saturated liquid enthalpy, h_l , equation are given in table (6). This table shows that the smaller percentage of error is achieved when using third order equation as:

$$h_l = A_{05} + A_{15}(P) + A_{25}(P)^2 + A_{35}(P)^3 \qquad (5)$$

Where h_l in kJ/kg, P in kPa. The range of applicability is from 70 to 2100 kPa.

Table (6) Coefficients of equation (5)

Coefficients	2_{nd} order	3_{rd} order
A_{05}	140.4	132.2
A_{15}	0.1274	0.1739
A_{25}	$-3.87 * 10^{-5}$	$-1.148 * 10^{-4}$
A_{35}	_	$3.723 * 10^{-8}$
Max. error	-4.6	-2.9

(f) Saturated vapor entropy

The coefficients of the saturated vapor entropy, S_g , equation are given in table (7). This table shows that the smaller percentage of error is achieved when using third order equation as given:

$$S_g = A_{06} + A_{16}(P) + A_{26}(P)^2 + A_{36}(P)^3 \qquad (6)$$

Where S_v in kJ/kg K, P in kPa. The range of applicability is from 70 to 2100 kPa.

Table (7) Coefficients of equation (6)

Coefficients	2_{nd} order	3_{rd} order
A_{06}	1.841	1.854
A_{16}	$-1.352 * 10^{-4}$	$-2.243 * 10^{-4}$
A_{26}	$6.612 * 10^{-8}$	$2.431 * 10^{-7}$
A_{36}	_	$-1.039 * 10^{-10}$
Max. error	0.28	0.21

(g) Saturated vapor specific volume

The coefficients of the saturated vapor specific volume, V_g , equation are given in table (8), this table shows that the smaller percentage of error is achieved when using third order equation as:

$$V_g = A_{07} + A_{17}(P) + A_{27}(P)^2 + A_{37}(P)^3 \qquad (7)$$

Where V_v in m^3/kg, P in kPa. The range of applicability is from 70 to 2100 kPa.

Table (8) Coefficients of equation (7)

Coefficients	2_{nd} order	3_{rd} order
A_{07}	0.1737	0.2264
A_{17}	$-3.626 * 10^{-4}$	$-7.33 * 10^{-4}$
A_{27}	$2.223 * 10^{-7}$	$9.591 * 10^{-7}$
A_{37}	_	$-4.325 * 10^{-10}$
Max. error	0.124	0.025

1.2 Superheated properties equations for R407c

(a) Superheated enthalpy

The coefficients of the superheated enthalpy, h_s , equation are given in table (9). This table shows that the smaller percentage of error is achieved when using first order equation for each pressure, P, and temperature, T, as:

$h_s = B_0 + B_1 (T)$ (8)

Where:

$B_0 = B_{001} + B_{011} (P)$

$B_1 = B_{101} + B_{111} (P)$

Where, h_s in kJ/kg, T in ^oC, and P in kPa. The range of applicability is ($-50 < T < 50$ ^oC) and ($70 < P < 2100$ kPa).

Table (9) Coefficients of equation (8)

Coefficients	1 st order	2 nd order
B_{001}	416.1	439.1
B_{011}	$-1.25 * 10^{-2}$	$2.17 * 10^{-2}$
B_{021}	_	$-4.5 * 10^{-5}$
B_{101}	0.8126	$-4.075 * 10^{-3}$
B_{111}	$2 * 10^{-4}$	$-1.02 * 10^{-4}$
B_{121}	_	$2.12 * 10^{-7}$
B_{201}	_	$4.387 * 10^{-6}$
B_{211}	_	$-4.176 * 10^{-8}$
B_{221}	_	$4.755 * 10^{-11}$
Max. error	4.3	7.2

(b) Superheated entropy

The coefficients of the superheated entropy, S_s , equation are given in table (10). This table shows that the smaller percentage of error is achieved when using first order equation for each pressure, P, and temperature, T, as:

$S_s = B_2 + B_3 (T)$ (9)

Where:

$B_2 = B_{002} + B_{012} (P)$

$B_3 = B_{102} + B_{112} (P)$

Where, S_s in kJ/ kg k , T in ^{o}C , and P in kPa. The range of applicability is from (- 50 < T < 50 ^{o}C) and (70 < P < 2100 kPa).

Table (10) Coefficients of equation (9)

Coefficients	1 st order	2 nd order
B_{002}	1.831	2.81
B_{012}	1.925	-0.0474
B_{022}	_	0.0006
B_{102}	$2.866 * 10^{-3}$	$- 1.5 * 10^{-3}$
B_{112}	$- 1.45 * 10^{-8}$	$1.02 * 10^{-3}$
B_{122}	_	$- 1.71 * 10^{-5}$
B_{202}	_	$- 4.5 * 10^{-5}$
B_{212}	_	$5.58 * 10^{-6}$
B_{222}	_	$1.23 * 10^{-7}$
Max. error	0.3	0.81

(c) Superheated specific volume

The coefficients of the superheated specific volume, V_s , equation are given in table (11). This table shows that the smaller percentage of error is achieved when using first order equation for each pressure, P, and temperature, T, as:

$$V_s = B_5 + B_6 (T) \qquad (10)$$

Where:

$B_5 = B_{003} + B_{013} (P)$

$B_6 = B_{103} + B_{113} (P)$

Where, V_s in m^3/ kg , T in ^oC , and P in kPa . The range of applicability is from (- 50 < T < 50 ^oC) and (70 < P < 2100 kPa).

Table (11) Coefficients of equation (10)

Coefficients	1 st order	2 nd order
B_{003}	$7.468 * 10^{-2}$	7.3087
B_{013}	$9.188 * 10^{-4}$	0.6177
B_{023}	_	$1.28 * 10^{-2}$
B_{103}	$3.26 * 10^{-4}$	$1.5 * 10^{-1}$
B_{113}	$6.595 * 10^{-8}$	$1.32 * 10^{-2}$
B_{123}	_	$- 2.78 * 10^{-4}$
B_{203}	_	$7.4 * 10^{-4}$
B_{213}	_	$- 6.61 * 10^{-5}$
B_{223}	_	$1.4 * 10^{-6}$
Max. error	0.4	6.1

1.3 Properties equations for R22

(a) Saturated pressure

The coefficients of the saturated pressure, P, equation are given in table (12). This table shows that the smaller percentage of error achieved when using third order equation as given:

$$P = C_{01} + C_{11} (T) + C_{21} (T)^2 + C_{31} (T)^3 \qquad (11)$$

Where P in kPa, T in ^oC. The range of applicability is from - 70 ^oC to 96 ^oC.

Table (12) Coefficients of equation (11)

Coefficients	2_{nd} order	3_{rd} order
C_{01}	497.6	497.7
C_{11}	16.52	16.21
C_{21}	0.1994	0.1967
C_{31}	_	$1.135 * 10^{-3}$
Max. error	3.1	1.2

(b) Saturated liquid enthalpy

The coefficients of the saturated liquid enthalpy, h_l , equation are given in table (13). This table shows that the smaller percentage of error is achieved when using third order equation as:

$$h_l = C_{02} + C_{12}(T) + C_{22}(T)^2 + C_{32}(T)^3 \qquad (12)$$

Where in h_l kJ/kg, T in ^oC. The range of applicability is from - 70 ^oC to 96 ^oC.

Table (13) Coefficients of equation (12)

Coefficients	2_{nd} order	3_{rd} order
C_{02}	44.59	44.6
C_{12}	1.173	1.172
C_{22}	$1.53 * 10^{-3}$	$1.339 * 10^{-3}$
C_{32}	_	$1.023 * 10^{-5}$
Max. error	-3.7	-2.1

(c) Saturated vapor enthalpy

The coefficients of the saturated vapor enthalpy, h_l , equation are given in table (14). This table shows that the smaller percentage of error is achieved when using third order equation as:

$$h_g = C_{03} + C_{13}(T) + C_{23}(T)^2 + C_{33}(T)^3 \qquad (13)$$

Where in h_g kJ/kg, T in ^oC. The range of applicability is from - 70 ^oC to 96 ^oC.

Table (14) Coefficients of equation (13)

Coefficients	2_{nd} order	3_{rd} order
C_{03}	249.9	249.9
C_{13}	0.3622	0.365
C_{23}	$-1.663 * 10^{-3}$	$-1.448 * 10^{-3}$
C_{33}	_	$-1.695 * 10^{-5}$
Max. error	-4.7	-2.6

(d) Superheated enthalpy

The coefficients of the superheated enthalpy, h_s , equation are given in table (15). This table shows that the smaller percentage of error is achieved when using first order equation for each pressure, P, and temperature, T, as:

$$h_s = D_0 + D_1(T) \qquad (14)$$

Where:

$$D_0 = D_{00} + D_{01}(P)$$

$$D_1 = D_{10} + D_{11}(P)$$

Where, h_s in kJ/kg , T in ^{o}C , and P in kPa. The range of applicability is from (- 70 < T < 96 ^{o}C) and (20.5 < P < 4969 kPa).

Table (15) Coefficients of equation (14)

Coefficients	1 st order	2 nd order
D_{00}	252.9	253.2
D_{01}	$-5.1 * 10^{-3}$	$3.233 * 10^{-3}$
D_{02}	_	$2.657 * 10^{-5}$
D_{10}	0.6889	0.6918
D_{11}	$5.85 * 10^{-5}$	$-2.563 * 10^{-5}$
D_{12}	_	$-3.24 * 10^{-7}$
D_{20}	_	$2.31 * 10^{-5}$
D_{21}	_	$3.22 * 10^{-8}$
D_{22}	_	$2.53 * 10^{-11}$
Max. error	4.2	7.6

2- Refrigeration cycle calculations

Standard refrigeration cycle, ideal cycle with superheating and sub-cooling and practical cycle can be used to predict the performance of the vapor compression cycle, which requires a complete set of refrigerant thermodynamic properties.

The above three cycles have the following characteristics:

1) No pressure losses occur inside all components of the three cycles except the pressure rise in the compression process.
2) Heat transfers between the system and the surroundings from the condenser and evaporator only.
3) Isentropic compression for both standard and ideal cycles and non-isentropic compression for the practical cycle.

The practical cycle is assumed to have non-isentropic compression in order to compare it with experimental results.

2.1 Standard vapor- compression cycle

This cycle consist of isobaric heat transfer in condenser and evaporator, isentropic compression and irreversible adiabatic expansion as shown in figure (1, a, b).

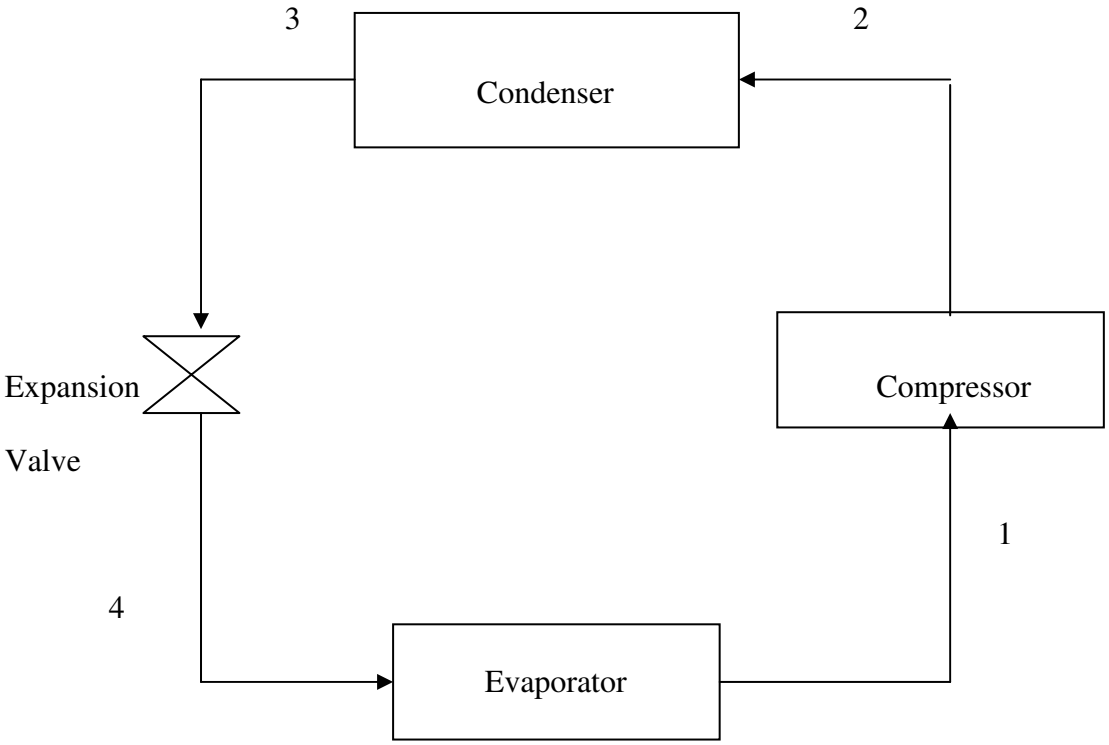

Fig (1, a) Schematic diagram of standard vapor- compression cycle

Temperature

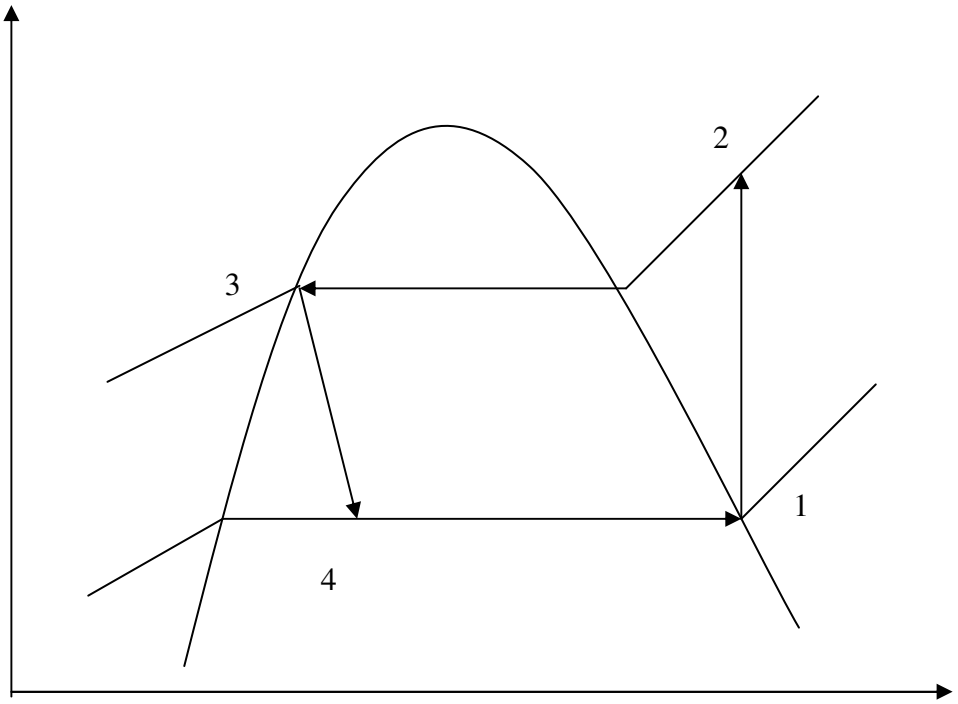

Entropy

Figure (1, b) Temperature- Entropy diagram of standard vapor- compression cycle

State 1: saturated vapor at evaporator outlet, compressor inlet.

State 2: superheated vapor at compressor outlet, condenser inlet.

State 3: saturated liquid at condenser outlet, expansion device inlet.

State 4: refrigerant mixture at expansion device outlet, evaporator inlet.

The various performance parameters of the standard cycle are calculated per kilowatt of refrigeration capacity i.e. $\dot{Q}_{ref} = 1$ kW

Refering to Figure (1), the refrigerant mass flow rate in (kg/s) per kW of refrigeration capcacity, $\dot{m}$, is obtained as follows:

$$\dot{m} = \frac{1}{(h_1 - h_4)} \quad (15)$$

where;

h_1 = Saturated vapor enthalpy leaving the evaporator kJ / kg.

h_4 = Enthalpy of refrigerant entering the evaporator kJ / kg.

= Enthalpy of saturated liquid leaving the condenser, h_3 , in kJ/kg.

The compressor power, $\dot{W}_c$, in (kW) per kW of refrigeration is given as:

$$\dot{W}_c = \dot{m}(h_2 - h_1) \quad (16)$$

where;

h_2 is the superheated vapor enthalpy leaving the compressor, kJ/kg.

The heat rejection, $\dot{Q}_{rej}$, in the condenser in (kW) per kilowatt of refrigeration is given as:

$$\dot{Q}_{rej} = \dot{m}(h_2 - h_3) \quad (17)$$

where;

h_3 is the saturated liquid enthalpy leaving the condenser, kJ/kg.

The coefficient of performance, *COP,* is the refrigeration effect, q_{ref} , divided by the compressor work, w_c .

$$COP = \frac{q_{ref}}{w_c} = \frac{h_1 - h_4}{h_2 - h_1} \quad (18)$$

2.2 Ideal vapor–compression cycle with superheating and sub-cooling:

Figure (2) shows the states of ideal vapor-compression cycle with superheating and sub-cooling, which is represented on the T-S diagram. The indicated states of figure (2) are:

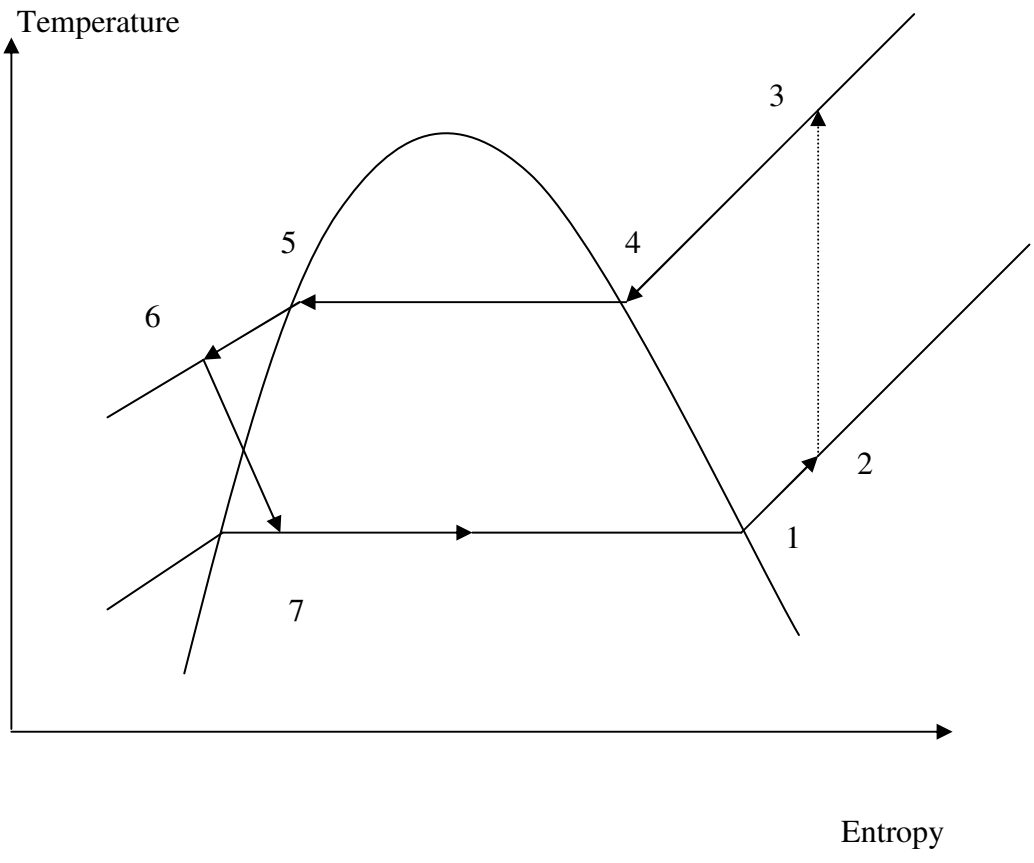

Figure (2) Temperature-Entropy diagram of the ideal vapor- compression cycle.

State 1: saturated vapor in the evaporator.

State 2: super heated vapor at evaporator outlet, and compressor inlet.

State 3: super heated vapor after the isentropic compression process.

State 4: saturated vapor in the condenser.

State 5: saturated liquid in the condenser.

State 6: sub-cooled liquid at condenser outlet, adiabatic expansion device inlet.

State 7: expansion device outlet and evaporator inlet.

The various performance parameters of the ideal cycle are calculated per kilowatt of refrigeration capacity i.e. $\dot{Q}_{ref} = 1$ kW:

Refering to Figure (2), the refrigerant mass flow rate in (kg/s) per kW of refrigeration capacity, $\dot{m}$, is obtained as follows:

$$\dot{m} = \frac{1}{(h_2 - h_7)} \qquad (19)$$

where;

h_2 = Superheated vapor enthalpy leaving the evaporator, kJ/kg.

h_7 = Enthalpy of refrigerant entering the evaporator, kJ / kg.

= Enthalpy of sub-cooled refrigerant leaving the condenser, h_6, kJ/kg.

The compressor power, $\dot{W}_c$, in (kW) per kW of refrigeration is given as:

$$\dot{w}_c = \dot{m}\left(h_3 - h_2\right) \tag{20}$$

where;

h_3 is the superheated vapor enthalpy leaving the compressor, kJ/kg.

The heat rejection, $\dot{Q}_{rej}$, in the condenser in (kW) per kilowatt of refrigeration is given as:

$$\dot{Q}_{rej} = \dot{m}\left(h_3 - h_6\right) \tag{21}$$

where;

h_6 is the sub-cooled liquid enthalpy leaving the condenser, kJ/kg.

The coefficient of performance, *COP,* is the refrigeration effect,q_{ref} , divided by the compressor work, w_c .

$$COP = \frac{q_{ref}}{w_c} = \frac{h_2 - h_7}{h_3 - h_2} \tag{22}$$

2.3 Practical vapor-compression cycle

This cycle is the same as that of the ideal vapor-compression cycle but with isentropic efficiency, η_s , doesn't equal to unity. i.e. $\eta_s \neq 1.0$

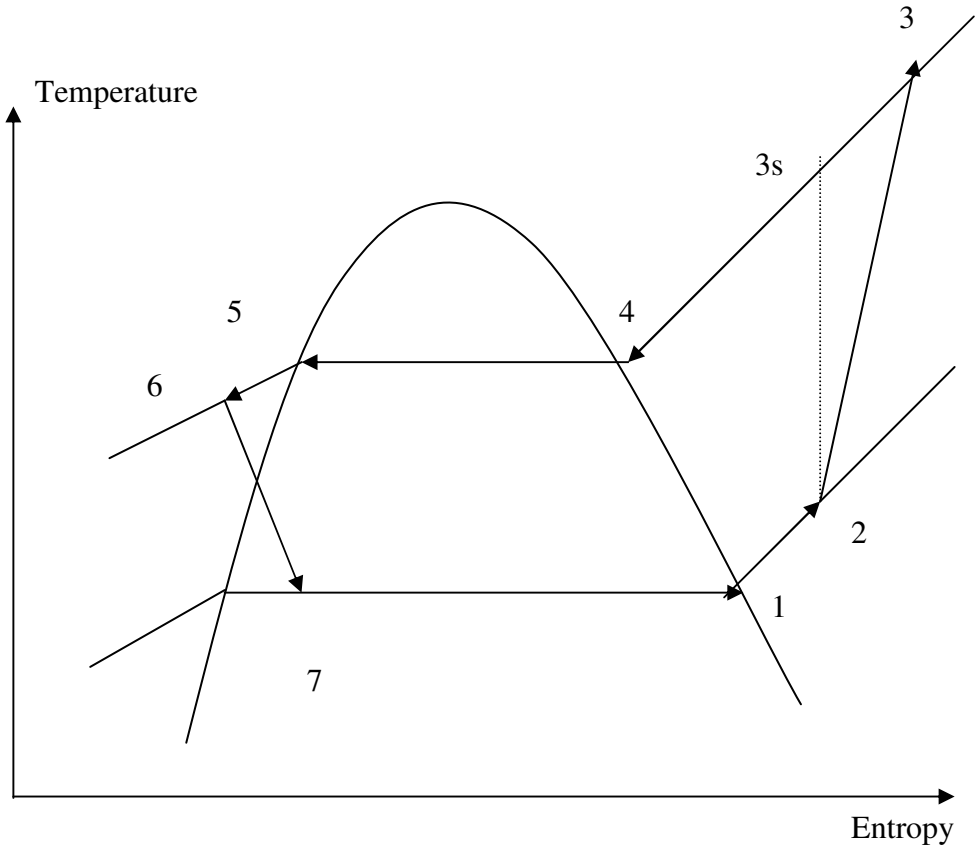

Figure (3) Temperature-entropy diagram of the practical vapor- compression cycle.

State 1: saturated vapor in the evaporator.

State 2: super heated vapor at evaporator outlet and compressor inlet.

State 3: super heated vapor at compressor outlet.

State 3s: super heated vapor for the isentropic compression process.

State 4: saturated vapor in the condenser.

State 5: saturated liquid in the condenser.

State 6: sub-cooled liquidat at condenser outlet, adiabatic expansion deviceinlet.

State 7: expansion device outlet and evaporator inlet.

The various performance parameters of the practical cycle are calculated per kilowatt of refrigeration capacity i.e. $\dot{Q}_{ref} = 1$ kW:

Refering to Figure (3), the refrigerant mass flow rate in (kg/s) per kW of refrigeration capacity, $\dot{m}$, is obtained as follows:

$$\dot{m} = \frac{1}{(h_2 - h_7)} \tag{23}$$

where;

h_2 = Superheated vapor enthalpy leaving the evaporator, kJ/kg.

h_7 = Enthalpy of refrigerant entering the evaporator, kJ / kg.

= Enthalpy of sub-cooled refrigerant leaving the condenser, h_6, kJ/kg.

$$\dot{w}_c = \dot{m}(h_3 - h_2) \tag{24}$$

h_3 is the superheated vapor enthalpy leaving the compressor, kJ/kg.

The heat rejection rate, $\dot{Q}_{rej}$, in the condenser in (kW) per kilowatt of refrigeration is given as:

$$\dot{Q}_{rej} = \dot{m}(h_3 - h_6) \tag{25}$$

h_6 is the sub-cooled liquid enthalpy leaving the condenser, kJ/kg.

The coefficient of performance, *COP,* is the refrigeration effect,q_{ref} , divided by the compressor work, w_c .

$$COP = \frac{q_{ref}}{w_c} = \frac{h_2 - h_7}{h_3 - h_2} \quad (26)$$

3- Computer algorithm

A computer simulation program was developed to calculate the thermodynamic properties and the performance parameters for the standard, ideal and practical refrigeration cycles, for the refrigerants R407c and R22. Matlab versions 5.3 and 6.1 were used as programming language. Computer program code is presented in Appendix A. This code includes the following:

1- The main program code, which calculates the performance parameters for both standard cycle and ideal one with superheating and sub-cooling, when the input is the evaporating temperature (T_e) or the condensing temperature (T_c), Figure (4).

2- The simulation program code, which produces a set of curves for each performance parameter, for both standard and ideal cycles.

3- The comparison program code, which produces a pair of comparison curves between standard and ideal cycles.

4- A specified program code, which calculates the performance parameters for practical cycle that uses the refrigerant R407c in order to compare it with experimental results.

5- The comparison program code, which produces a pair of comparison curves between refrigerants R407c and R22 for both standard and ideal cycles.

6- A specified program code, which calculates the performance parameters for practical cycle for refrigerant R22 in order to compare it with experimental results.

3.1 Main program

In this program, the input parameters are assigned, and the output results are arranged. It consists from the following steps:

* Input data

1- The value of the constant (T_e) or (T_c) in ^oC.

2- The value of the degree of superheating in ^oC.

3- The value of the degree of sub-cooling in ^oC.

4- The value of isentropic efficiency.

* Calculating saturated vapor, saturated liquid, superheated vapor and sub-cooled liquid thermodynamics properties.

At every pair of evaporator and condenser temperatures, the program will calculate suitable pressures, temperatures and enthalpies at inlet and outlet of evaporator, compressor, condenser and expansion device.

* Calculating performance parameters

* Main program output

1- Mass flow rate in kg/s per 1 kw of refrigeration.

2- Compressor work in kW per 1 kW of refrigeration.

3- Heat rejection rate in kW per 1 kW of refrigeration.

4- Coefficient of performance.

5- Compressor discharge temperature in ^{o}C.

3.2 Simulation program

This program produces a set of curves for each performance parameter, for both standard and ideal cycles. It includes two cases:

1- Simulation program for constant condensing temperature and variable evaporating temperature.

2- Simulation program for constant evaporating temperature and variable condensing temperature.

3.3 Comparison programs

1- The first comparison program produces a pair of comparison curves between standard and ideal cycles for refrigerant R407c for two cases:

   a) A pair of curves for each performance parameter at T_c = 40 ^{o}C and variable evaporating temperature.

   b) A pair of curves for each performance parameter at T_e = 10 ^{o}C and variable condensing temperature.

2- The second comparison program produces a pair of comparison curves for each standard and ideal cycles for refrigerants R407c and R22 as follows:

   a) A pair of curves for each performance parameter for standard cycle at T_c = 40 ^{o}C and variable evaporating temperature.

   b) A pair of curves for each performance parameter for standard cycle at T_e = 10 ^{o}C and variable condensing temperature.

c) A pair of curves for each performance parameter for ideal cycle at T_c = 40 ^oC and variable evaporating temperature.

d) A pair of curves for each performance parameter for ideal cycle at T_e = 10 ^oC and variable condensing temperature.

3.4 A specified program

1- The specified program code calculates performance parameters for the practical cycle for refrigerant R407c in order to compare it with experimental results for the following two cases:

a) For each performance parameter it produces curves at T_c = 40 ^oC and variable evaporating temperature.

b) For each performance parameter it produces curves at T_e = 10 ^oC and variable condensing temperature.

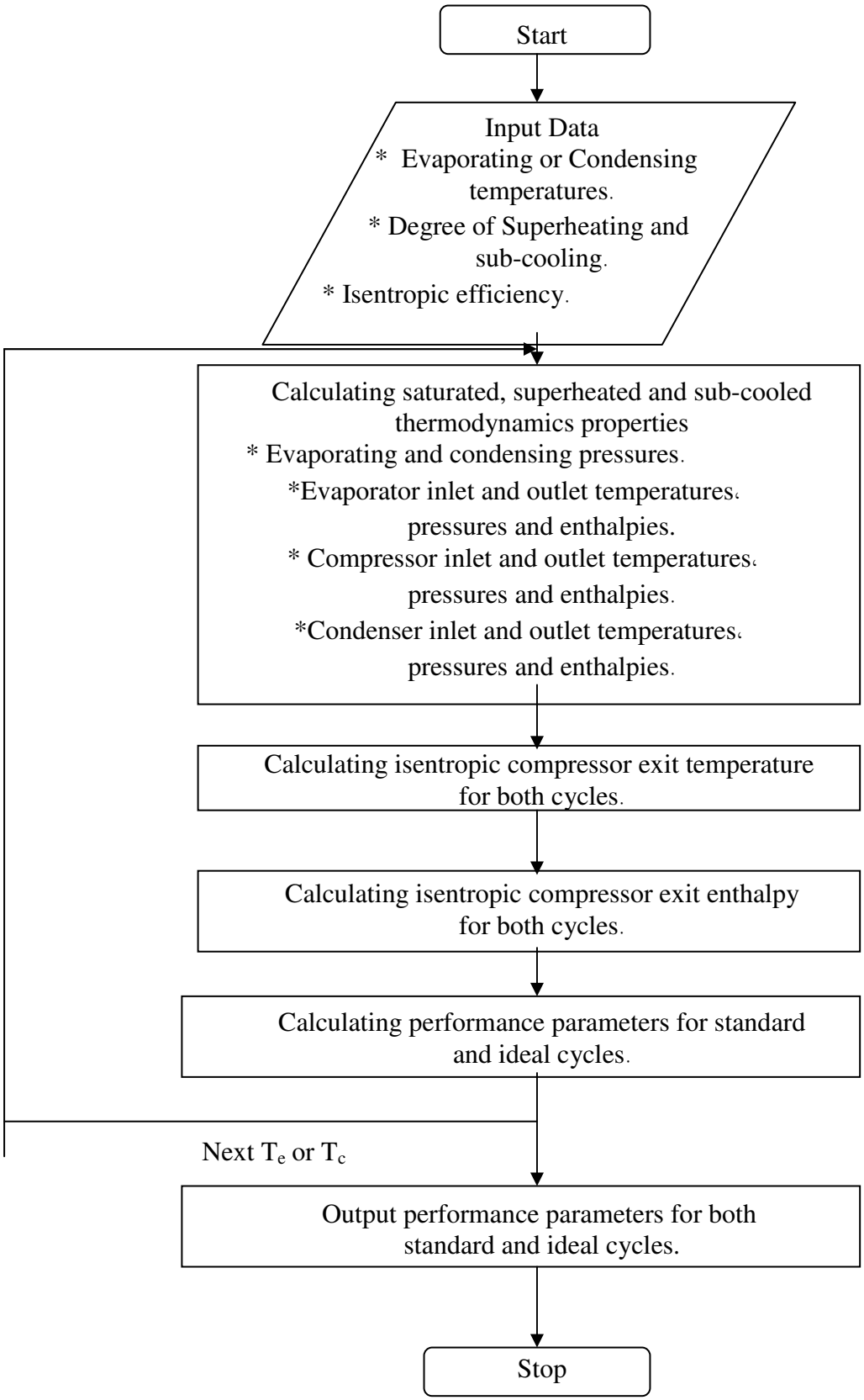

Figure (4) Main program flow chart

RESULTS AND DISCUSSIONS

The results of the standard cycle and ideal one with superheating and sub-cooling for the evaporator temperatures range from –10 to 15 ^{o}C, and condenser temperatures range from 30 to 50 ^{o}C, are plotted in Figures (5 to 34) and numerically presented in Tables (B.1 to B.30) in Appendix B.

The results investigated for both cycles per one kW refrigeration capacity are mass flow rate, compressor power, heat rejection rate, coefficient of performance and compressor discharge temperature.

Comparison results are obtained for the following:

1- Comparison between standard and ideal cycles performance parameters of refrigerant R407c.
2- Comparison between standard and ideal cycles performance parameters of refrigerant R407c and R22 wich presented in Figures (35 to 42) and Tables (B.31 to B.38).
3- Comparison between practical cycle performance results with experimental data for refrigerant R407c is presented in Figures (43 to 50) and Tables (B.39 to B.46).

1- Performance parameters results for R407c

All performance parameters results are presented per one kW refrigeration capacity.

1.1 Mass flow rate

Variation of the mass flow rate, $\dot{m}$, with the evaporating and condensing temperatures, for standard and ideal cycles are shown in Figures (5 to 8) and Tables (B.1 to B.4).

Since, the mass flow rate was calculated per one kilowatt of refrigeration, then $\dot{m}$ is inversely proportional to the specific enthalpy at the outlet of the evaporator as seen from equations (15 and 19).

Figures (5 and 6) show for the evaporating temperature, T_e , variation results that, $\dot{m}$, decreases as T_e increases due to the increases of the specific enthalpy at the outlet as T_e increases, which causes $\dot{m}$ to decrease for standard and ideal cycle.

On the other hand, the mass flow rate, $\dot{m}$, is directly proportional to the specific enthalpy at the inlet of the evaporator.

Figures (7 and 8) show that $\dot{m}$ increases as the condensing temperature, T_c increases, due to the increase of specific enthalpy at the inlet of the evaporator as T_c increases for standard and ideal cycles.

Figures (9 and 10) compare the variation of $\dot{m}$ with T_e and T_c , respectively, for standard and ideal cycles. These figures show that the mass flow rate of standard cycle is higher than that of ideal cycle for all values of T_e and T_c. This is due to the fact that specific enthalpy difference at the inlet and the outlet of the evaporator for T_e and T_c variation results for the standard cycle is lower than that for ideal cycle.

1.2 Compressor power

Variation of compressor power, $\dot{W}_c$, with evaporating and condensing temperatures for both cycles are shown in Figures (11 to 14) and Tables (B.7 to B.10). The compressor power was calculated per one kilowatt of refrigeration capacity, and it is proportional directly with the mass flow rate, $\dot{m}$, and with the specific enthalpy difference across the compressor, Δh_c, as seen in equations (16 and 20).

For the case of T_e variation results for both cycles, it is noticed that as T_e increases, the compressor power decreases because of $\dot{m}$ and Δh_c decrease as Te increase. Figures (11 and 12) show that the compressor power decreases as T_e increases for standard and ideal cycles for all values of T_c investigated.

On the other hand, as T_c increases at constant T_e values, the compressor power increases because of $\dot{m}$ and Δh_c increase as shown in Figure (13) for the standard cycle and Figure (14) for the ideal cycle.

Figures (15 and 16) compare the compressor power, $\dot{W}_c$, consumed as T_e and T_c increase for standard and ideal cycles. Both figures indicate that $\dot{W}_c$ for standard cycle is slightly higher than that for ideal cycle. This difference in $\dot{W}_c$ increases as T_e or T_c increases, because the difference in $\dot{m}$ for both cycles increases as T_e or T_c increases, as shown in Figures (9 and 10), respectively.

1.3 Heat rejection rate

Figures (17 to 20) and Tables (B.13 to B.16) show the variation of the heat rejection rate, $\dot{Q}_{rej}$, with the evaporating and condensing temperatures for both standard and ideal cycles. The heat rejection rate was calculated per one kilowatt of refrigeration capacity, and it is proportional directly with the mass flow rate, $\dot{m}$, and the specific enthalpy difference across the condenser, Δh_{con} , as seen in equations (17 and 2).

Figures (17 and 18) show for the T_e variation results that, $\dot{Q}_{rej}$ decreases as T_e increases at constant T_c due to the decrease of the mass flow rate and the enthalpy difference across the condenser for standard and ideal cycles.

On the other hand, as T_c increases at constant T_e values, $\dot{Q}_{rej}$ increases because of the mass flow rate and the enthalpy difference across the condenser increase as shown in Figures (19 and 20) for both standard and ideal cycles, respectively.

Figures (21 and 22) compare the heat rejection rate, $\dot{Q}_{rej}$, of standard cycle with that of ideal cycle for the variation of T_e and T_c, respectively. These figures show that the heat rejection rate for standard cycle is slightly higher than that of ideal cycle for all values of T_e and T_c. This difference in $\dot{Q}_{rej}$ increases as T_e or T_c increases, because the difference in $\dot{m}$ for both cycles increases as T_e or T_c increases, as discussed in section 1.1.

1.4 Coefficient of performance (COP)

Coefficient of performance, COP, is plotted against evaporating and condensing temperatures as shown in Figures (23 to 26) and Tables (B.19 to B.22) for both standard and ideal cycles. As seen in equations (18 and 22), the COP is proportional directly to the refrigeration effect, q_{ref} , and inversely with compressor work, w_c.

For the case of T_e variation results at constant T_c for both cycles, Figures (23 and 24) show that as T_e increases the COP increases, because of compressor work decrease and refrigeration effect increase.

On the other hand, Figures (25 and 26) indicate that COP decreases as T_c increases at constant T_e values, because of increasing of the compressor work and decreasing the refrigeration effect.

Figures (27 and 28) compare the coefficent of performance, COP, with T_e and T_c, respectively, for standard and ideal cycles. These figures show that the COP of ideal cycle is higher than that of standard cycle. This is due to superheating and sub-cooling effect in the ideal cycle which cause the refrigeration effect,q_{ref} ,to increase.

1.5 Compressor discharge temperature

The compressor discharge temperature variation is plotted against evaporating and condensing temperatures as shown in Figures (29 to 32) and Tables (B.25 to B.28) for both standard and ideal cycles.

Figures (29 and 30) show that as T_e increases at constant T_c, the discharge temperature decreases, due to increasing the evaporating pressure, which decrease the pressure difference across the compressor. So the superheating will decrease.

While Figures (31 and 32) show that the discharge temperature increases as T_c increases, due to the increasing of the condensing pressure that leads to increase the pressure difference across the compressor. So, the superheating will increase.

Figures (33 and 34) compare the discharge temperature of standard cycle with that of ideal cycle for the variation of T_e and T_c, respectively. These figures show that the compressor discharge temperature of the ideal cycle is higher than that of standard cycle for all values of T_e and T_c due to the compressor inlet temperature rise because of superheating state, which increase the compressor exit temperature.

2- Comparison between R407c and R22 refrigerants for standard and ideal cycle with superheating and subcooling

By using a simulation program, pair of curves was plotted to compare between a certain performance parameters of refrigerants R407c and R22. These performance parameters are the mass flow rate and COP. Selection of mass flow rate because of its representation as a basic quantity calculated from a definite amount of refrigeration capacity (1 kilowatt) and used as a basic controller for calculating all performance parameters. While, COP selection because it give us a good idea about the ratio between refrigeration effect and the compressor work, which means controlling the cost of the system operating.

2.1 Mass flow rate

A variation of mass flow rate, $\dot{m}$, for R407c and R22 with the evaporating and condensing temperatures, for standard and ideal cycles are shown in Figures (35 to 38) and Tables (B.31 to B.34).

Figures (35 and 36) show that as T_e increases at T_c = 40 ^{o}C for standard and ideal cycles, the mass flow rate decreases for both refrigerants due to the increasing of the specific enthalpy difference across the evaporator as indicated by equations (15 and 19).

The mass flow rate for R407c is higher than that of R22 for all values of T_e. The mass flow rate of R407c at T_e = 10 ^oC is equal to 0.0072 kg/s and of R22 is equal to 0.0063 kg/s per one kW of refrigeration for standard cycle (increasing by14.3%). While, for ideal cycle is equal to 0.0062 and 0.0058 kg/s per one kW of refrigeration (increasing by 6.9%), respectively.

Figures (37 and 38) show that as T_c increases at T_e =10 ^oC for standard and ideal cycles, the mass flow rate increases for both refrigerants due to the decreasing of the enthalpy difference across the evaporator as indicated by equations (15 and 19). The mass flow rate for R407c is higher than that of R22 for all values of T_c. The mass flow rate of R407c at T_c = 40 ^oC is equal to 0.0072 kg/s and of R22 is equal to 0.0063 kg/s per one kW of refrigeration for standard cycle (increasing by 14.3 %). While, for ideal cycle is equal to 0.0062 and 0.0058 kg/s per one kW of refrigeration (increasing by 6.9 %), respectively.

2.2 Coefficient of performance (COP)

Coefficient of performance, COP, variation of R407c and R22 with evaporating temperature and condensing temperature for both standard and ideal cycles are shown in Figures (39 to 42) and Tables (B.35 to B.38).

Figures (39 and 40) indicate that COP increases at T_c = 40 ^oC when increasing the evaporating temperature, T_e due to decrease in compressor work and the increase of refrigeration effect. The COP of R407c is lower than that of R22 for all values of T_e. The COP of R407c at T_e = 10 ^oC is about 81.6 % of that of R22 for standard cycle and about 84.14 % for ideal cycle.

Figures (41 and 42) show that COP decreases at T_e = 10 ^oC when increasing the condensing temperature due to increase in compressor work and the decrease of

refrigeration effect. The COP of R407c is lower than that of R22 for all values of T_e. The COP of R407c at T_c = 40 ^oC is about 81.3 % of that of R22 for standard cycle and about 84.3 % for ideal cycle.

3- Comparison between practical cycle results and experimental results

Mass flow rate, compressor power, heat rejection rate and coefficient of performance are obtained for practical cycle using the simulation program, while experimental results were obtained by Herz (2003). The comparison between practical and experimental results is done at the same conditions and over the same ranges of evaporating and condensing temperature variations.

3.1 Mass flow rate

The mass flow rate variation, $\dot{m}$, for practical and experimental results are plotted against the evaporating and condensing temperatures in Figures (43 and 44) and presented numerically in Tables (B.39 and B.40). The mass flow rate is directly proportional to the refrigeration capacity which given from experimental results, and inversly proportional to the enthalpy difference across the evaporator as seen from equation (23).

Figure (43) shows the variation of mass flow rate with T_e at constant T_c = 40 ^oC. This figure indicates that, $\dot{m}$, increases as T_e increases due to the increasing of refrigeration capacity and decreasing the enthalpy difference across the evaporator. The practical

cycle mass flow rate is higher than that of experimental results for all values of T_e, with 8.42 % at T_e = 10 °C.

Figure (44) shows the variation of mass flow rate with T_c at constant T_e = 12 °C. This figure indicates that, $\dot{m}$, decreases as T_c increases due to the decreasing of refrigeration capacity. The practical cycle mass flow rate is slightly higher than that of experimental results for all values of T_c, with 2.42 % at T_c = 40 °C.

3.2 Compressor power

Figures (45 and 46) and Tables (B.41 and B.42) show the variation of compressor power, $\dot{W}_c$, with evaporating and condensing temperatures for practical and experimental results. The compressor power is directly proportional to the mass flow rate and the enthalpy difference across the compressor as seen from equation (24).

Figure (45) shows the variation of compressor power with T_e at constant T_c = 40 °C. This figure indicates that the compressor power decreases as T_e increases due to the decrease of enthalpy difference across the compressor. The compressor power of experimental results is higher than that of practical cycle for all values of T_e, with 38.77 % at T_e = 10 °C.

Figure (46) shows the variation of compressor power with T_c at constant T_e = 12 °C. This figure indicates that the compressor power increases as T_c increases due to the increase of enthalpy difference across the compressor. The compressor power of experimental results is higher than that of practical cycle for all values of T_e, with 33.2 % at Tc = 40 °C.

3.3 Heat rejection rate

Figures (47 and 48) and Tables (B.43 and B.43) show the variation of heat rejection rate, $\dot{Q}_{rej}$, with evaporating and condensing temperatures for practical and experimental results. The heat rejection rate is directly proportional to the mass flow rate and the enthalpy difference across the condenser as seen from equation (25).

Figure (47) shows the variation of $\dot{Q}_{rej}$ with T_e at constant T_c = 40 ^oC. This figure indicates that the heat rejection rate increases as T_e increases due to the increase of mass flow rate. The heat rejection rate of experimental results is higher than that of practical cycle for all values of T_e, with 8.4 % at T_e = 10 ^oC.

Figure (48) shows the variation of $\dot{Q}_{rej}$ with T_c at constant T_e = 12 ^oC. This figure indicates that the heat rejection rate decreases as T_c increases due to the decrease of mass flow rate. The heat rejection rate of experimental results is higher than that of practical cycle for all values of T_c, with 6 % at T_c = 40 ^oC.

3.4 Coefficient of performance

The variation of coefficient of performance, COP, with evaporating and condensing temperatures for practical and experimental results are shown in Figures (49 and 50) and Tables (B.45 and B.46). The COP is proportional directly to the refrigeration effect, q_{ref} , and inversely with compressor work, w_c as seen from equation (26).

Figure (49) shows the variation of COP with T_e at constant T_c = 40 ^oC. This figure indicates that the COP increases as T_e increases due to the increase of refrigeration capacity and decrease of compressor power. The practical COP is higher than that of experimental results by 63.3 % at T_e = 10 ^oC.

Figure (50) shows the variation of COP with T_c at constant T_e = 12 ^oC. This figure indicates that the COP decreases as T_c increases due to the decrease of refrigeration capacity and increase of compressor power. The practical COP is higher than that of experimental results by 49.7 % at T_c = 40 ^oC.

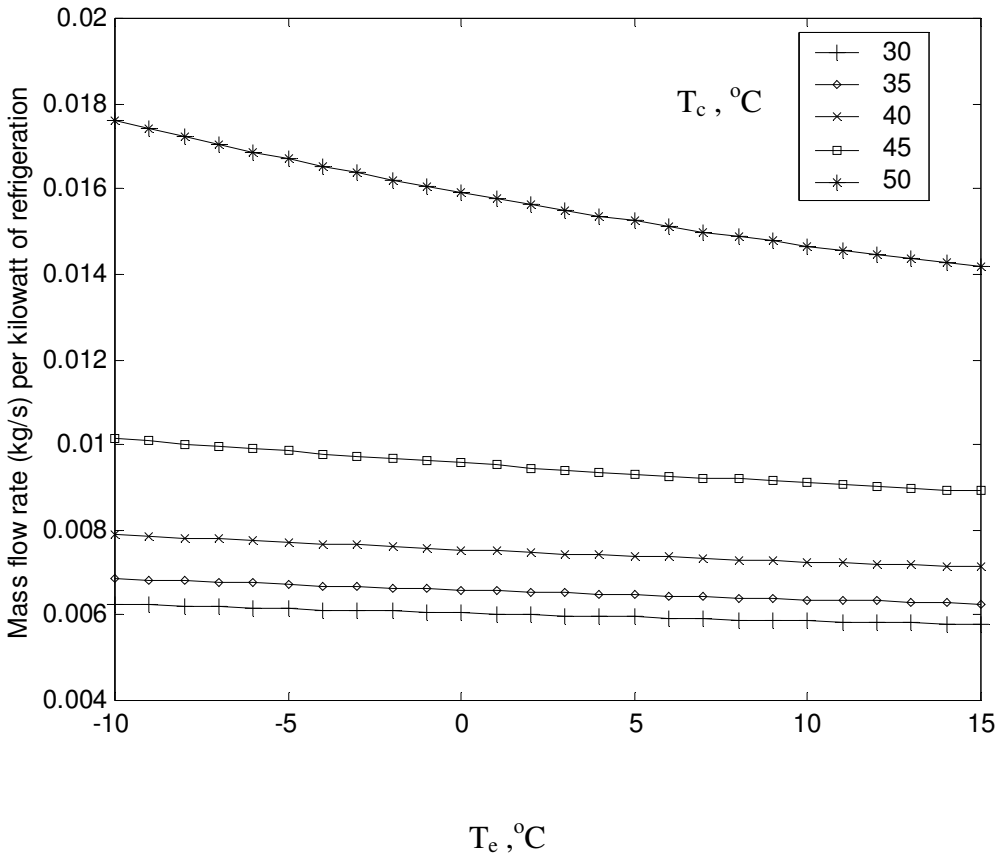

Fig (5) Mass flow rate versus T_e for different values of T_c for standard cycle

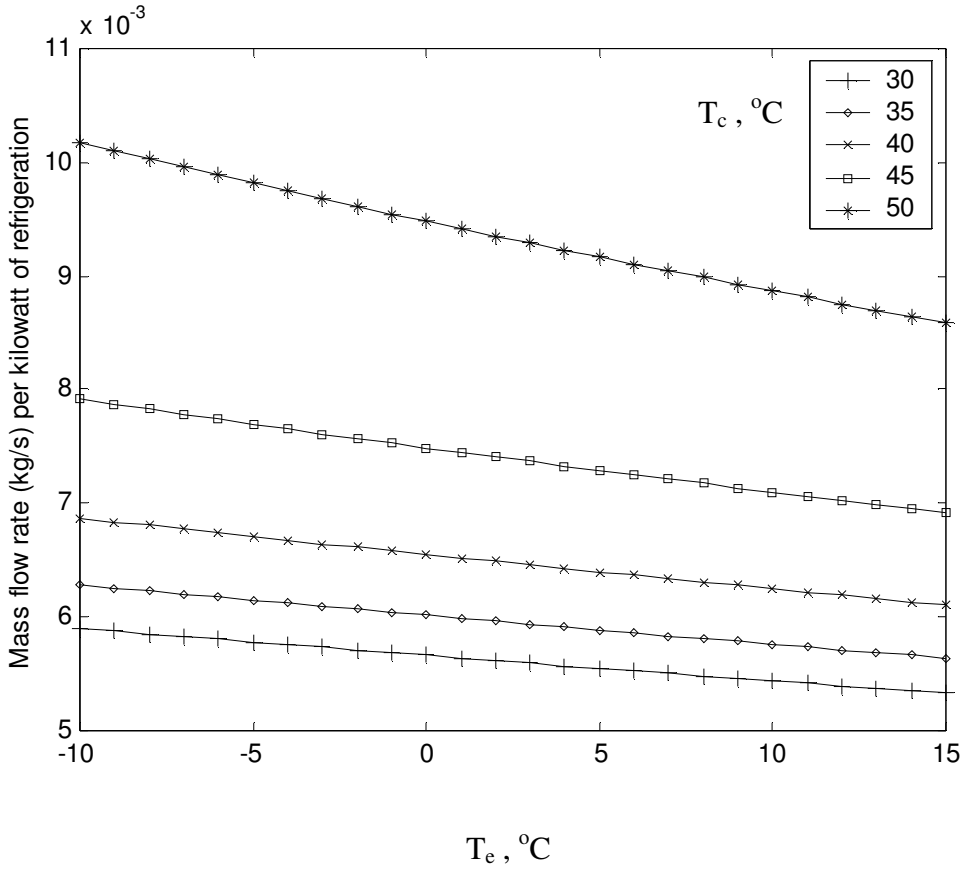

Fig (6) Mass flow rate versus T_e for different values of T_c for ideal cycle

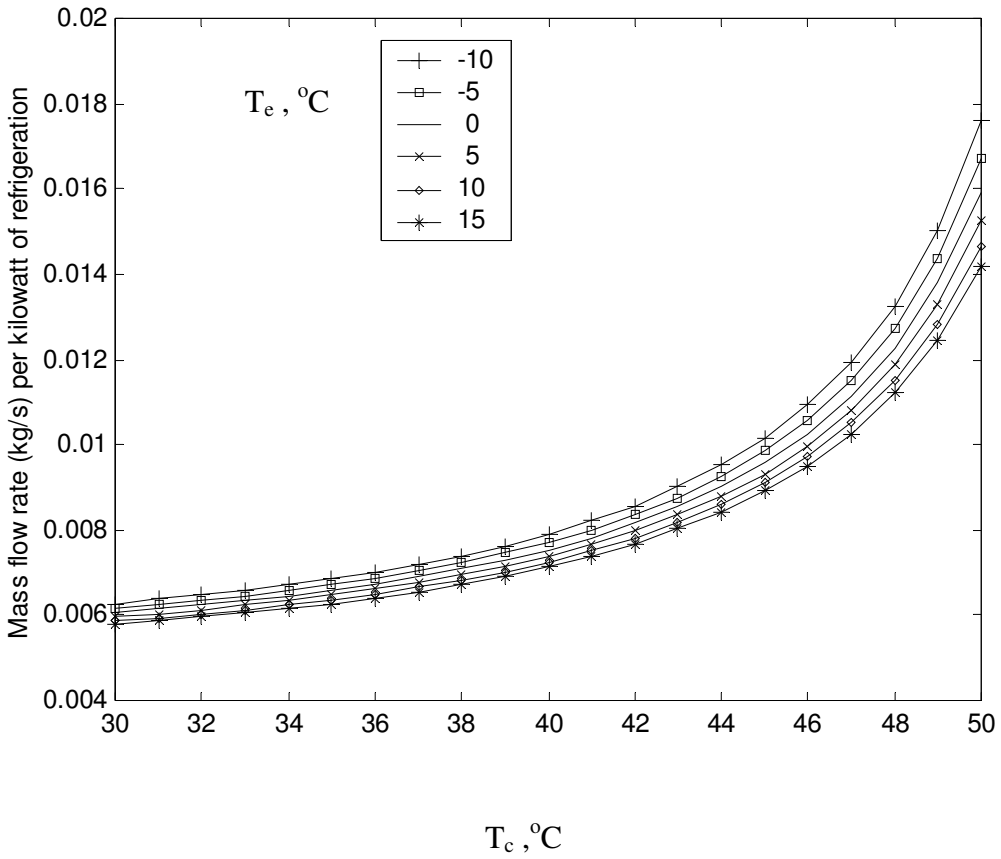

Fig (7) Mass flow rate versus T_c for different values of T_e for standard cycle

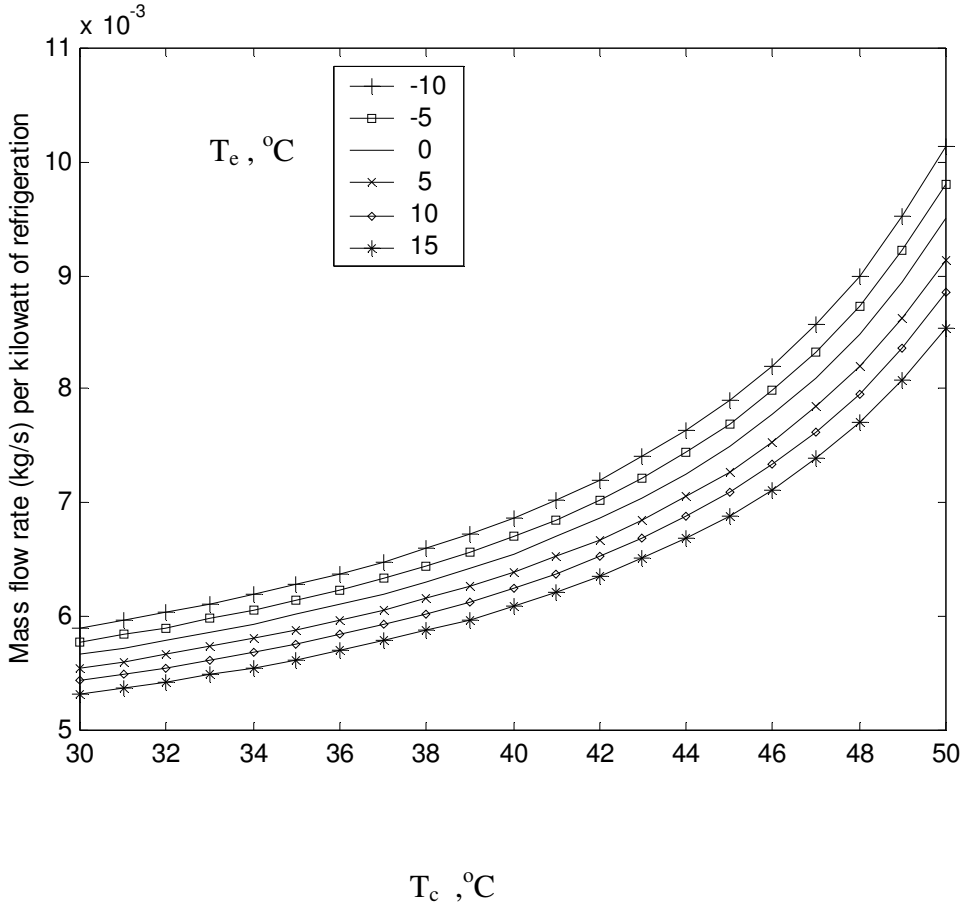

Fig (8) Mass flow rate versus Tc for different values of Te for ideal cycle

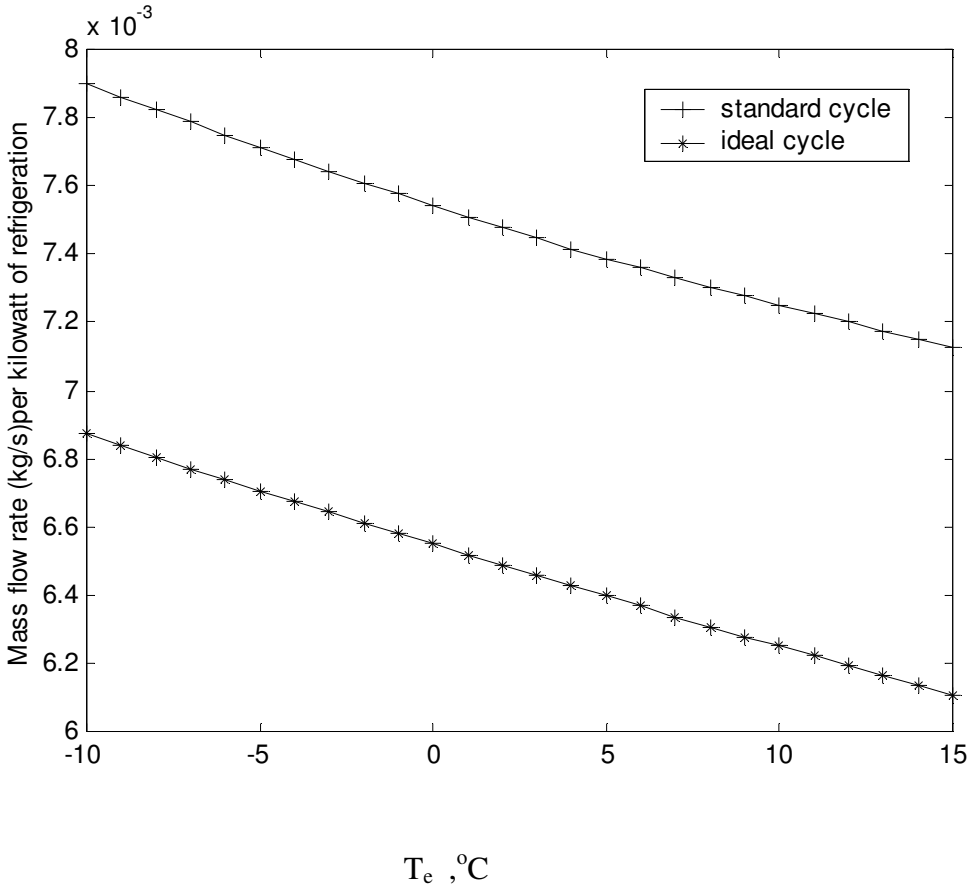

Fig (9) Standard and ideal mass flow rate versus T_e at $T_c = 40\ ^oC$

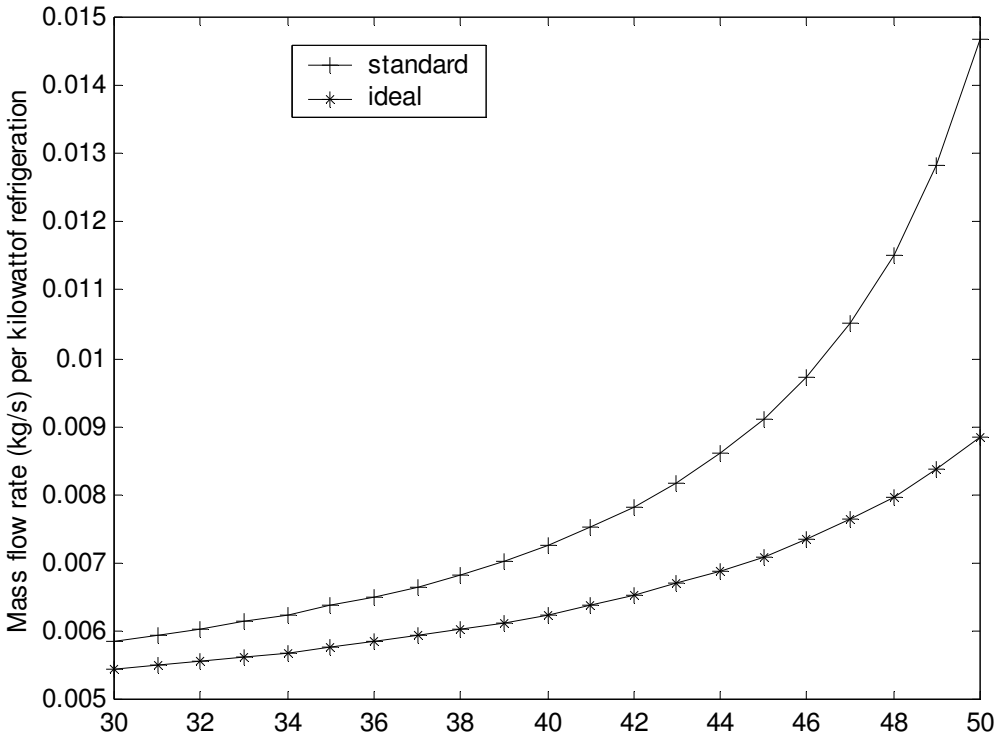

Fig (10) Standard and ideal mass flow rate versus T_c at T_e = 10 °C

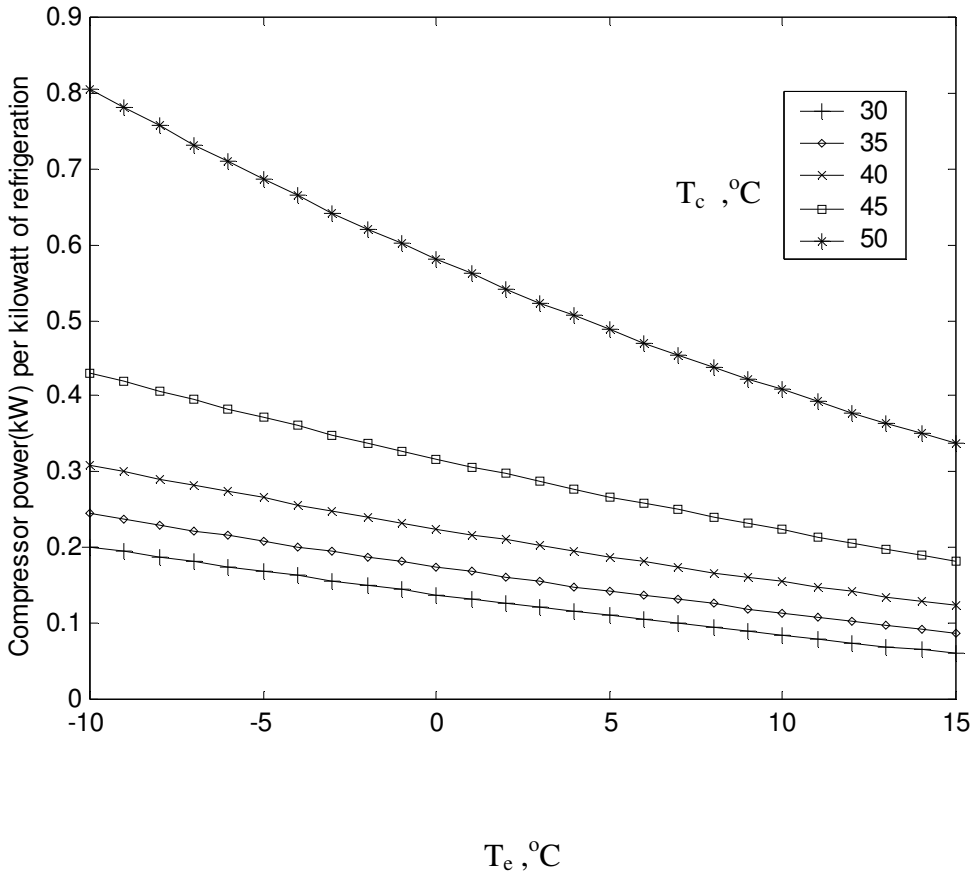

Fig (11) Compressor power versus T_e for different values of T_c for standard cycle

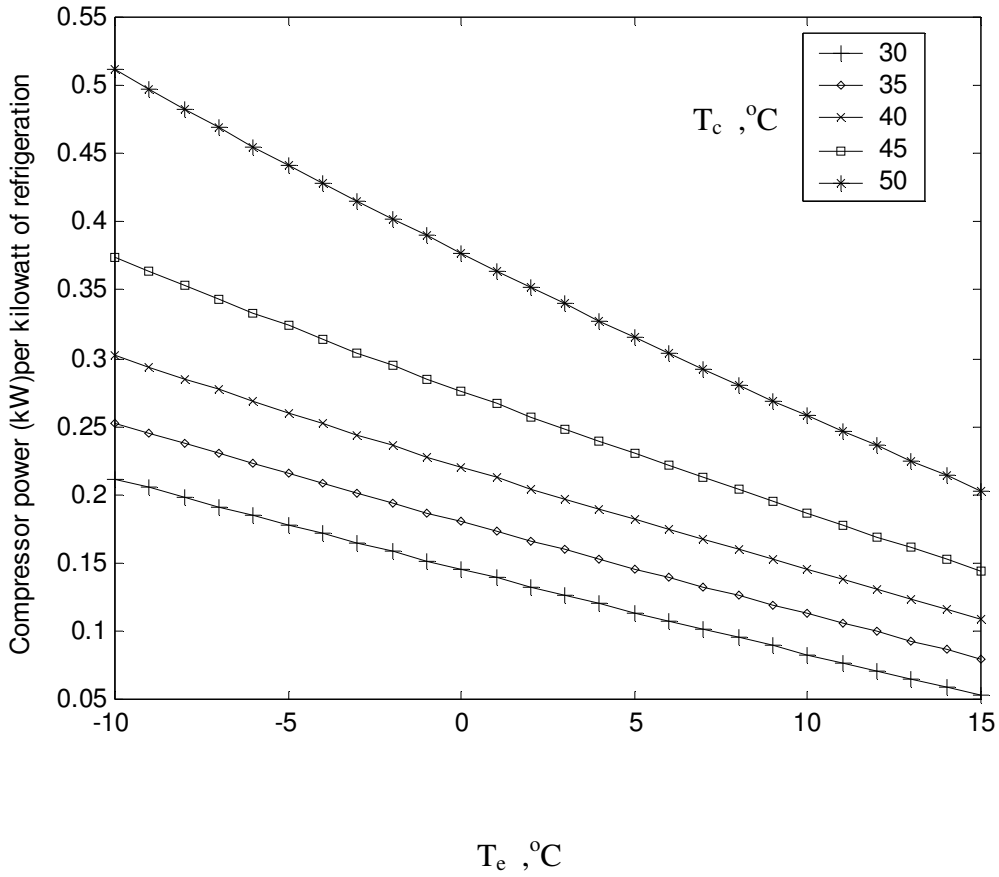

Fig (12) Compressor power versus T_e for different values of T_c for ideal cycle

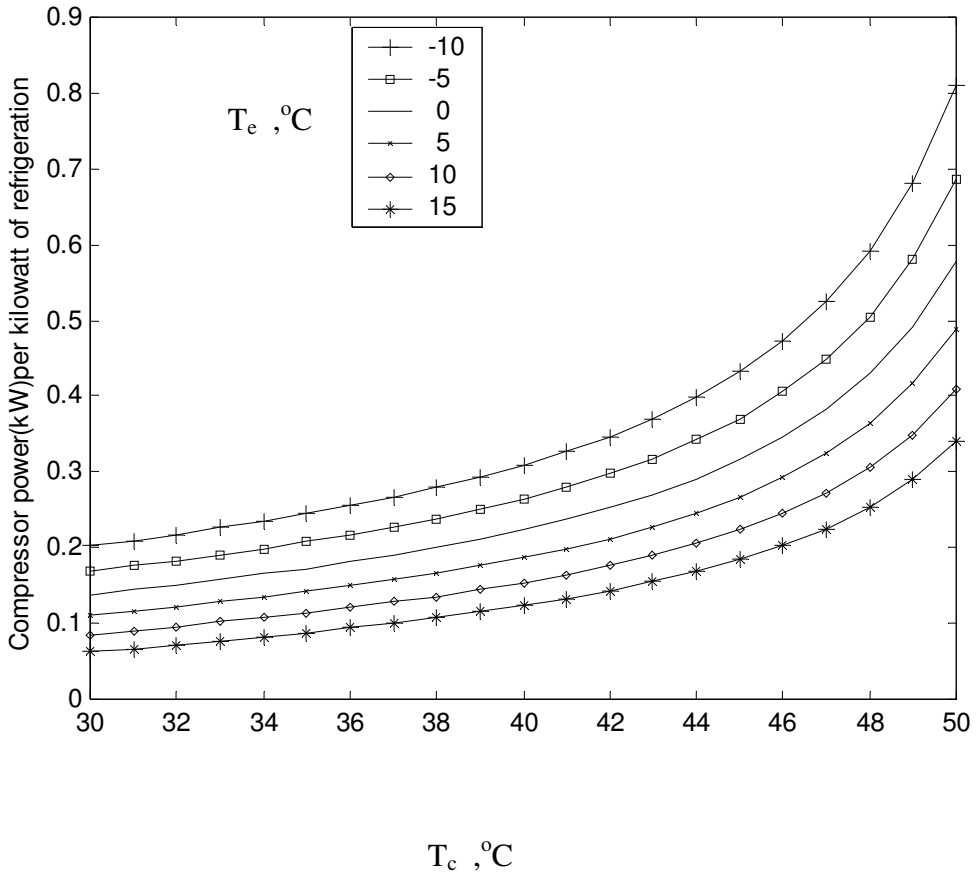

Fig (13) Compressor power versus T_c for different values of T_e for standard cycle

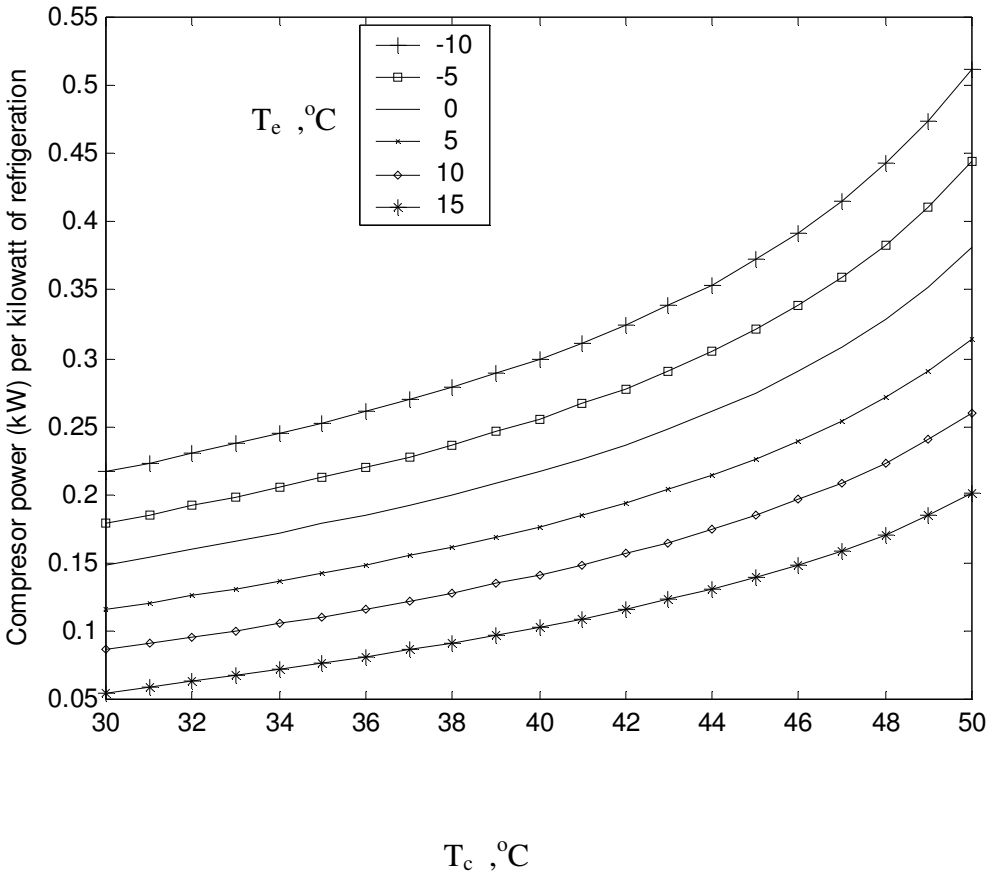

Fig (14) Compressor power versus T_c for different values of T_e for ideal cycle

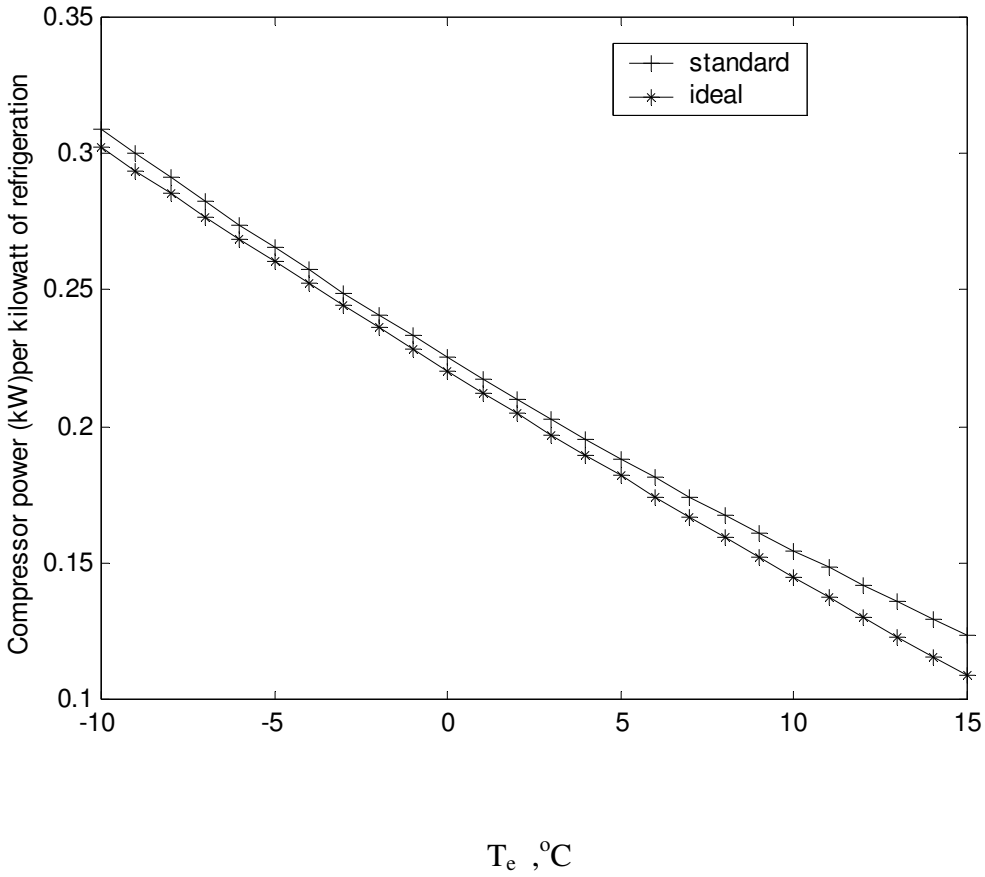

Fig (15) Standard and ideal compressor power versus T_e at T_c = 40 °C

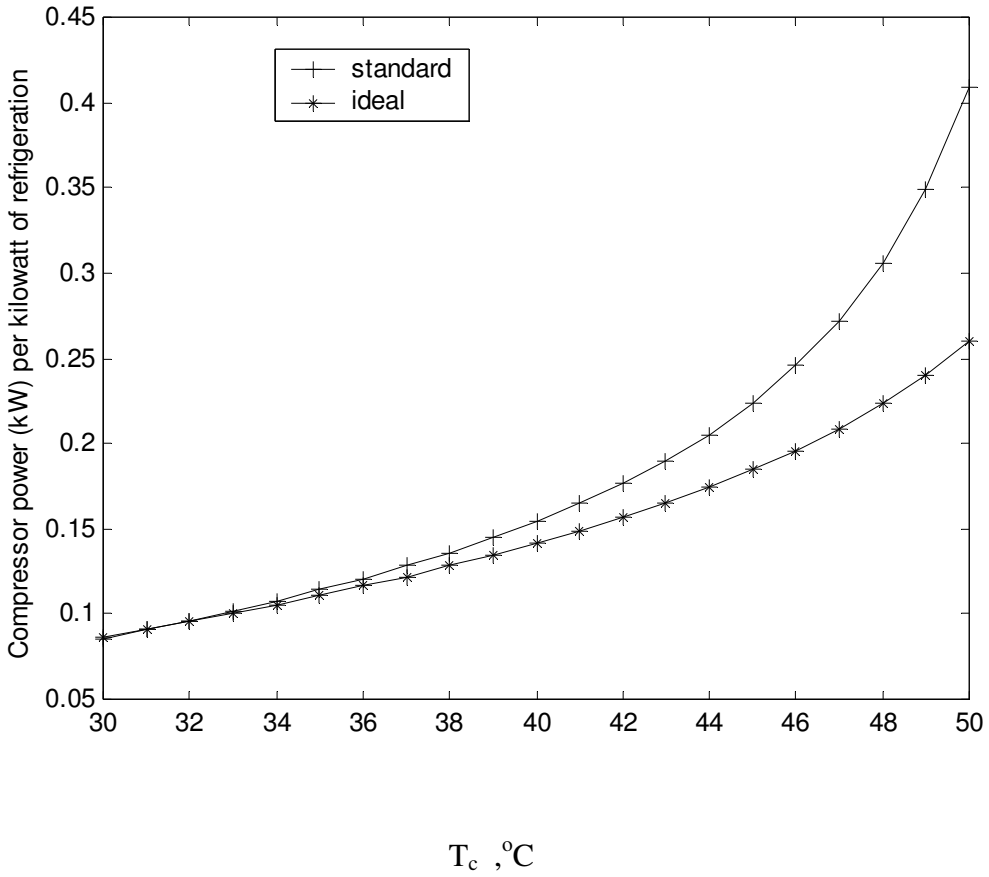

Fig (16) Standard and ideal compressor power versus T_c at T_e = 10 °C

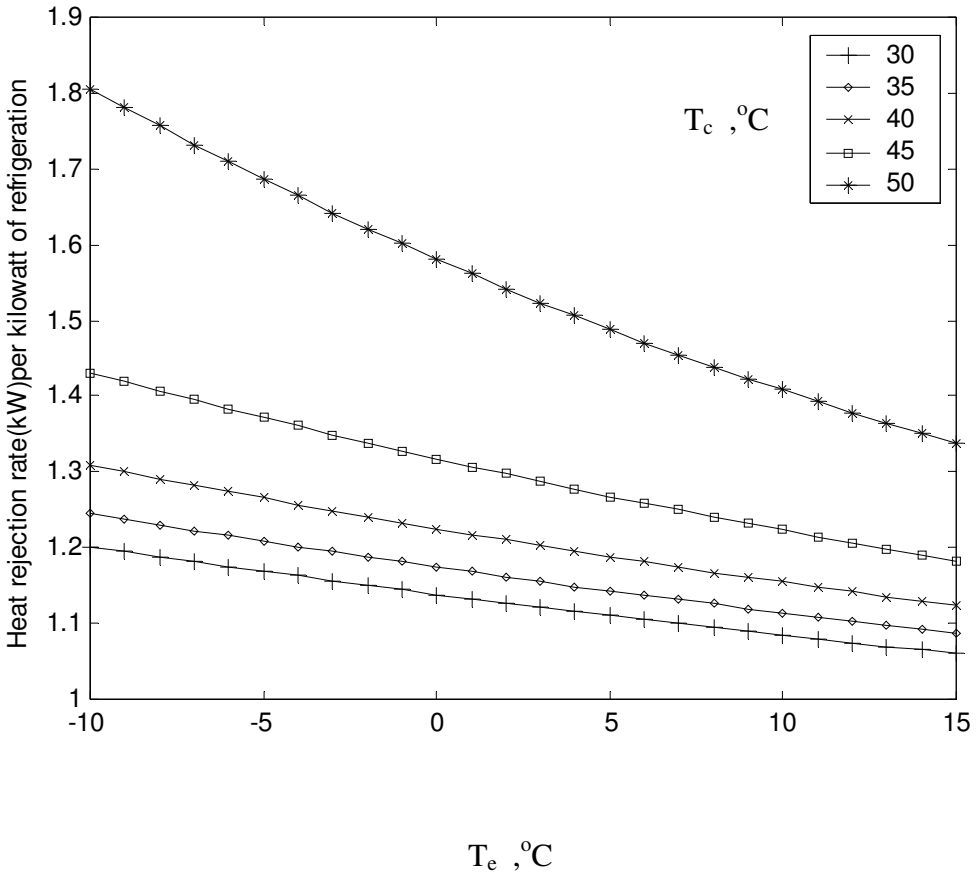

Fig (17) Heat rejection rate versus T_e for different values of T_c for standard cycle

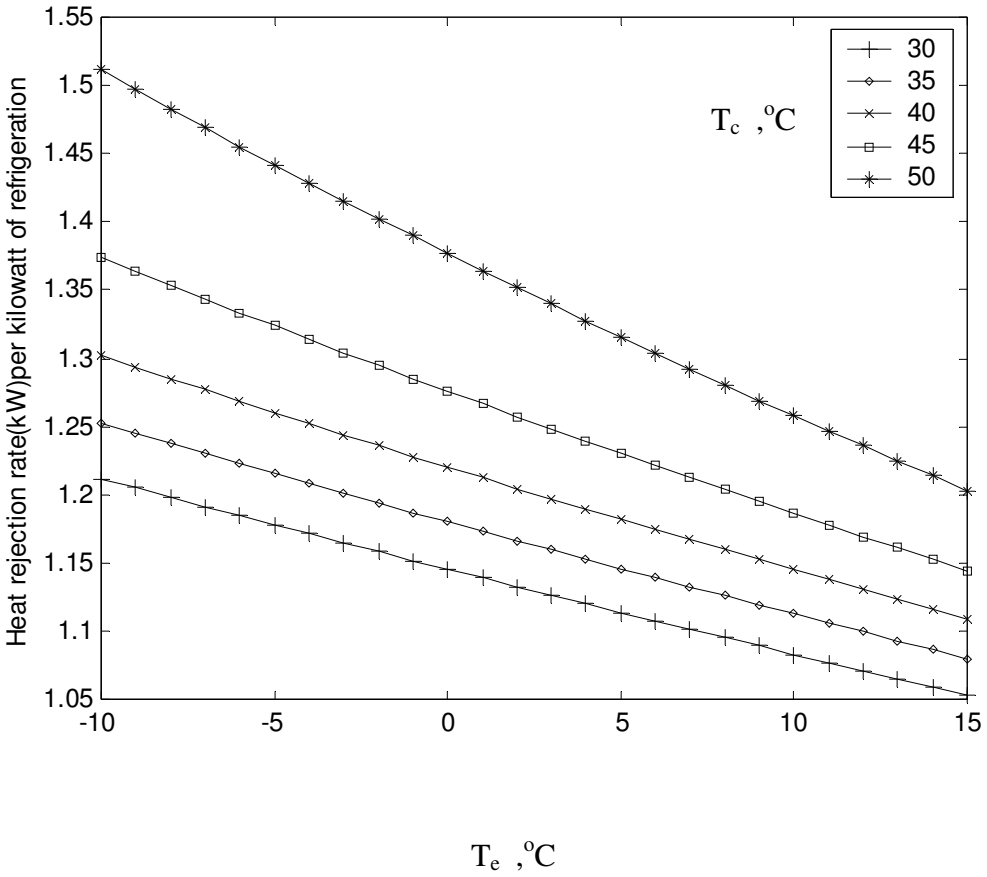

Fig (18) Heat rejection rate versus T_e for different values of T_c for ideal cycle

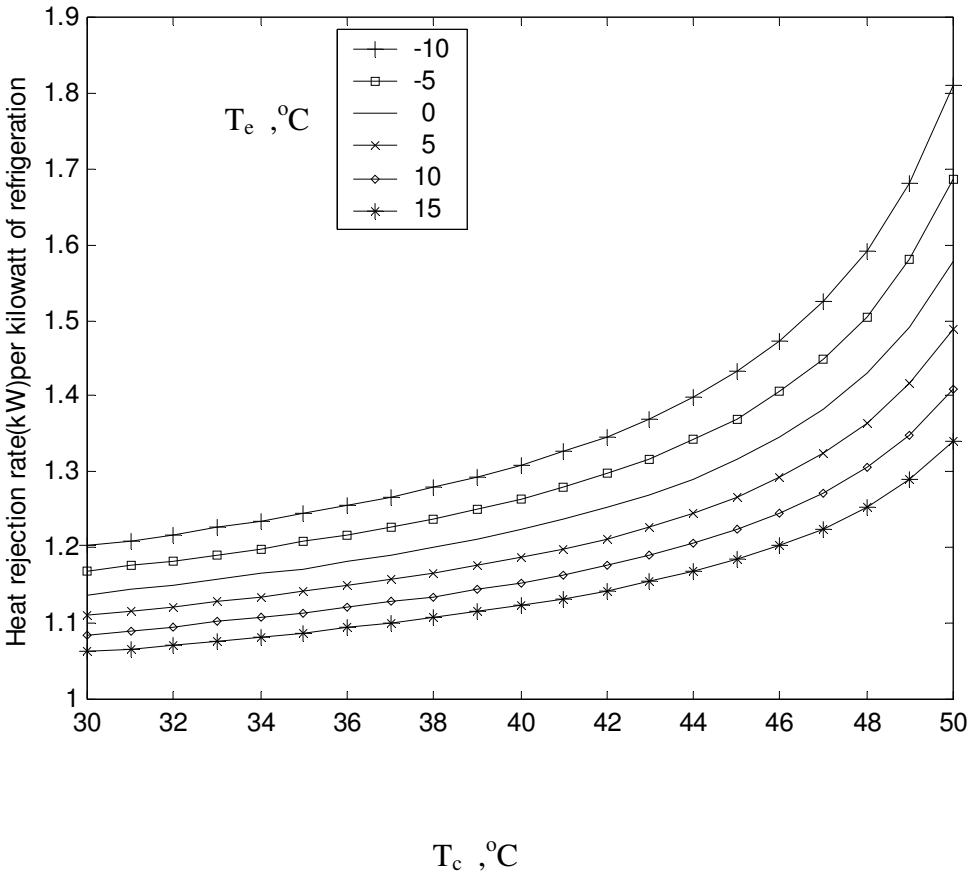

Fig (19) Heat rejection rate versus T_c for different values of T_e for standard cycle

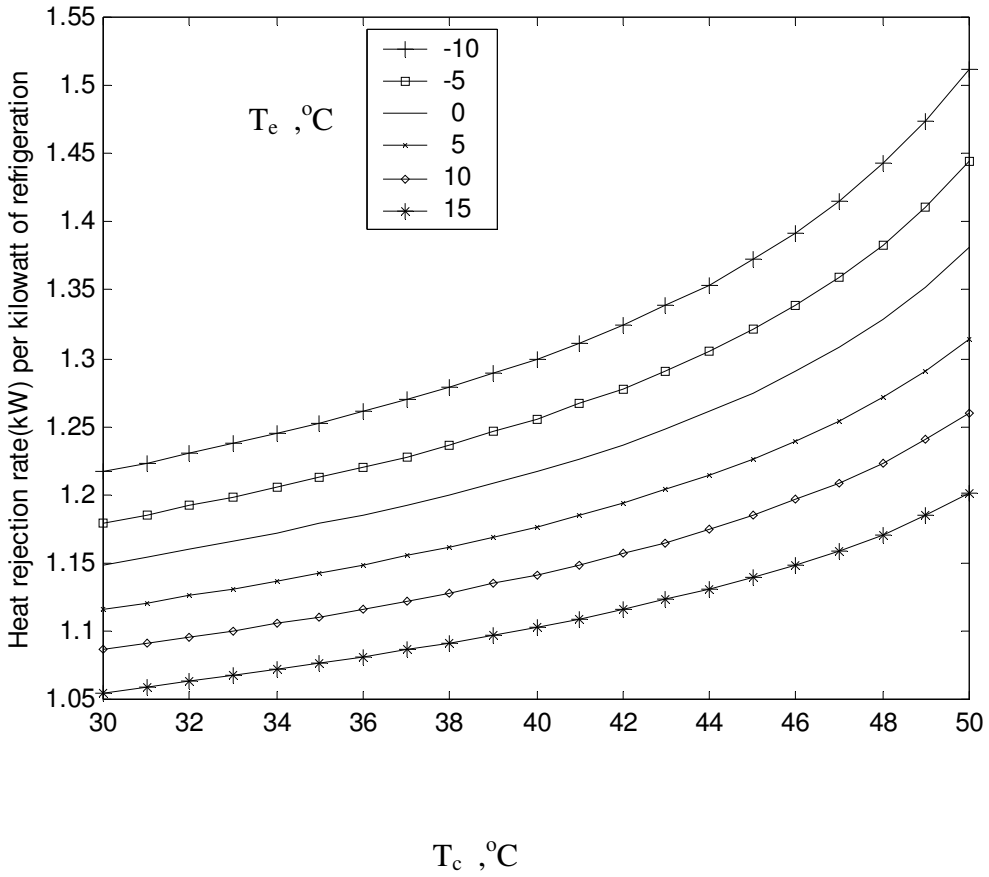

Fig (20) Heat rejection rate versus T_c for different values of T_e for ideal cycle

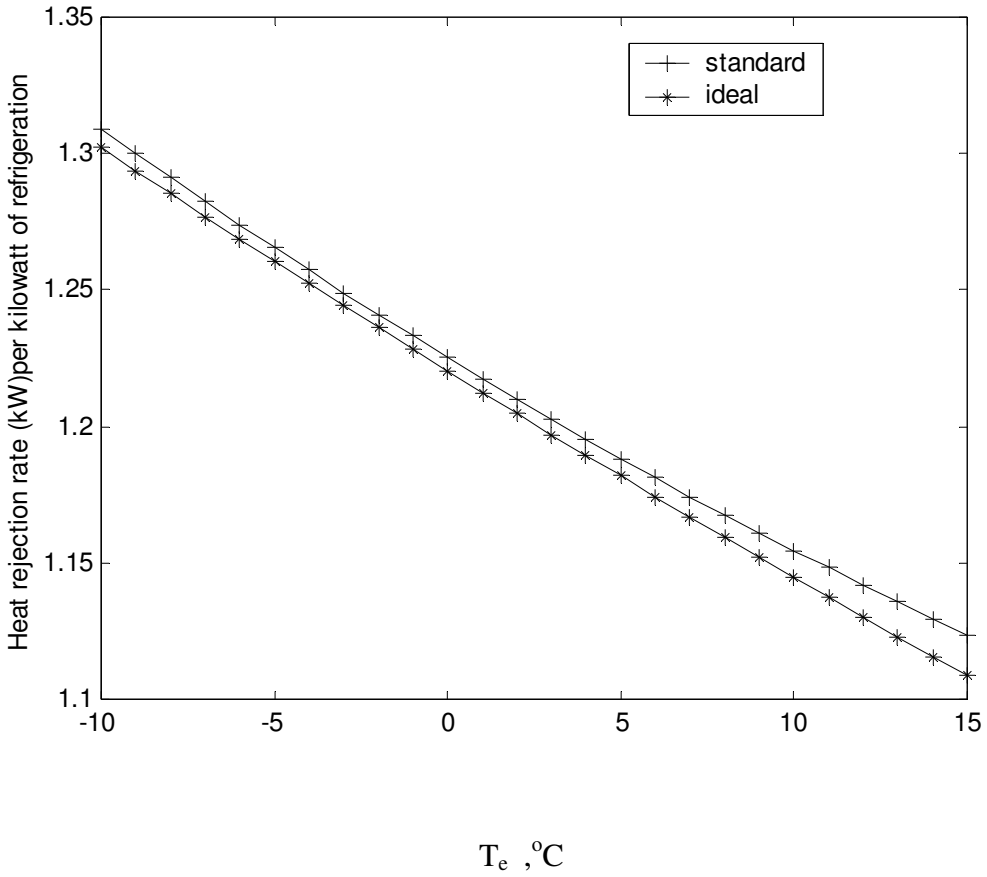

Fig (21) Standard and ideal heat rejection rate versus T_e at $T_c = 40\ ^oC$

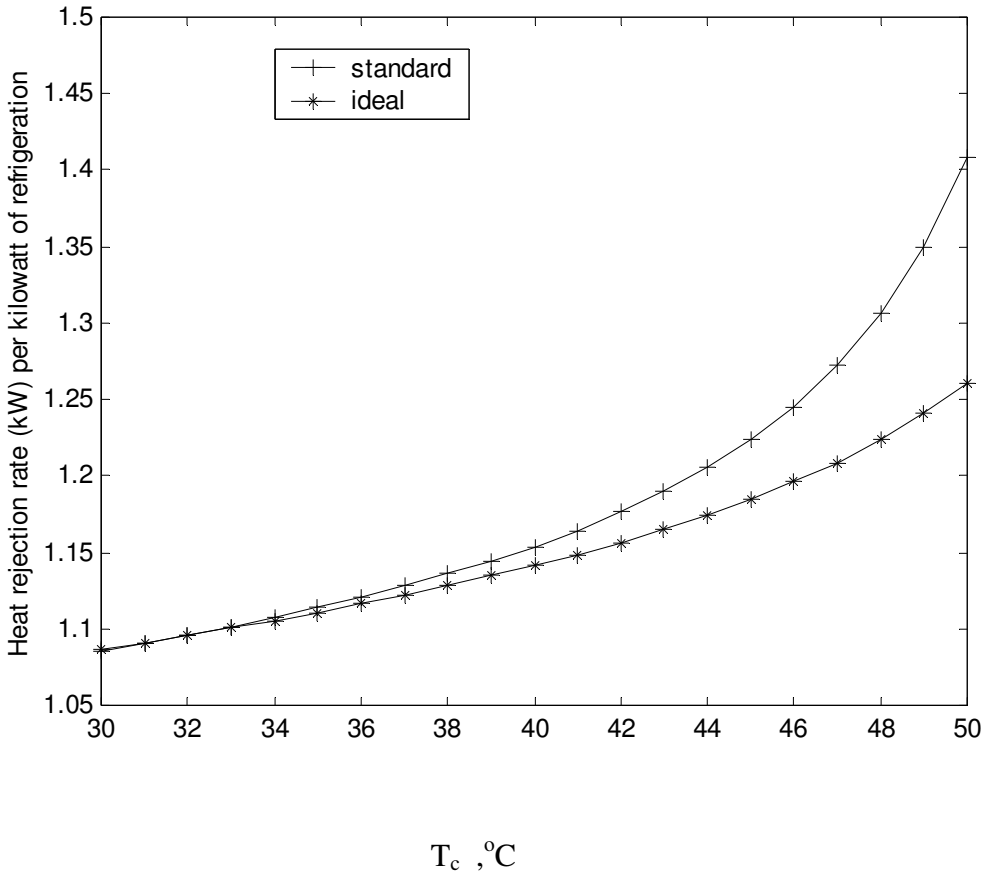

Fig (22) Standard and ideal heat rejection rate versus T_c at $T_e = 10\ ^oC$

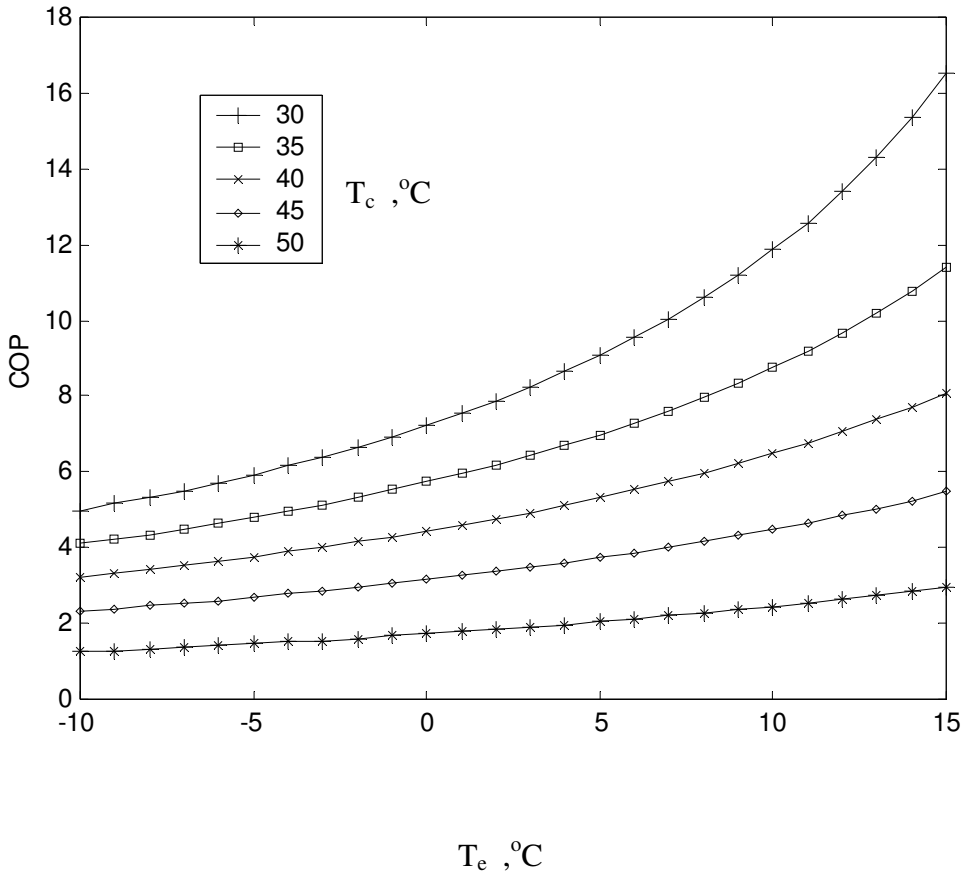

Fig (23) Coefficient of performance versus T_e for different values of T_c for standard cycle

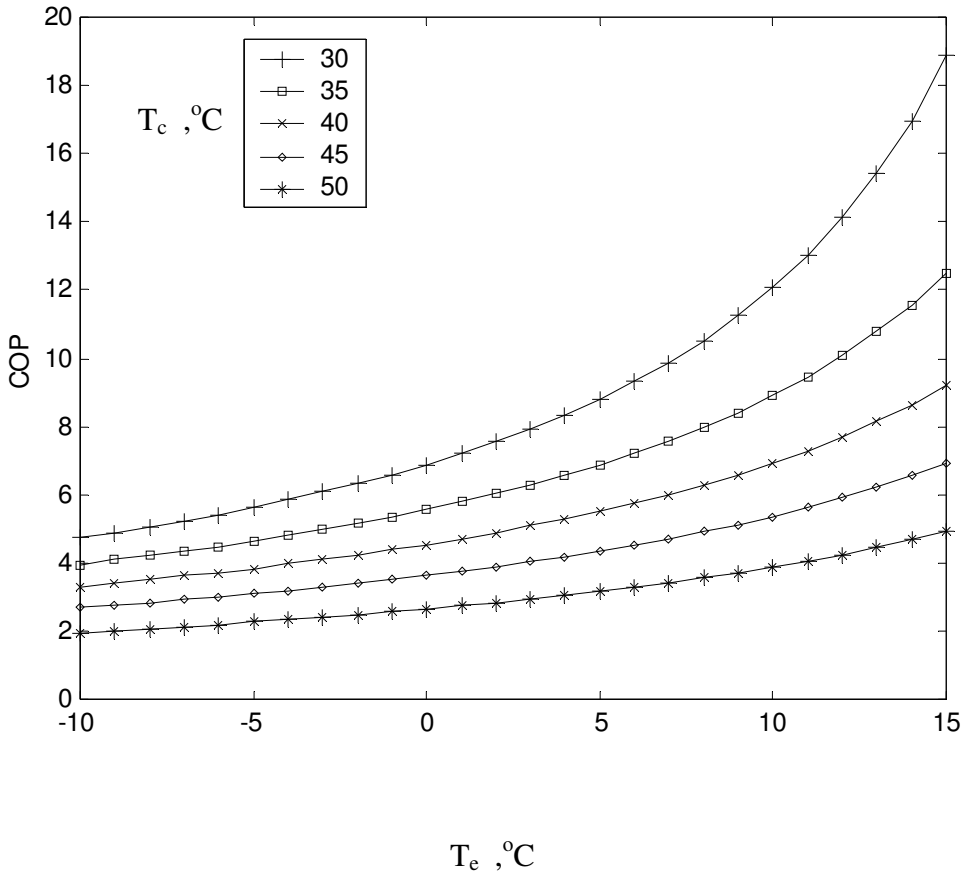

Fig (24) Coefficient of performance versus T_e for different values of T_c for ideal cycle

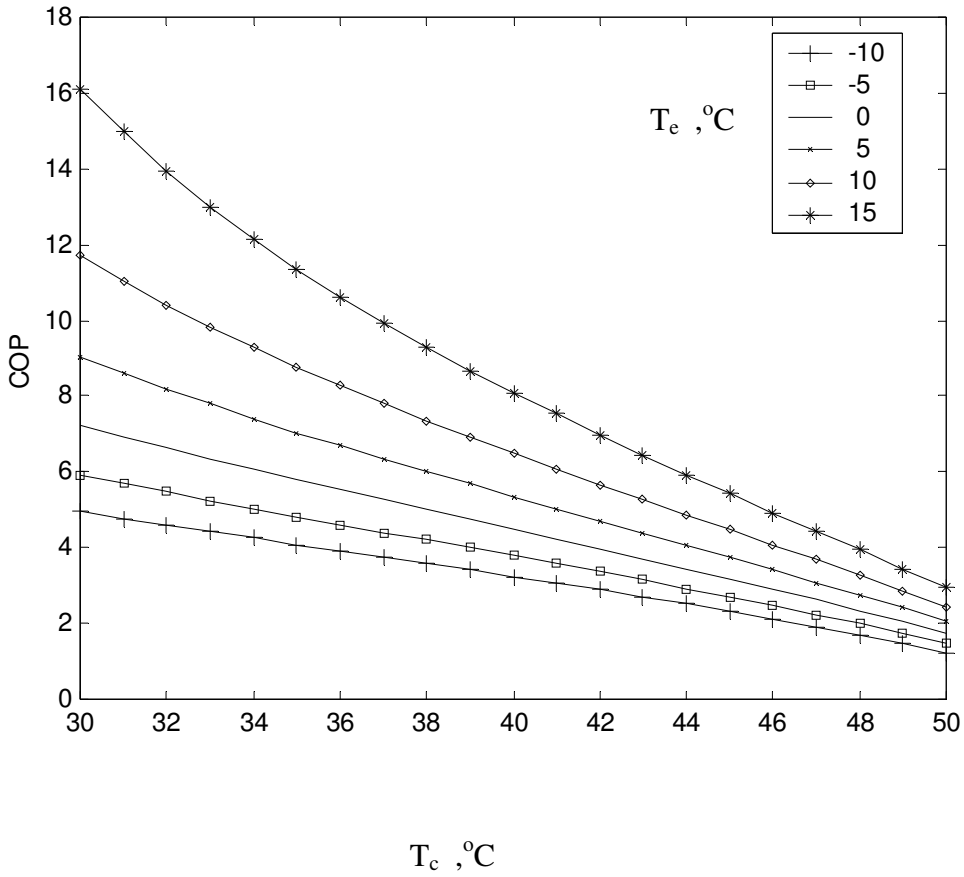

Fig (25) Coefficient of performance versus T_c for different values of T_e for standard cycle

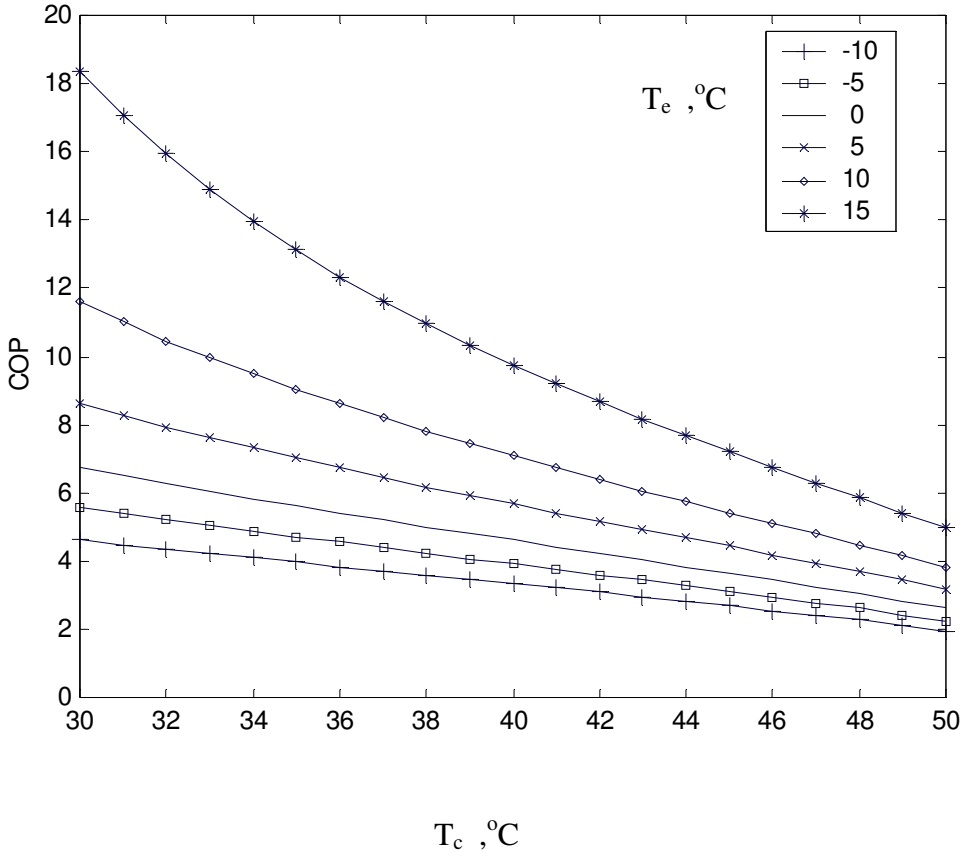

Fig (26) Coefficient of performance versus T_c for different values of T_e for ideal cycle

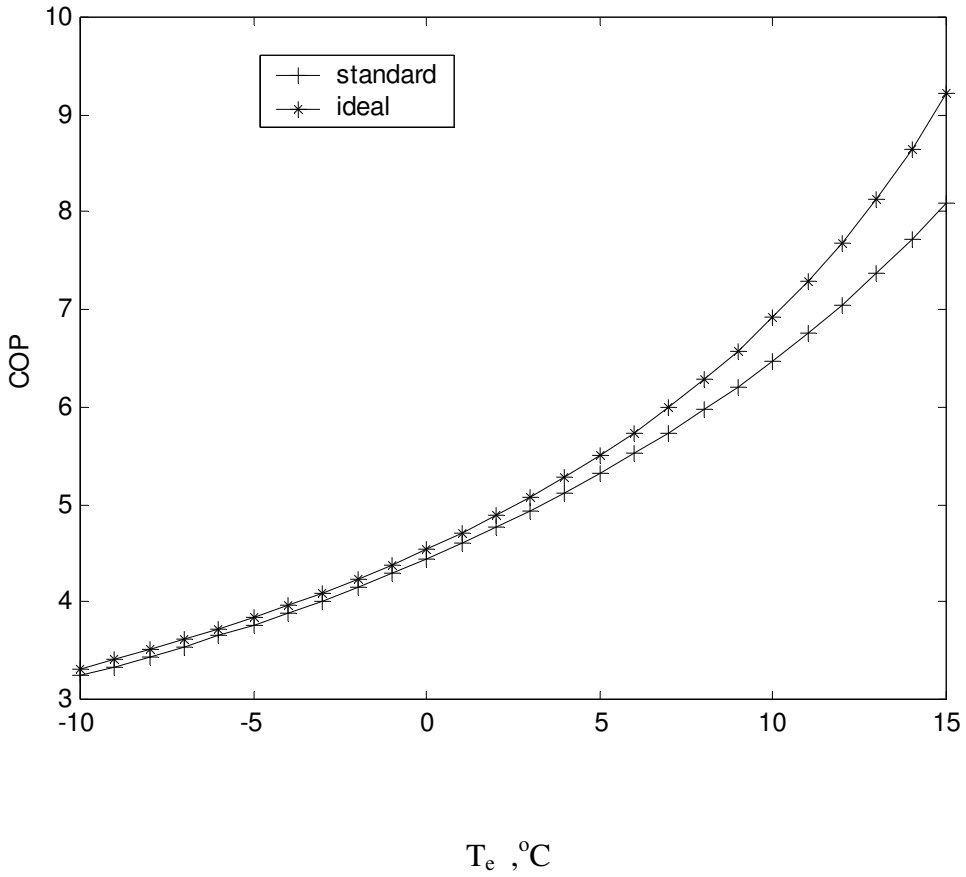

Fig (27) Standard and ideal coefficient of performance versus T_e at T_c = 40 °C

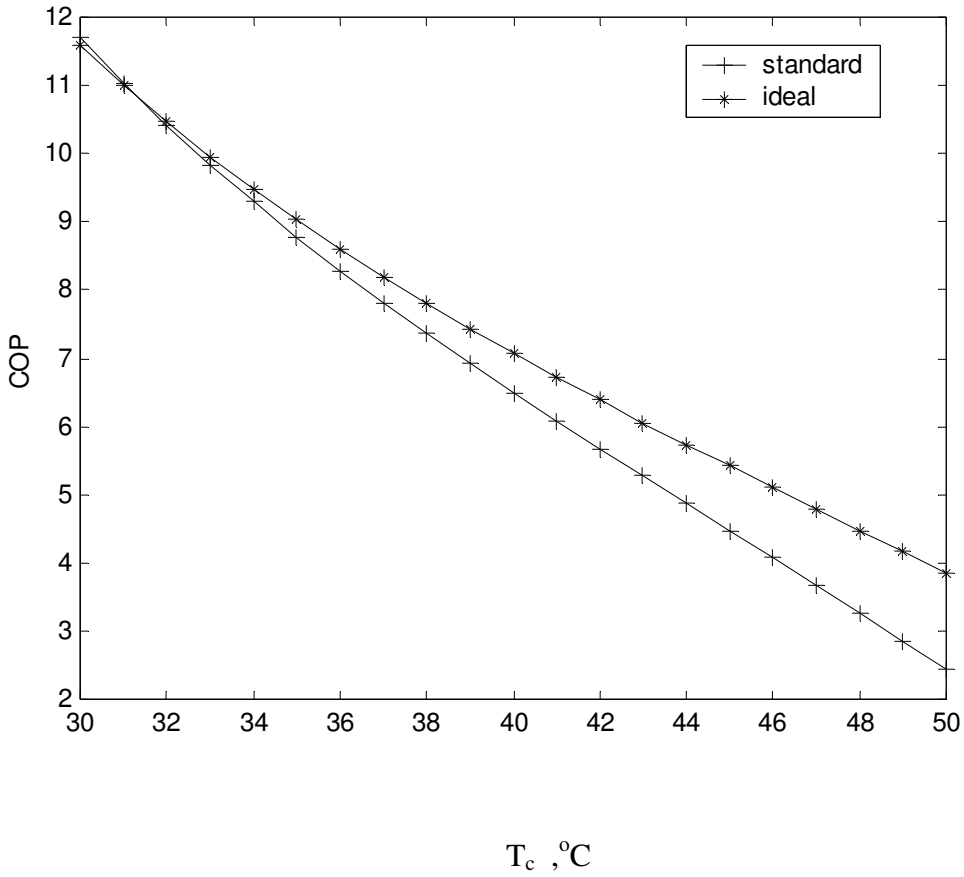

Fig (28) Standard and ideal coefficient of performance versus T_c at T_e = 10 °C

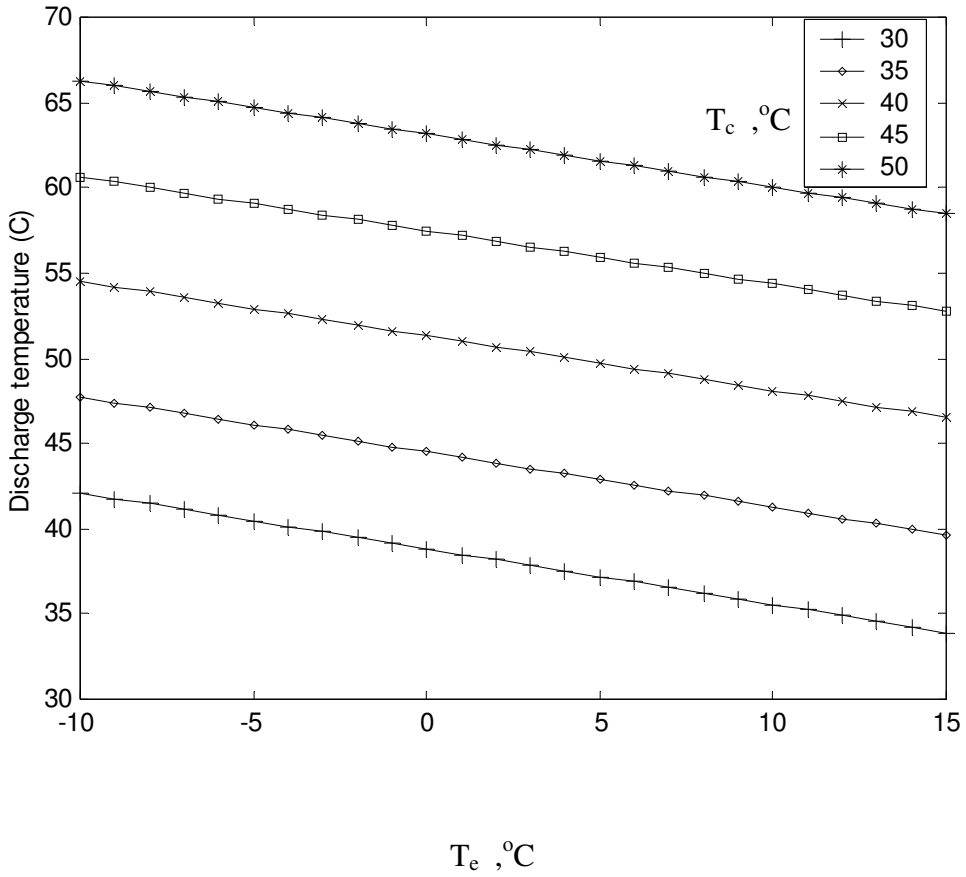

Fig (29) Compressor discharge temperature versus T_e for different values of T_c for standard cycle

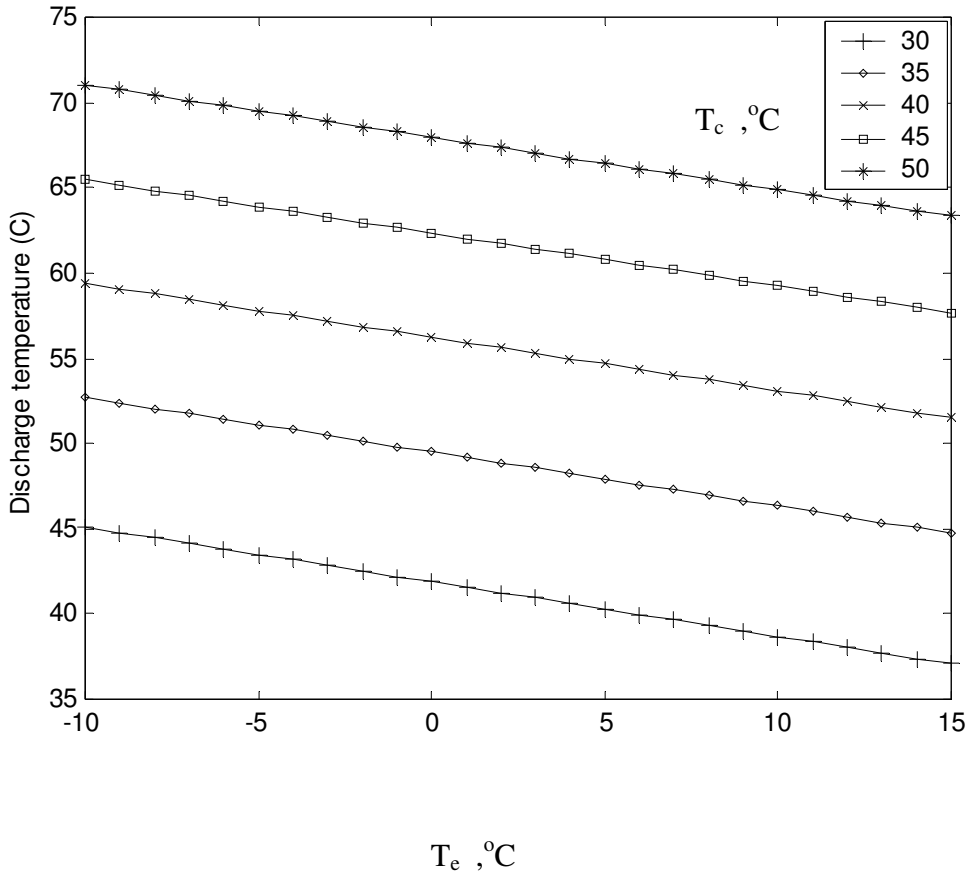

Fig (30) Compressor discharge temperature versus T_e for different values of T_c for ideal cycle

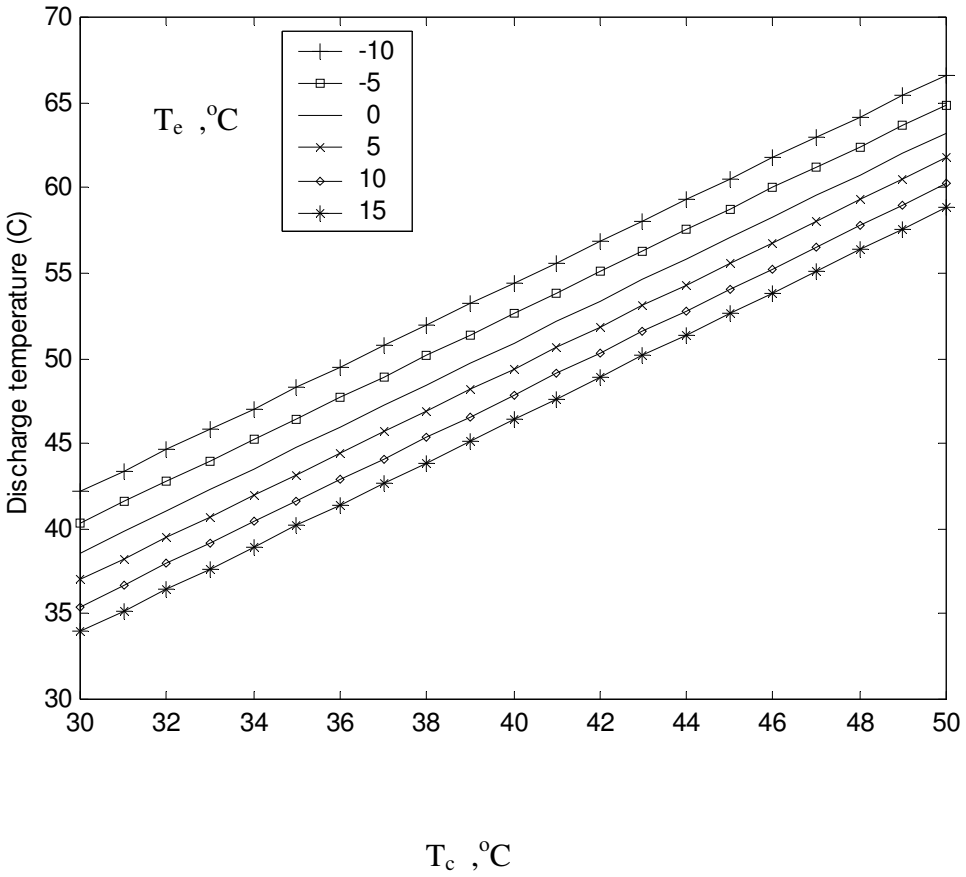

Fig (31) Compressor discharge temperature versus T_c for different values of T_e for standard cycle

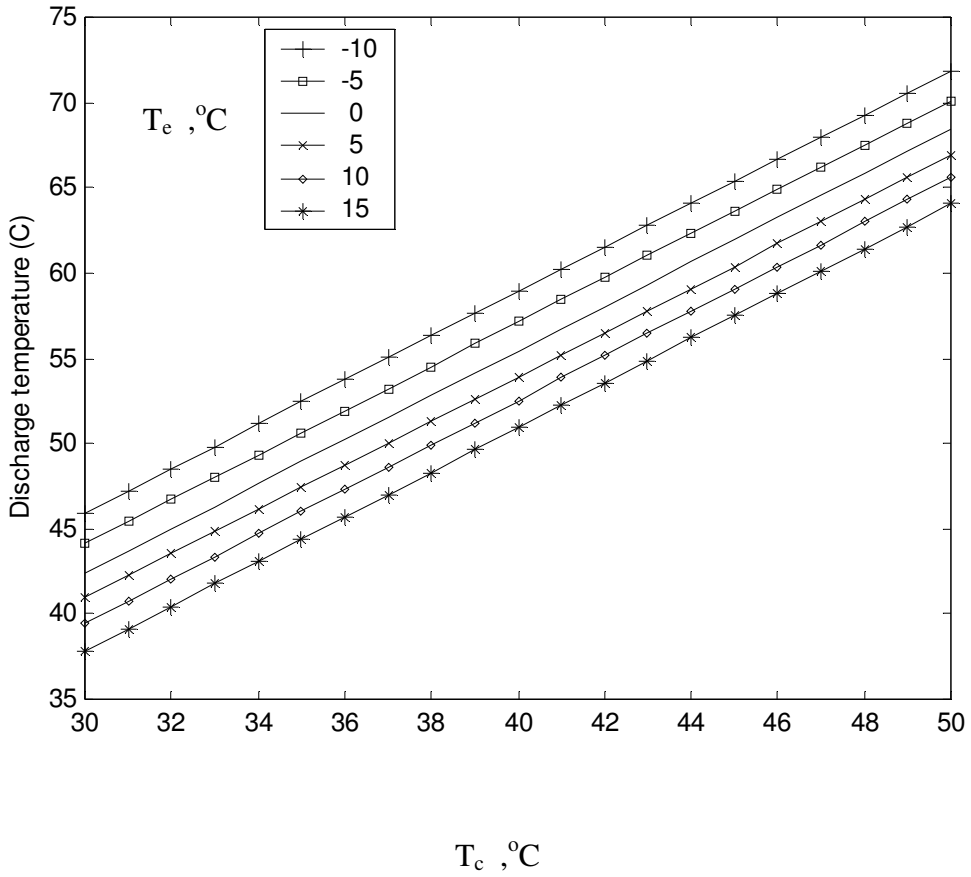

Fig (32) Compressor discharge temperature versus T_c for different values of T_e for ideal cycle

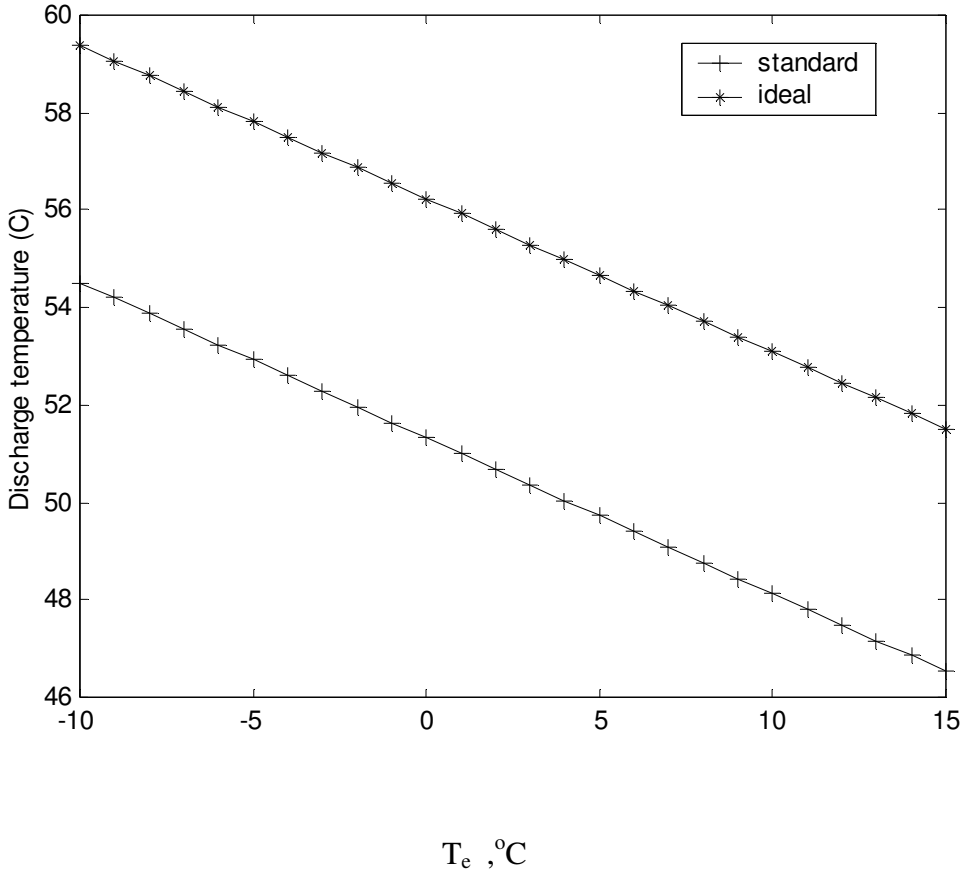

Fig (33) Standard and ideal compressor discharge temperature versus T_e at T_c = 40 °C

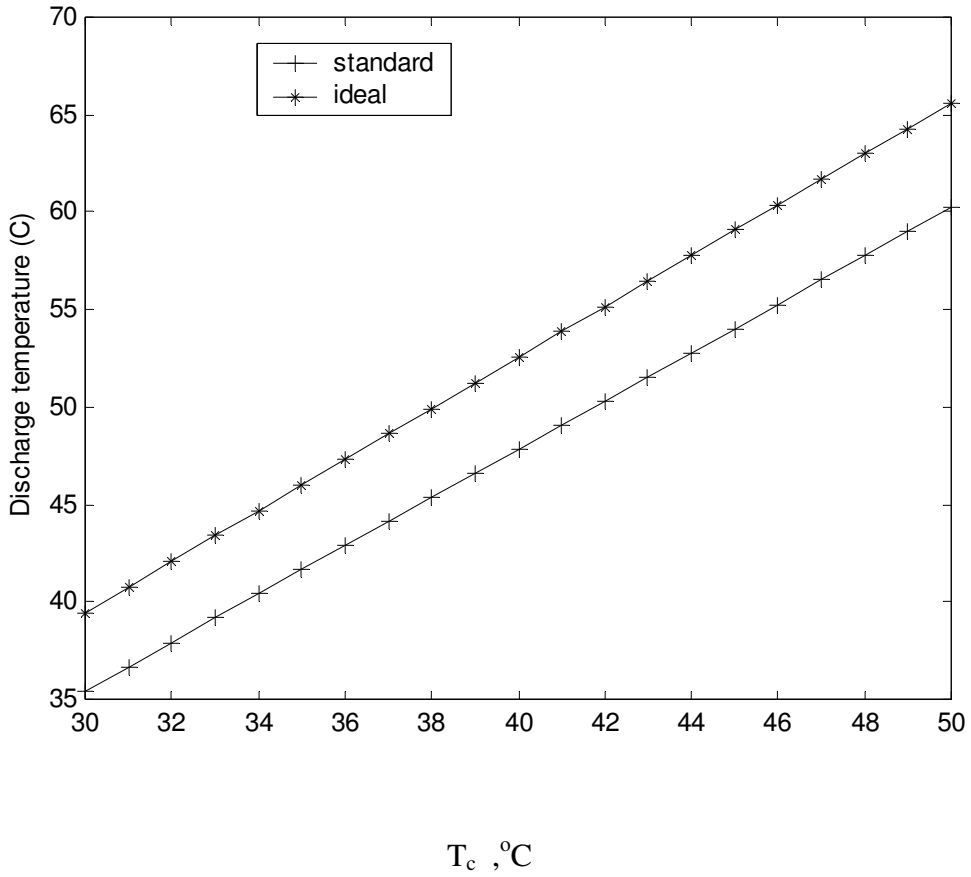

Fig (34) Standard and ideal compressor discharge temperature versus T_c at T_e = 10 °C

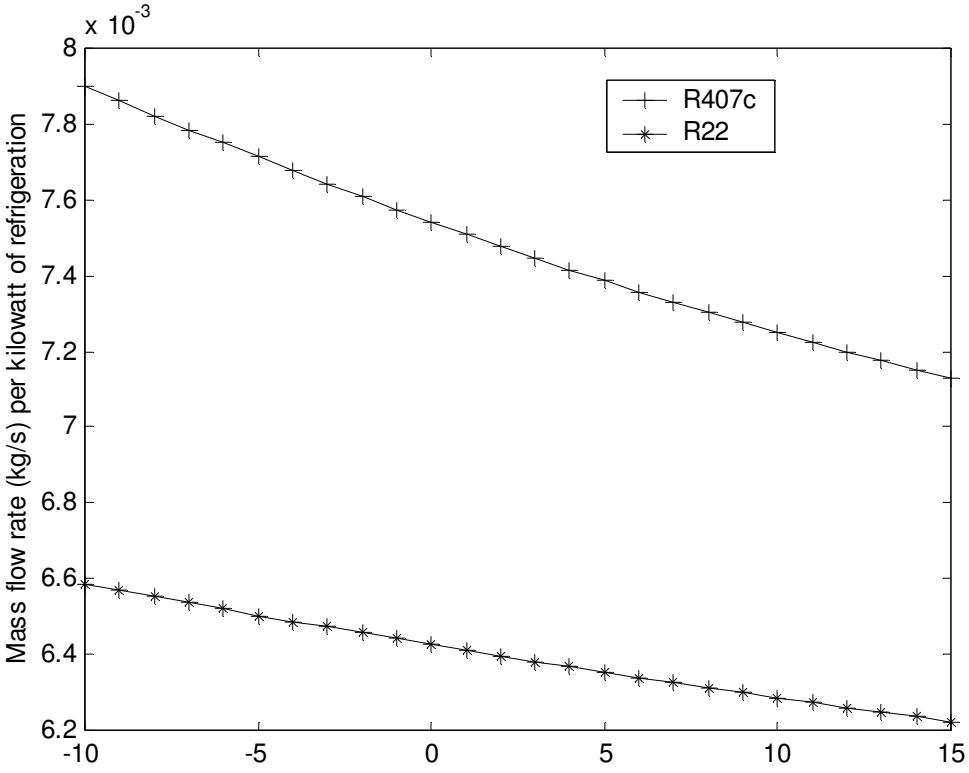

Fig (35) Comparison between mass flow rate of R407c and R22 versus T_e at T_c = 40 ^oC for standard cycle.

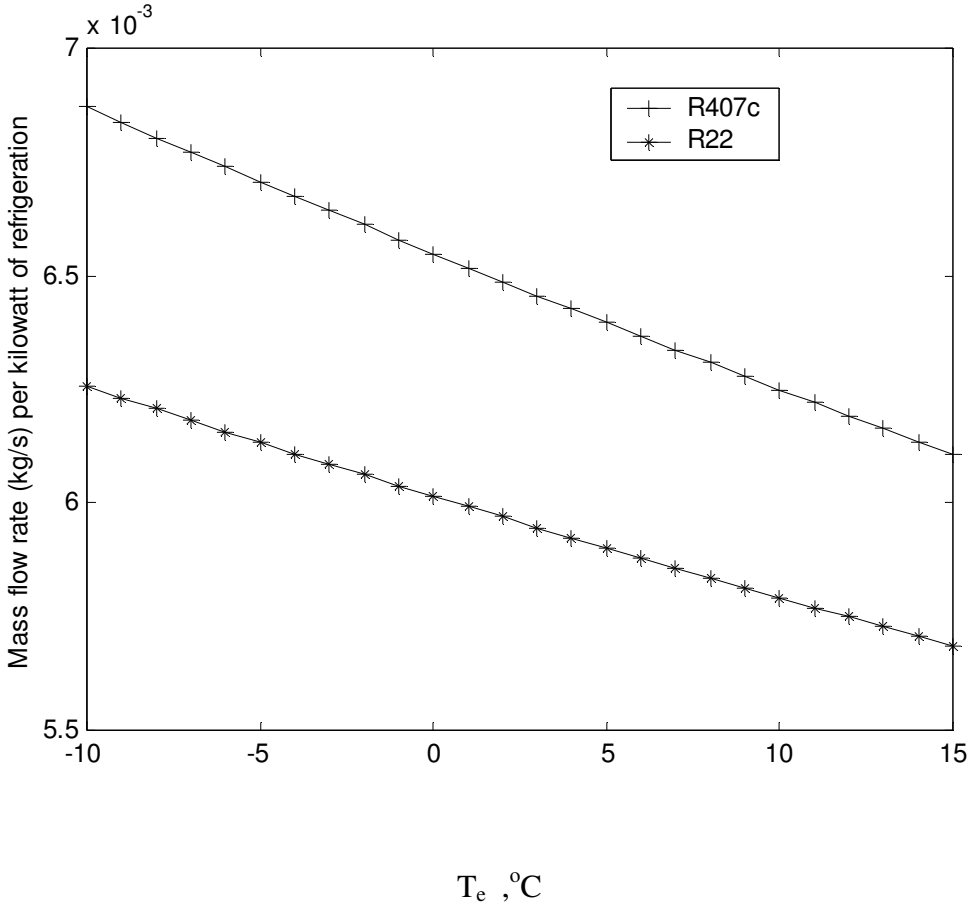

Fig (36) Comparison between mass flow rate of R407c and R22 versus T_e at T_c = 40 °C for ideal cycle.

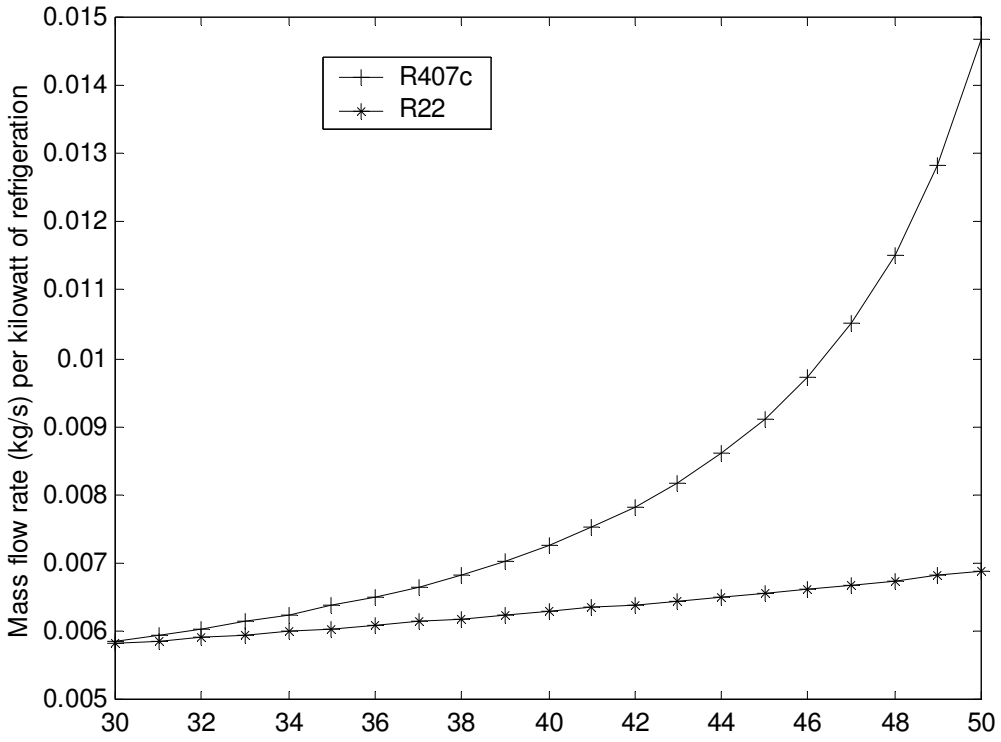

Fig (37) Comparison between mass flow rate of R407c and R22 versus T_c at T_e = 10 °C for standard cycle.

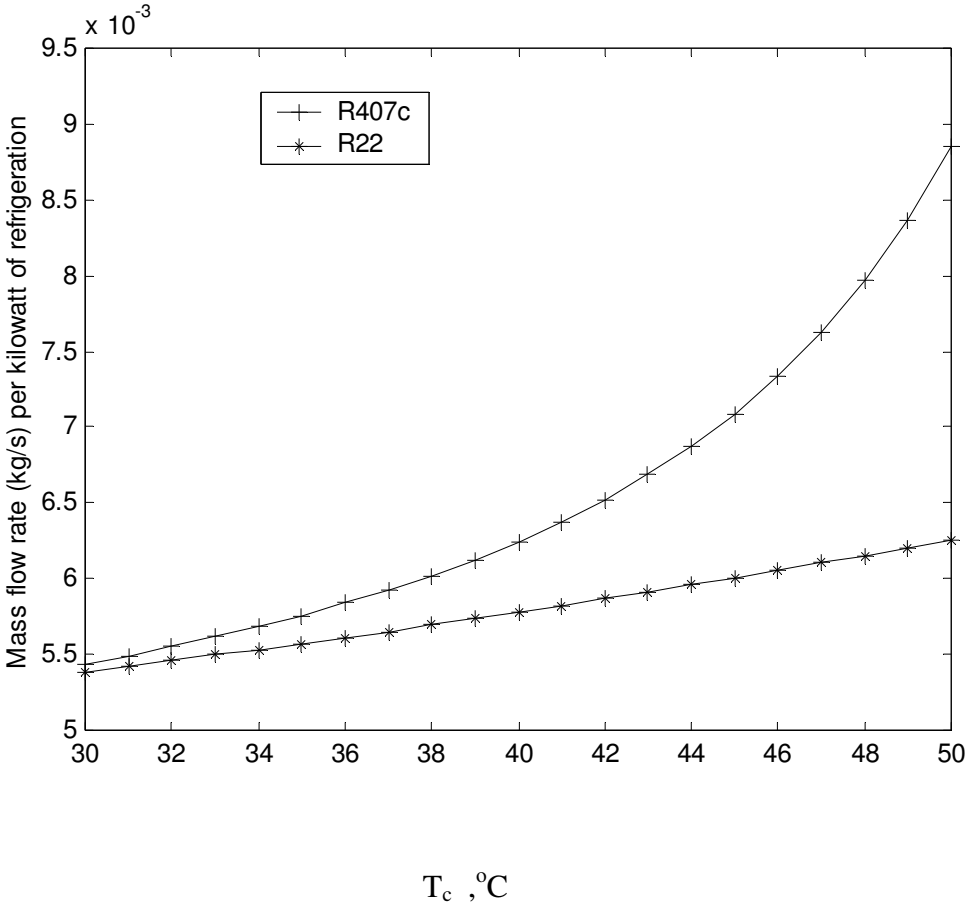

Fig (38) Comparison between mass flow rate of R407c and R22 versus T_c at T_e = 10 °C for ideal cycle.

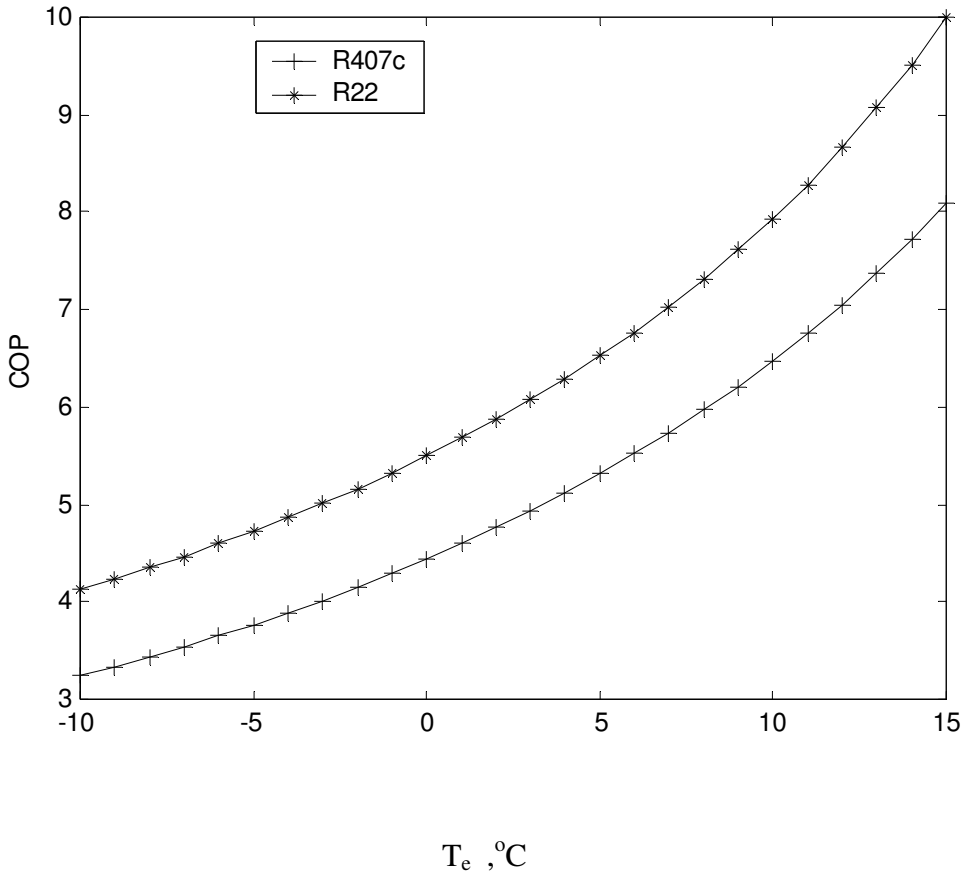

Fig (39) Comparison between coefficient of performance of R407c and R22 versus T_e at T_c = 40 °C for standard cycle.

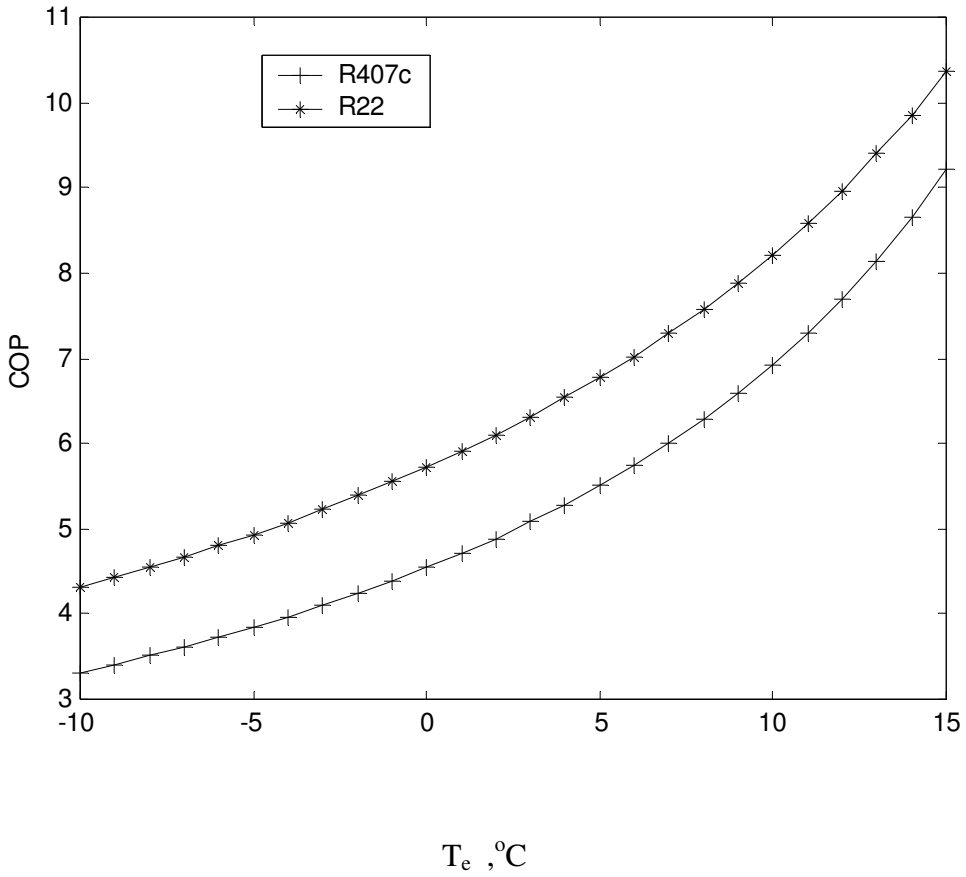

Fig (40) Comparison between coefficient of performance of R407c and R22 versus T_e at T_c = 40 °C for ideal cycle.

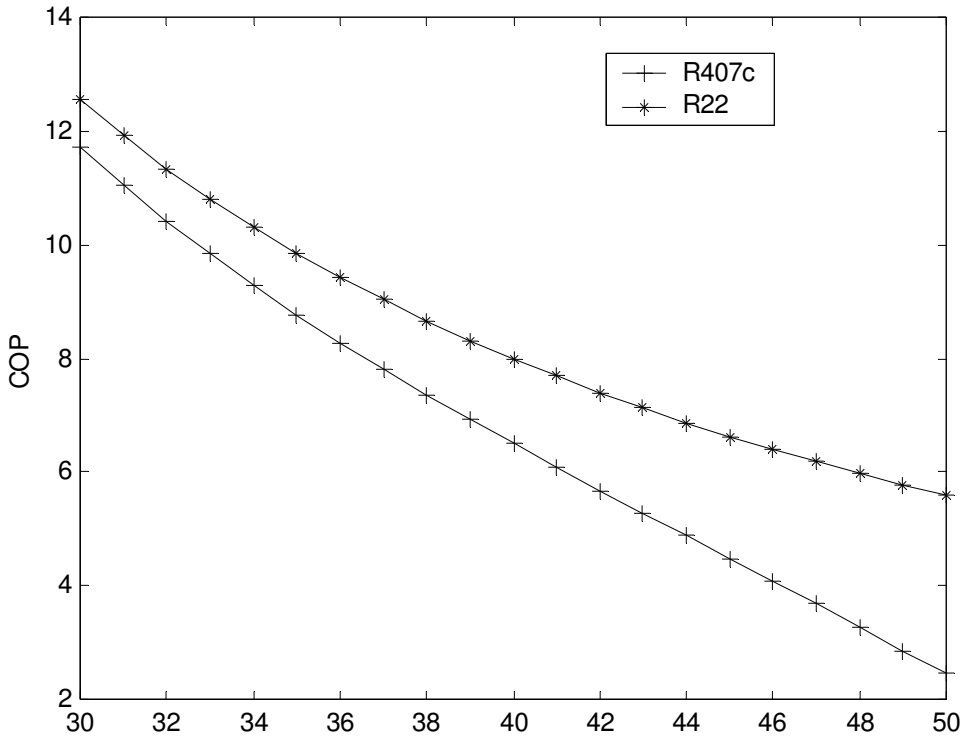

Fig (41) Comparison between coefficient of performance of R407c and R22 versus T_c at T_e = 10 °C for standard cycle.

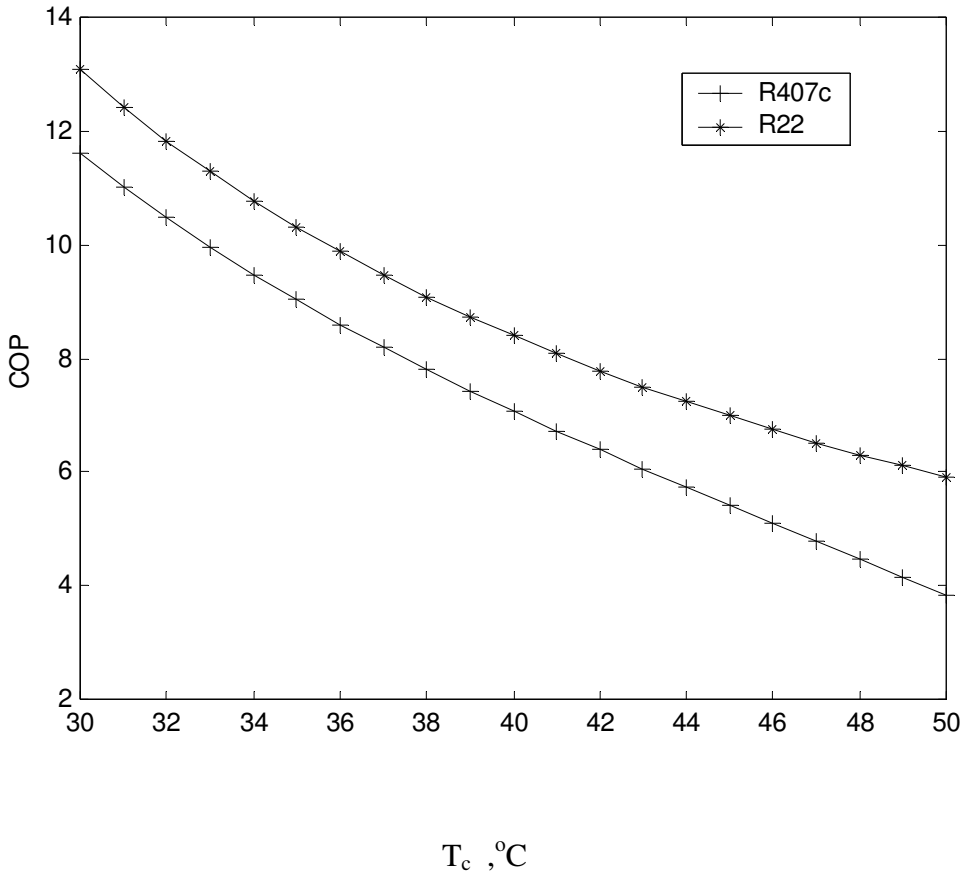

Fig (42) Comparison between coefficient of performance of R407c and R22 versus T_c at T_e = 10 °C for ideal cycle.

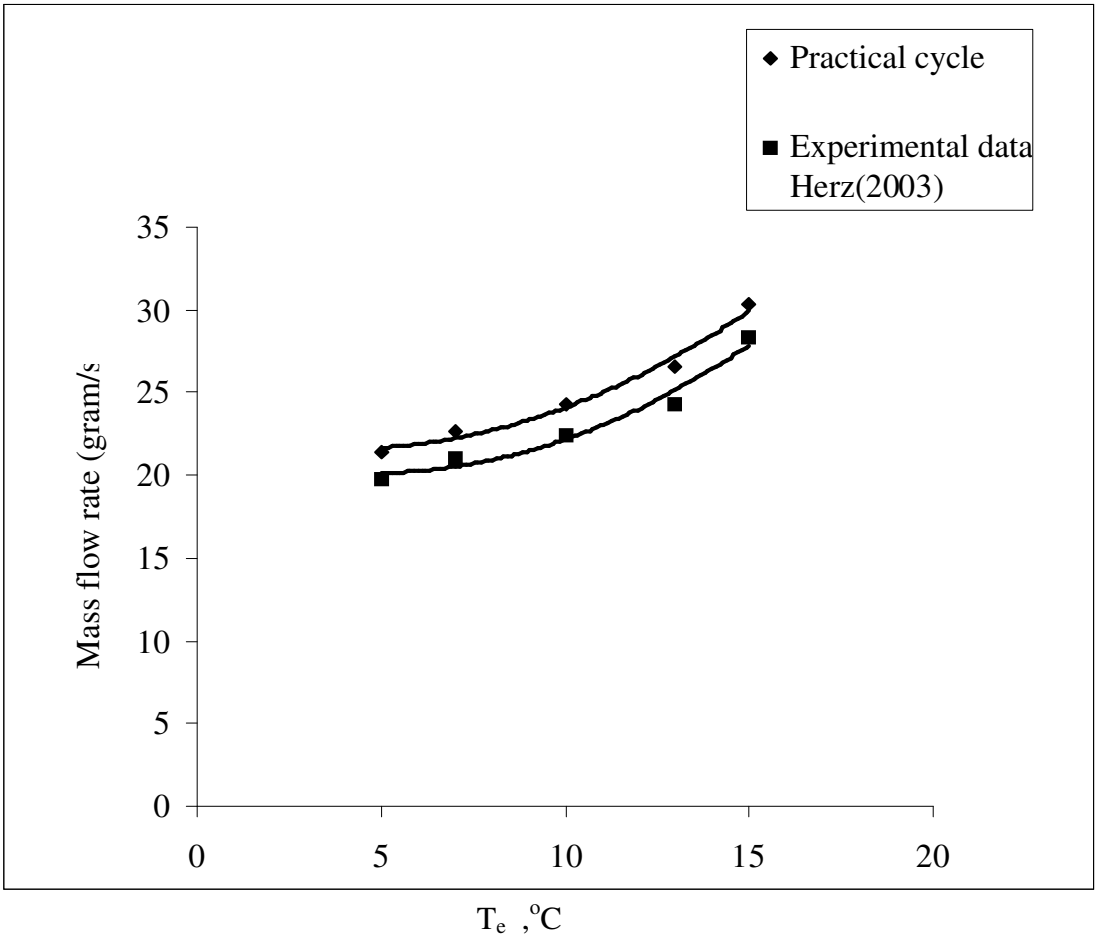

Fig (43) Variation of mass flow rate versus T_e at T_c = 40 °C

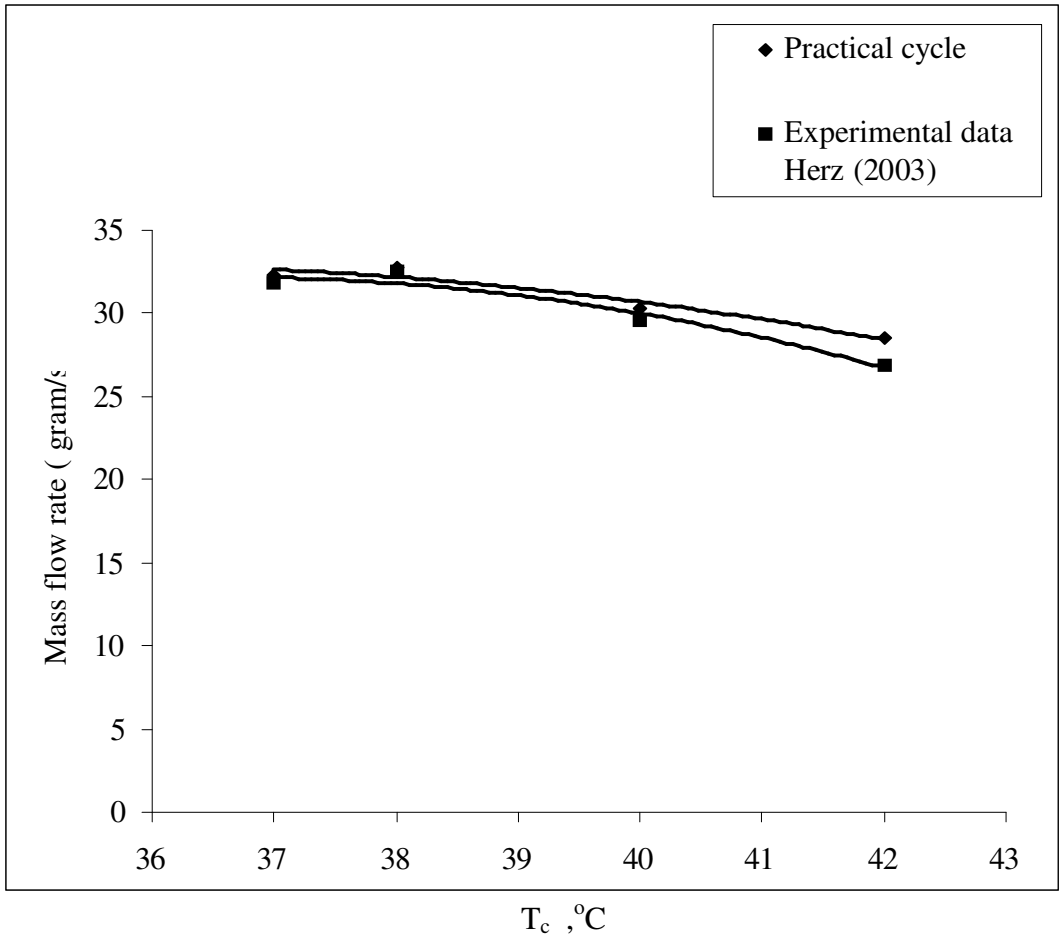

Fig (44) Variation of mass flow rate versus T_c at T_e = 12 °C

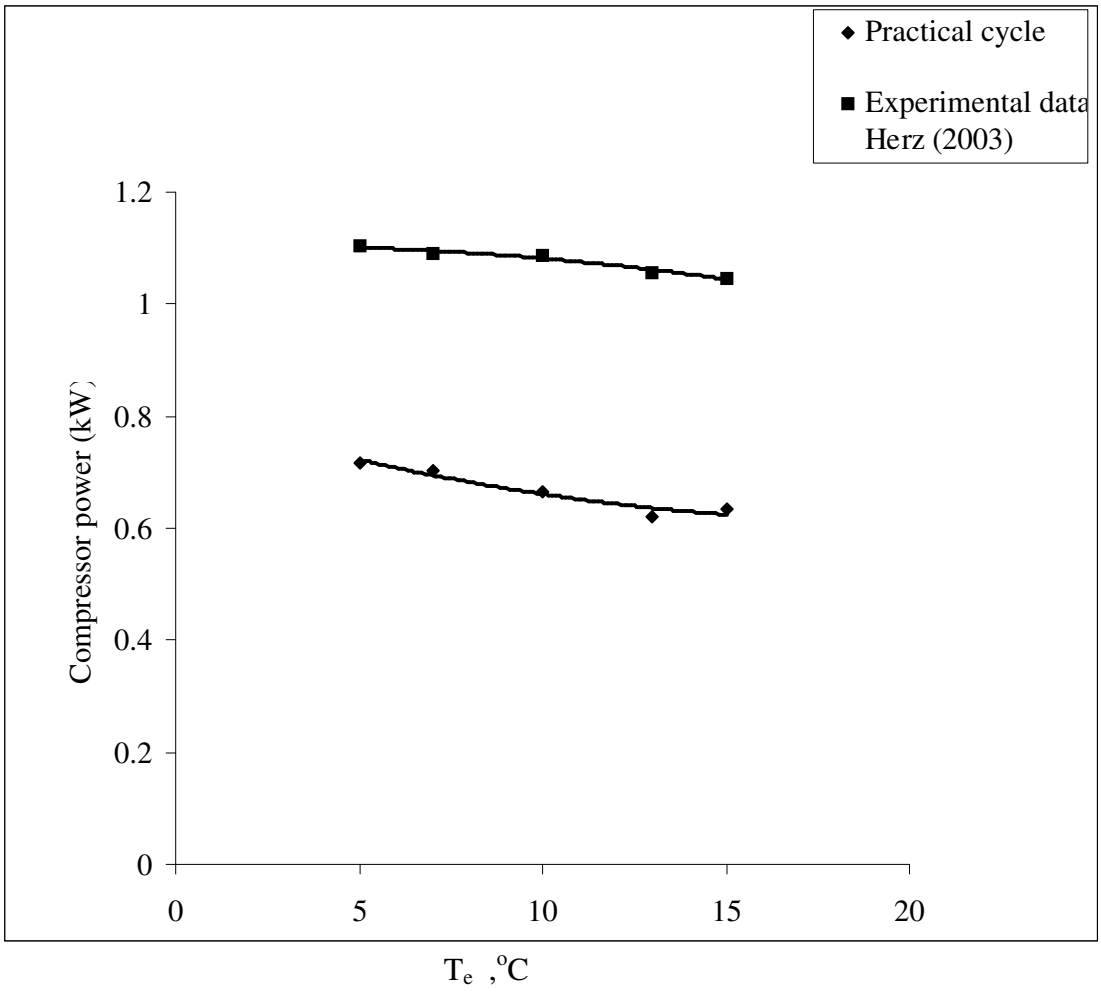

Fig (45) Variation of compressor power versus T_e at T_c = 40 °C

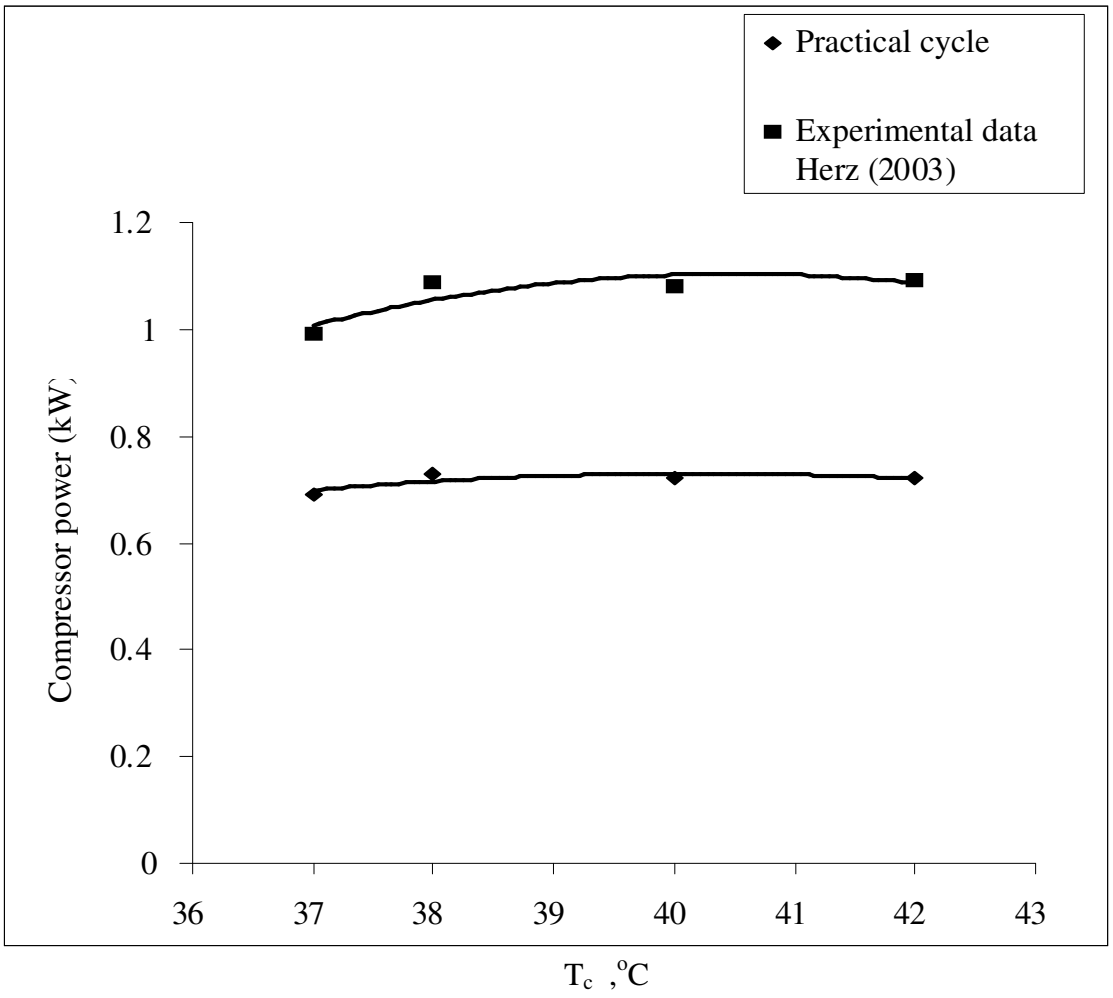

Fig (46) Variation of compressor power versus T_c at T_e = 12 °C

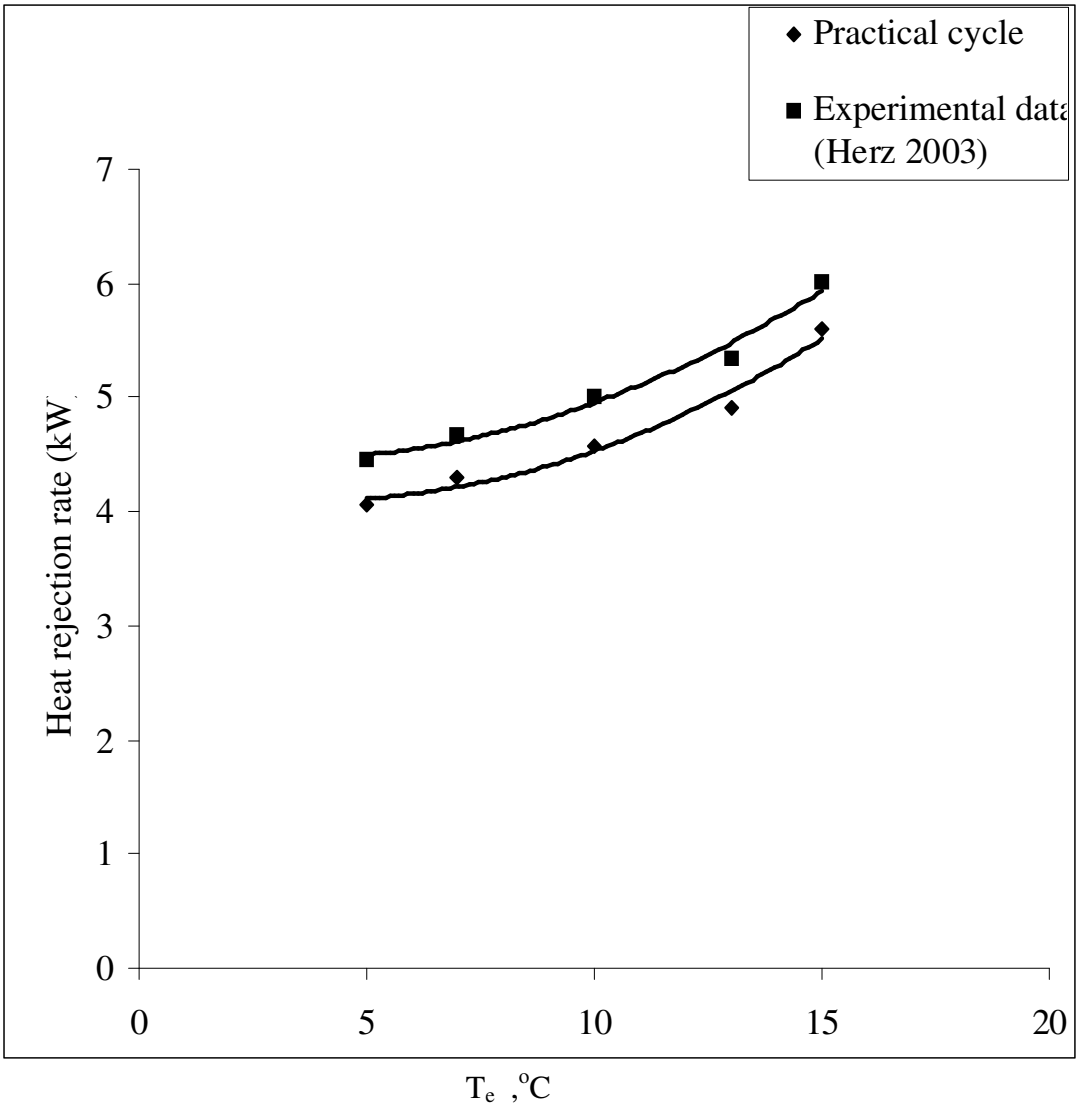

Fig (47) Variation of heat rejection rate versus T_e at T_c = 40 °C

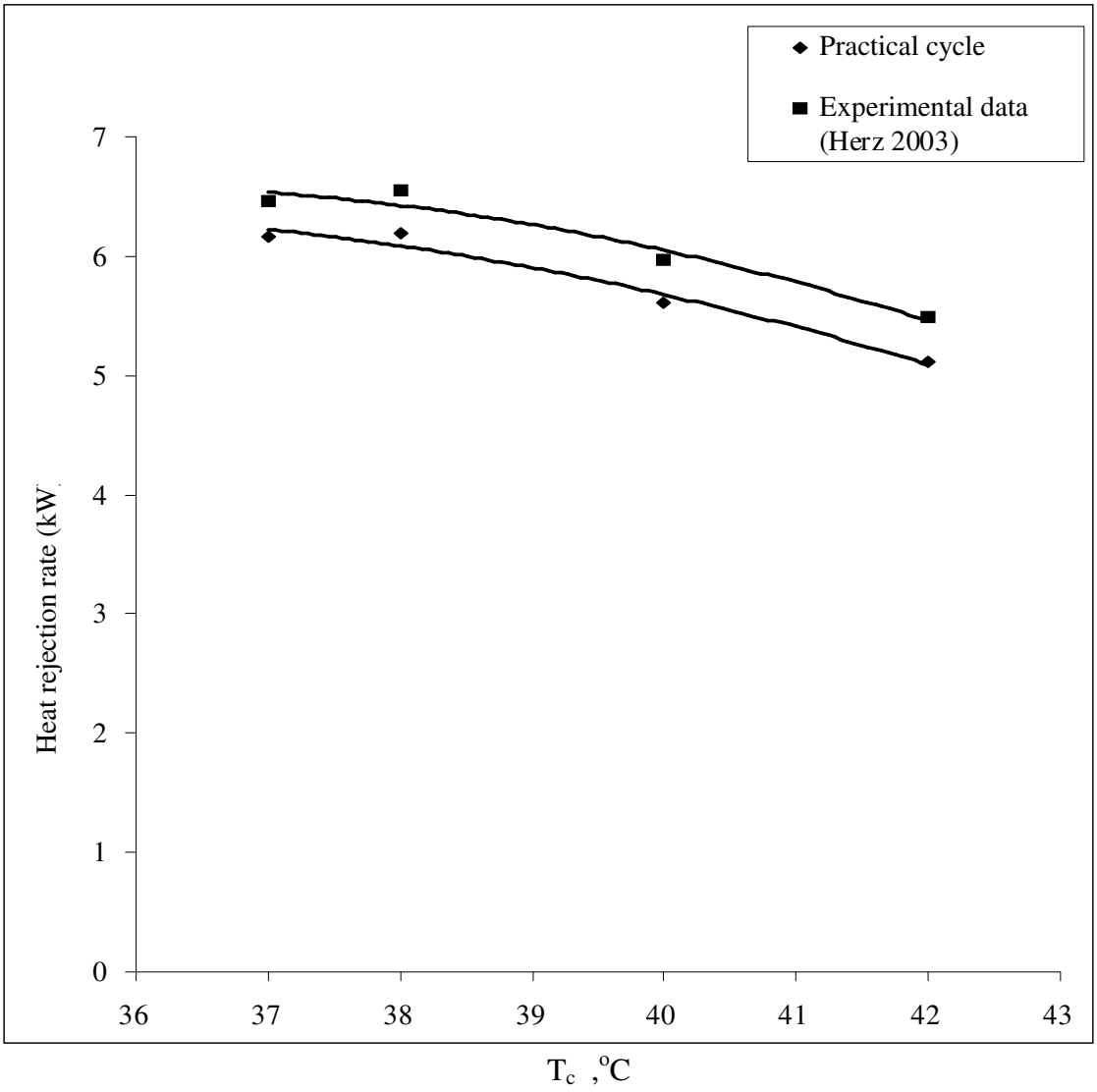

Fig (48) Variation of heat rejection rate versus T_c at T_e = 12 °C

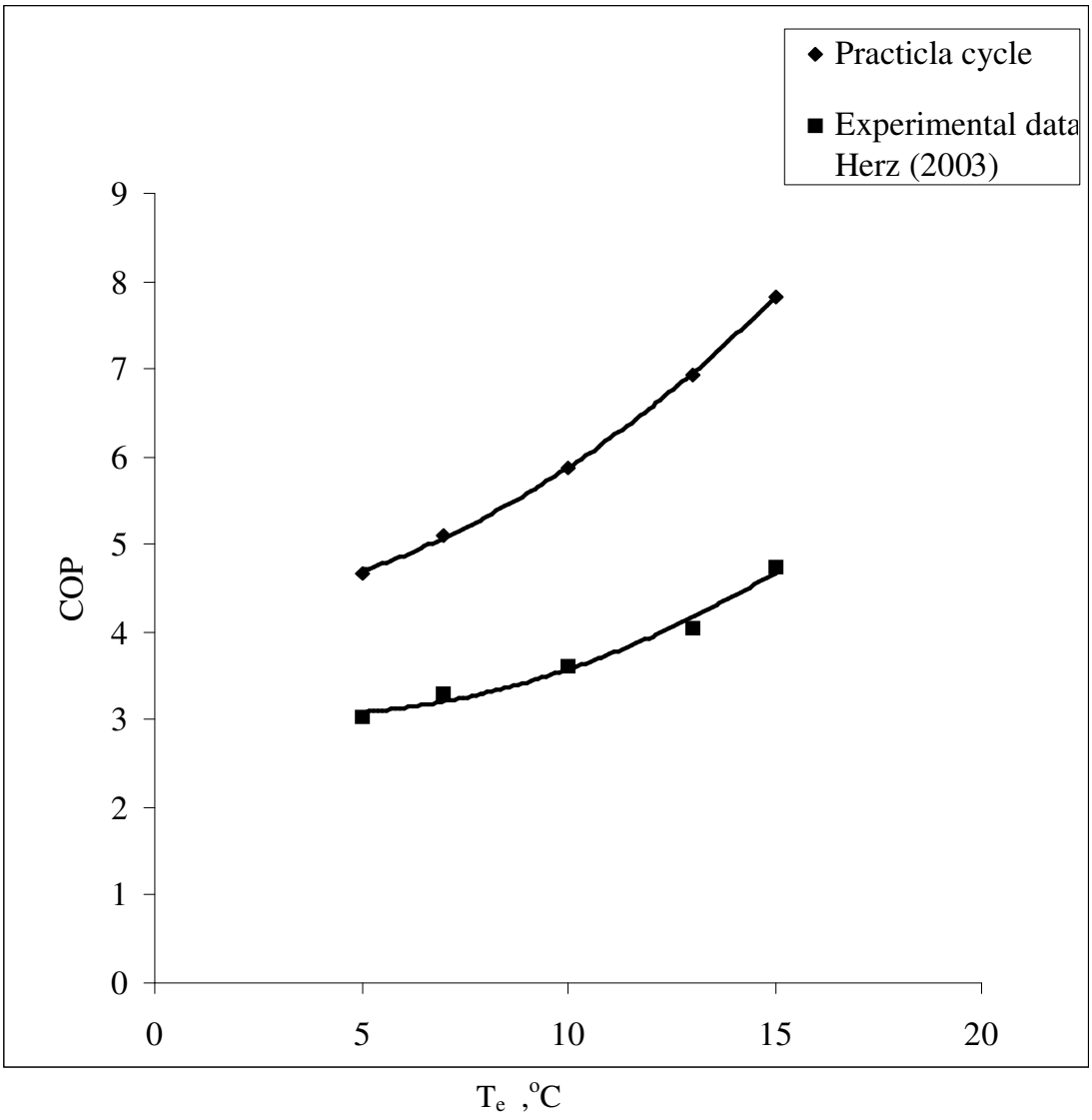

Fig (49) Variation of coefficient of performance versus T_e at T_c = 40 °C

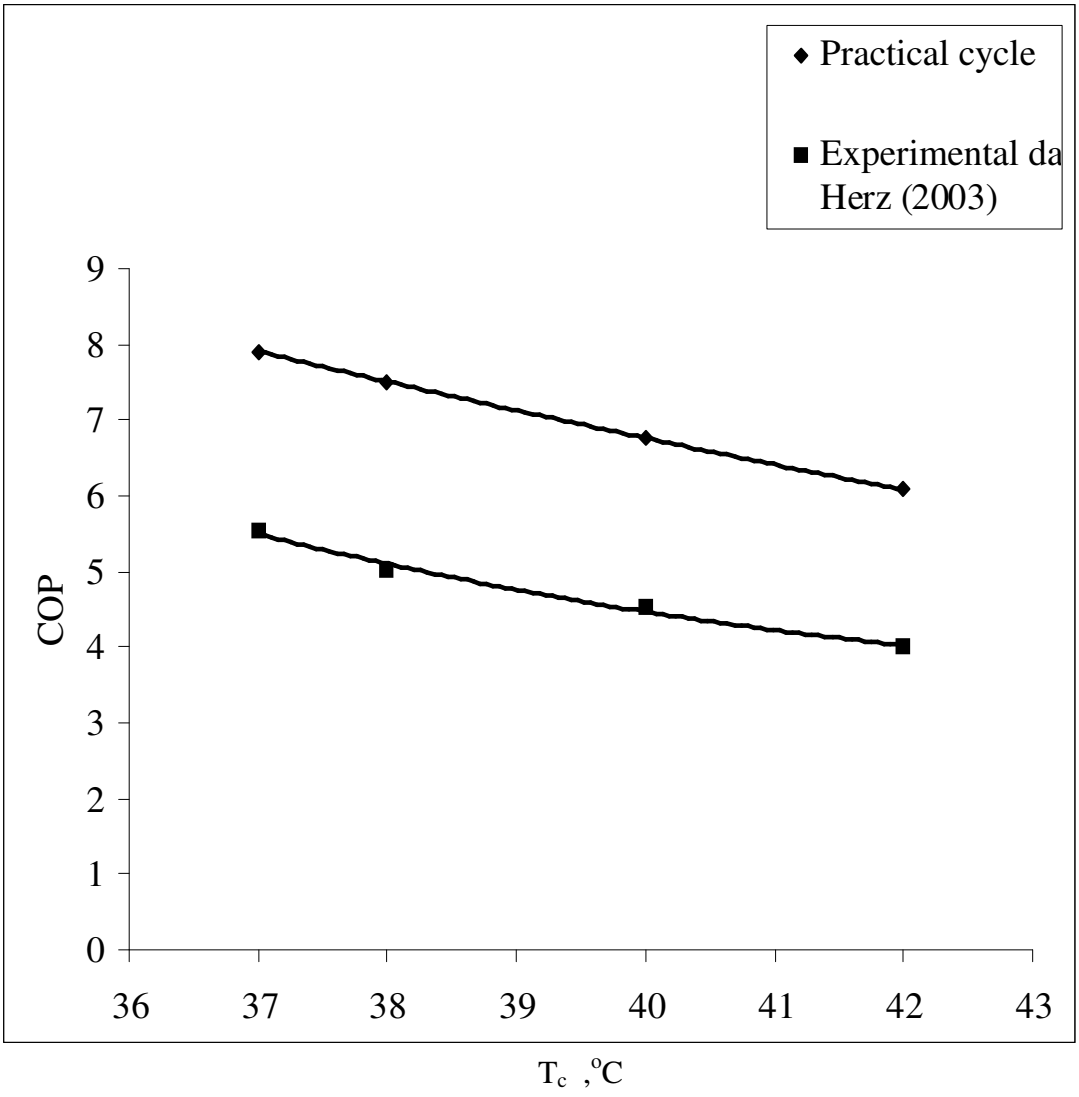

Fig (50) Variation of coefficient of performance versus T_c at T_e = 12 °C

CONCLUSIONS AND RECOMMENDATIONS

1- General

In this work, a simulation program was used to study the performance parameters for a window type air conditioning unit when using R407c as an alternative refrigerant to R22. A performanc comparison between R407c and R22 was carried out using a simulation program for standard, ideal and practical cycles.

2- Conclusions

The following conclusions are obtained:

1- The mass flow rate of refrigerant R407c is equal to 0.0062 (kg/s) at T_e = 10 ^oC and T_c = 40 ^oC for ideal cycle. This quantity is lower than that of standard cycle by 13.8 % at same T_e and T_c values.

2- The mass flow rate of R407c when replaced by R22 decreased by 14.3 % for standard cycle and by 6.9 % for ideal cycle at T_e = 10 ^oC and T_c = 40 ^oC.

3- The mas flow rate of practical cycle is higher than that of experimental results by 7.7 % at T_e = 10 ^oC and T_c = 40 ^oC.

4- The compressor power variation over the evaporating temperature range from –10^oC to 15 ^oC at T_c = 40 ^oC is decreased by 60 % for standard cycle and by 64 % for ideal cycle. The compressor power variation over the condensing temperature range from 30 ^oC to 50 ^oC at T_e = 10 ^oC is increased by 79.1 % for standard cycle and by 66.9% for ideal cycle.

5- The coefficient of performance of the standard cycle increased from 3.24 to 8.09 when T_e increased from -10 ^oC to 15 ^oC, and for ideal cycle increased from 3.31 to 9.21 at T_c= 40 ^oC. On the other hand, the COP of the standard cylce decreased from

11.70 to 2.45 when T_c increased from 30 ^oC to 50 ^oC, and for ideal cycle decreases from 11.60 to 3.84 at T_e = 10 ^oC.

6- The coefficient of performance of R407c is equal to 6.9 for ideal cycle with 5 ^oC superheating and sub-cooling which is higher than that of standard cycle by 6.4 % at T_e = 10 ^oC and T_c = 40 ^oC.

7- The coefficient of performance of R407c at T_e = 10 ^oC and T_c = 40 ^oC reached a value that is 81.6% of that of R22 for standard cycle and 84.2 % for ideal cycle with 5 ^oC superheating and sub-cooling.

8- The variation of COP with T_e and T_c for the practical cycle obtained by simulation program was compared with that of the experimental results; the same trend was observed. The COP values of both cycles at T_e = 12 ^oC and T_c = 40 ^oC are approximately 6.6 and 4.2, respectively. This indicates that the COP value of experimental cycle is lower than that of the practical one by 57.1 %.

9- Based on the above conclusions, the simulation model can be used in testing refrigeration systems using the refrigerant under study with different conditions, which means that the cost of using laboratory equipment for experimental tests and effort can be reduced.

10- The previous results show that refrigerant R407c is a suitable replacement for R 22 in window type air conditioning units for T_c range from 30 to 40 ^oC and T_e range form 0 to 15 ^oC.

3- Recommendations

1- The suitability of other alternative refrigerants can be tested using the simulation computer method.

2- The computer simulation method can be used to determine the variation of the performance parameters of other refrigeration systems.

REFERENCES

American Society of Heating, Refrigeration and Air Conditioning Engineers, (1993). **ASHRAE Handbook of Fundamentals**. Atlanta.

Burke, M., Carre, S. and Kruse, H. (1994). Oil behavior of the HFC R32, R125, R134a and their mixtures. **Proceedings of Refrigeration Science and Technology (The Day after)**. VDI, Berichte, Italy, 223-230.

Corr, S., Murphy, F.T. and Wilkinson, S. (1994). **Composition shifts of zeotropic HFC refrigerants in service**. ASHRAE Transactions. 100(2): 538-545.

Dawood, W.K. (2001). **Performance study of a 20-Ton chiller when using R407c as a replacement to R22**. Unpublished M.Sc. Thesis, University of Jordan, Amman, Jordan.

Douglass, J.D., Braun, J.E., Groll, E.A. and Tree, D.R. (1991). A cost based method for comparing alternative refrigerants applied to R-22 system. **International Journal of Refrigeration**, 22, 107-125.

German Compressor Manufacturing Company (BITZER). (1998). **Substitute for R22**. (BITZER Publication). Kuhlmachineebau Gmbh, Germany.

German Compressor Manufacturing Company (BITZER). (1999). **Refrigerant Report No.5**. (BITZER Publication). Kuhlmachineebau Gmbh, Germany.

Herz, A.K. (2003). **Performance study of Window-Type Air Conditioning Unit Using R-407c as an Alternative Refrigerant.** Unpublished M.Sc. Thesis, University of Jordan, Amman, Jordan.

Mongey, B., Hewitt, N.J. and McMullan, J.T. (1996). R407c as an alternative to R22 in refrigeration systems. **International Journal of Energy Research.** 20 (3), 245-254.

Pananonda, D. (1998). **The performance study of a refrigeration system by comparison of theory and experiments between refrigerants HCFC22 and HFC407c.** Thesis. Central Library of KMITNB.

Sleiti A.K. (2001). **Development of a computer simulation program to study the performance of A/C split units working on R-407c**. Unpublished M.Sc. Thesis, University of Jordan, Amman, Jordan.

Stoecker, W., and Jones, J. (1987). **Refrigeration and Air conditioning**, (2nd ed.). New York: McGraw-Hill.

The American Society of Mechanical Engineers. (1998). **Choosing the right refrigerant.** New York.

Wylen, G.J., Sonntag, R.E. and Borgnakke, C. (1994). **Fundamentals of Classical thermodynamics**, (4th ed.). New York: John Wiley and Sons.

APPENDIX A

COMPUTER PROGRAM CODES

******** Main Program ********

This program is designed to calculate performance parameters for constant condensing temperature and variable evaporating temperature.

% T_c = 30 ^oC

T_c = input (' Enter the value of evaporator temperature Te = ');
T11 = T_e;
T_c = input (' Enter the value of condenser temperature Tc = ');
dosh = input (' Enter the degree of superheating dosh = ');
dosc = input (' Enter the degree of sub-cooling dosc = ');

```
% Standard cycle

T11=Te;
P11=451.9+15.81*(T11)+0.215*(T11)^2+(1.3*10^-   3)*(T11)^3;
h11=384.9+0.1001*(P11)-(9.579*10^-5)*(P11)^2+(3.742*10^-
8)*(P11)^3;
T21=38.83-0.3272*T11;
h21=436.9-0.3137*T11;
T41=30;
P41=560.2+18.19*T41+0.2247*(T41^2)+(1.179*10^-3)*(T41^3);
h41=132.2+0.1739*(P41)-(1.148*10^-4)*(P41)^2+(3.723*10^-
8)*(P41)^3;
h51=h41;
%Refrigeration capacity = 1 kW
mfr11=1/(h11-h51);
woc11=mfr11*(h21-h11);
hrr11=mfr11*(h21-h41);
```

```
COP11=(h11-h51)/(h21-h11);
Tcompout11=T21;
[T11;mfr11;woc11;hrr11;COP11;Tcompout11]'

% Ideal cycle with superheating and sub-cooling

T11i=Te;
T21i=T11i+dosh;
P21i=451.9+15.81*T11i+0.215*(T11i^2)+(1.3*10^-3)*(T11i^3);
B01i=416.1-(1.25*10^-2)*P21i;
B11i=0.8126+(2*10^-4)*P21i;
h21i=B01i+B11i*T21i;
h3s1i=440.6-(0.3072)*T11i;
T3s1i=41.89-(0.3211)*T11i;
h31i=h21i+((h3s1i-h21i)/Iseff);
T31i=46.59-0.5122*T11i;
T51i=30;
T61i=T51i-dosc;
P61i=560.2+18.19*T61i+0.2247*(T61i^2)+(1.179*10^-
3)*(T61i^3);
h61i=132.2+0.1739*P61i-(1.148*10^-4)*(P61i^2)+(3.723*10^-
8)*(P61i^3);
h71i=h61i;
%Refrigeration capacity = 1 kW
mfr11i=1/(h21i-h71i);
woc11i=mfr11i*(h3s1i-h21i);
hrr11i=mfr11i*(h3s1i-h61i);
COP11i=(h21i-h71i)/(h3s1i-h21i);
Tcompout11i=T3s1i;
[T11i;mfr11i;woc11i;hrr11i;COP11i;Tcompout11i]'
```

The program is repeated for T_c =35, 40, 45 and 50 °C.

This program is developed to calculate performance parameters for constant evaporating temperature and variable condensing temperature.

% T_e = -10 °C

T_e = input (' Enter the value of evaporator temperature Te = ');
T11 = T_e;
T_c = input (' Enter the value of condenser temperature Tc = ');
dosh = input (' Enter the degree of superheating dosh = ');
dosc = input (' Enter the degree of sub-cooling dosc = ');

```
% Standard cycle

Te = -10;
dosh=5;
dosc=5;
Iseff=0.85;

% Standard cycle

Tc1=i+29;
T41=Tc1;      P41=560.2+18.19*T41+0.2247*(T41^2)+(1.179*10^-
3)*(T41^3);
h41=132.2+0.1739*P41-(1.148*10^-4)*(P41^2)+(3.723*10^-
8)*(P41^3);
h51=h41;
P21=451.9+15.81*T41+0.215*(T41^2)+(1.3*10^-3)*(T41^3);
T21=5.44+1.224*Tc1;
h21=419.6+0.6888*Tc1;
T11=-10;
P11=451.9+15.81*T11+0.215*(T11^2)+(1.3*10^-3)*(T11^3);
h11=384.9+0.1001*P11-(9.58*10^-5)*(P11^2)+(3.742*10^-
8)*(P11^3);
%Refrigeration capacity = 1 kW
mfr11=1/(h11-h51);
woc11=mfr11*(h21-h11);
```

```
hrr11=mfr11*(h21-h41);
COP11=(h11-h51)/(h21-h11);
Tcompout11=T21;
[T41;mfr11;woc11;hrr11;COP11;Tcompout11]'

% Ideal cycle with superheating and sub-cooling

Tc1i=i+29;
T51i=Tc1i;
T61i=T51i-dosc;
P61i=560.2+18.19*T61i+0.2247*(T61i^2)+(1.179*10^-
3)*(T61i^3);
h61i=132.2+0.1739*P61i-(1.148*10^-4)*(P61i^2)+(3.723*10^-
8)*(P61i^3);
h71i=h61i;
T41i=Tc1i;
P41i=451.9+15.81*T41i+0.215*(T41i^2)+(1.3*10^-3)*(T41i^3);
T31i=12.86+1.349*Tc1i;
h31i=425.7+0.8378*Tc1i;
h3s1i=422.9+0.7152*Tc1i;
T3s1i=7.135+1.294*Tc1i;
h21i=6.66*h3s1i-5.66*h31i;
%Refrigeration capacity = 1 kW
mfr11i=1/(h21i-h71i);
woc11i=mfr11i*(h3s1i-h21i);
hrr11i=mfr11i*(h3s1i-h61i);
COP11i=(h21i-h71i)/(h3s1i-h21i);
Tcompout11i=T3s1i;
[T51i;mfr11i;woc11i;hrr11i;COP11i;Tcompout11i]'
```

The program is repeated for T_e =-5,0,5,10 and 15 °C.

******** Simulation Program ********

```
%This program is constructed to calculate performance
parameters for constant condensing temperature and variable
evaporating temperature

% Tc=30 °C;  % Condenser temperature

dosh=5;       % Degree of superheating
dosc=5;       % Degree of sub-cooling
Iseff=0.85;   % Isentropic efficiency

% Standard cycle

for i=1:1:26;
   Te1(i)=i-11;
T11(i)=Te1(i);
P11(i)=451.9+15.81*(T11(i))+0.215*(T11(i))^2+(1.3*10^-
3)*(T11(i))^3;
h11(i)=384.9+0.1001*(P11(i))-(9.579*10^-
5)*(P11(i))^2+(3.742*10^-8)*(P11(i))^3;
T21(i)=38.83-0.3272*T11(i);
h21(i)=436.9-0.3137*T11(i);
T41(i)=30;
P41(i)=560.2+18.19*T41(i)+0.2247*(T41(i)^2)+(1.179*10^-
3)*(T41(i)^3);
h41(i)=132.2+0.1739*(P41(i))-(1.148*10^-
4)*(P41(i))^2+(3.723*10^-8)*(P41(i))^3;
h51(i)=h41(i);
%Refrigeration capacity = 1 KW
mfr11s1(i)=1/(h11(i)-h51(i));
woc11s1(i)=mfr11(i)*(h21(i)-h11(i));
hrr11s1(i)=mfr11(i)*(h21(i)-h41(i));
COP11s1(i)=(h11(i)-h51(i))/(h21(i)-h11(i));
Tcompout11s1(i)=T21(i);
```

```
[COP11s1,COP12s1,COP13s1,COP14s1,COP15s1]'
plot(T11,COP11,'+',T12,COP12,'r',T13,COP13,'g',T14,COP14,'b
',T15,COP15,*,);
xlabel('Te  (°C)')
ylabel('COP')
```

The program is repeated for T_c = 35, 40, 45 and 50 °C.

```
% This program is designed to calculate performance
parameters for constant evaporating temperature and
variable condensing temperature

Te=-10 °C;          % Evaporating temperature

dosh=5;             % Degree of superheating
dosc=5;             % Degree of sub-cooling
Iseff=0.85;         % Isentropic efficiency

% Standard cycle

for i=1:1:21;
Tc1(i)=i+29;
T41(i)=Tc1(i);
P41(i)=560.2+18.19*T41(i)+0.2247*(T41(i)^2)+(1.179*10^-
3)*(T41(i)^3);
h41(i)=132.2+0.1739*P41(i)-(1.148*10^-
4)*(P41(i)^2)+(3.723*10^-8)*(P41(i)^3);
h51(i)=h41(i);
P21(i)=451.9+15.81*T41(i)+0.215*(T41(i)^2)+(1.3*10^-
3)*(T41(i)^3);
T21(i)=5.44+1.224*Tc1(i);
h21(i)=419.6+0.6888*Tc1(i);
```

```
T11(i)=-10;
P11(i)=451.9+15.81*T11(i)+0.215*(T11(i)^2)+(1.3*10^-
3)*(T11(i)^3);
h11(i)=384.9+0.1001*P11(i)-(9.58*10^-
5)*(P11(i)^2)+(3.742*10^-8)*(P11(i)^3);
%Refrigeration capacity = 1kw
mfr11s2(i)=1/(h11(i)-h51(i));
woc11s2(i)=mfr11(i)*(h21(i)-h11(i));
hrr11s2(i)=mfr11(i)*(h21(i)-h41(i));
COP11s2(i)=(h11(i)-h51(i))/(h21(i)-h11(i));
Tcompout11s2(i)=T21(i);

[COP11s2,COP12s2,COP32s2,COP14s2,COP15s2,COP16s2]'
plot(Tc1,COP11s2,'+',Tc2,COP12s2,'r',Tc3,COP13s2,'g',Tc4,CO
P14s2,'b',Tc5,COP15s2,'y',Tc6,COP16,'*');

xlabel('Tc  (°C)')
ylabel('COP')
```

The program is repeated for T_e = -5,0,5,10 and 15 °C.

```
% This program is developed to calculate performance
parameters for constant condensing temperature and variable
evaporating temperature

Tc=30 °C;          % Condensing temperature

dosh=5;            % Degree of superheating
dosc=5;            % Degree of sub-cooling
Iseff=0.85;        % Isentropic efficiency

% Ideal cycle with superheating and sub-cooling

for i=1:1:26;
```

```
Te11(i)=i-11;
T11(i)=Te11(i);
T21(i)=T11(i)+dosh;
   P21(i)=451.9+15.81*T11(i)+0.215*(T11(i)^2)+(1.3*10^-
3)*(T11(i)^3);
B01(i)=416.1-(1.25*10^-2)*P21(i);
B11(i)=0.8126+(2*10^-4)*P21(i);
h21(i)=B01(i)+B11(i)*T21(i);
h3s1(i)=440.6-(0.3072)*T11(i);
T3s1(i)=41.89-(0.3211)*T11(i);
h31(i)=h21(i)+((h3s1(i)-h21(i))/Iseff);
T31(i)=46.59-0.5122*T11(i);
T51(i)=30;
T61(i)=T51(i)-dosc;
P61(i)=560.2+18.19*T61(i)+0.2247*(T61(i)^2)+(1.179*10^-
3)*(T61(i)^3);
h61(i)=132.2+0.1739*P61(i)-(1.148*10^-
4)*(P61(i)^2)+(3.723*10^-8)*(P61(i)^3);
h71(i)=h61(i);
%Refrigeration capacity = 1 kw
mfr11i1(i)=1/(h21(i)-h71(i));
woc11i1(i)=mfr11(i)*(h3s1(i)-h21(i));
hrr11i1(i)=mfr11(i)*(h3s1(i)-h61(i));
COP11i1(i)=(h21(i)-h71(i))/(h3s1(i)-h21(i));
Tcompout11i1(i)=T3s1(i);

[COP11i1.COP12i1,COP13i1,COP14i1,COP15i1]'
plot(Te11,COP11i1,'+',Te12,COP12i1,'r',Te13,COP13i1,'g',Te1
4,COP14i1,'b',Te15,COP15i1,'+');

xlabel(' Te  (°C)')

ylabel('COP')
```

The program is repeated for T_c = 35,40,45 and 50 °C.

```
% This program is designed to calculate performance
parameters for constant evaporating temperature and
variable condensing temperature

Te=-10 °C;          % Evaporating temperature

dosh=5;             % Degree of superheating
dosc=5;             % Degree of sub-cooling
Iseff=0.85;         % Isentropic efficiency

% Ideal cycle with superheating and sub-cooling

for i=1:1:21;

Tc1(i)=i+29;
T51(i)=Tc1(i);
T61(i)=T51(i)-dosc;
P61(i)=560.2+18.19*T61(i)+0.2247*(T61(i)^2)+(1.179*10^-
3)*(T61(i)^3);
h61(i)=132.2+0.1739*P61(i)-(1.148*10^-
4)*(P61(i)^2)+(3.723*10^-8)*(P61(i)^3);
h71(i)=h61(i);
T41(i)=Tc1(i);
P41(i)=451.9+15.81*T41(i)+0.215*(T41(i)^2)+(1.3*10^-
3)*(T41(i)^3);
T31(i)=12.86+1.349*Tc1(i);
h31(i)=425.7+0.8378*Tc1(i);
h3s1(i)=422.9+0.7152*Tc1(i);
T3s1(i)=7.135+1.294*Tc1(i);
```

```
h21(i)=6.66*h3s1(i)-5.66*h31(i);
%Refrigeration capacity= 1kw
mfr11i2(i)=1/(h21(i)-h71(i));
woc11i2(i)=mfr11(i)*(h3s1(i)-h21(i));
hrr11i2(i)=mfr11(i)*(h3s1(i)-h61(i));
COP11i2(i)=(h21(i)-h71(i))/(h3s1(i)-h21(i));
Tcompout11i2(i)=T3s1(i);

[COP11i2,COP12i2,COP13i2,COP14i2,COP15i2,COP16i2]'

plot(Tc1,COP11i2,'+',Tc2,COP12i2,'r',Tc3,COP13i2,'g',Tc4,CO
P14i2,'b',Tc5,COP15i2,'y',Tc6,COP16i2,'*]

xlabel(' Tc (°C)')
ylabel('COP ')
```

The program is repeated for T_e = -5,0,5,10 and 15 °C.

******** Comparison Programs ********

(1)

```
%This program is designed to compare performance parameters
between the standard and ideal cycles for constant
condensing temperature Tc = 40 °C, and variable evaporating
temperatures.

% Tc=40 °C;

dosh=5;
dosc=5;
Iseff=0.85;

% standard cycle

for i=1:1:26;
   Te3(i)=i-11;
T13(i)=Te3(i);
P13(i)=451.9+15.81*(T13(i))+0.215*(T13(i))^2+(1.3*10^-
3)*(T13(i))^3;
h13(i)=384.9+0.1001*(P13(i))-(9.579*10^-
5)*(P13(i))^2+(3.742*10^-8)*(P13(i))^3;
T23(i)=51.32-0.3198*T13(i);
h23(i)=443.9-0.3223*T13(i);
T43(i)=40;
P43(i)=560.2+18.19*T43(i)+0.2247*(T43(i)^2)+(1.179*10^-
3)*(T43(i)^3);
h43(i)=132.2+0.1739*(P43(i))-(1.148*10^-
4)*(P43(i))^2+(3.723*10^-8)*(P43(i))^3;
h53(i)=h43(i);
%Refrigeration capacity = 1 KW
mfr13s(i)=1/(h13(i)-h53(i));
woc13s(i)=mfr13(i)*(h23(i)-h13(i));
hrr13s(i)=mfr13(i)*(h23(i)-h43(i));
```

```
COP13s(i)=(h13(i)-h53(i))/(h23(i)-h13(i));
Tcompout13s(i)=T23(i);


% Ideal cycle with superheating and sub-cooling


Te3(i)=i-11;
T13(i)=Te3(i);
T23(i)=T13(i)+dosh;
P23(i)=451.9+15.81*T13(i)+0.215*(T13(i)^2)+(1.3*10^-
3)*(T13(i)^3);
B03(i)=416.1-(1.25*10^-2)*P23(i);
B13(i)=0.8126+(2*10^-4)*P23(i);
h23(i)=B03(i)+B13(i)*T23(i);
h3s3(i)=448.6-(0.3185)*T13(i);
T3s3(i)=56.24-(0.3149)*T13(i);
h33(i)=h23(i)+((h3s3(i)-h23(i))/Iseff);
T33(i)=62.1-0.4979*T13(i);
T53(i)=40;
T63(i)=T53(i)-dosc;
P63(i)=560.2+18.19*T63(i)+0.2247*(T63(i)^2)+(1.179*10^-
3)*(T63(i)^3);
h63(i)=132.2+0.1739*P63(i)-(1.148*10^-
4)*(P63(i)^2)+(3.723*10^-8)*(P63(i)^3);
h73(i)=h63(i);
%Refrigeration capacity = 1 kw
mfr13i(i)=1/(h23(i)-h73(i));
woc13i(i)=mfr13(i)*(h3s3(i)-h23(i));
hrr13i(i)=mfr13(i)*(h3s3(i)-h63(i));
COP13i(i)=(h23(i)-h73(i))/(h3s3(i)-h23(i));
Tcompout13i(i)=T3s3(i);

end;
```

```
[COP13s,COP13i]'
plot(Te3,COP13s,'+',Te3,COP13I,'*')

xlabel('Te (°C)')
ylabel('COP')


%This program is designed to compare performance parameters
between standard and ideal cycles for constant evaporating
temperature Te = 10 °C, and variable condensing
temperatures.

% Te=10 °C;

dosh=5;
dosc=5;
Iseff=0.85;

% Standard cycle

for i=1:1:21;
Tc5(i)=i+29;
T45(i)=Tc5(i);
P45(i)=560.2+18.19*T45(i)+0.2247*(T45(i)^2)+(1.179*10^-
3)*(T45(i)^3);
h45(i)=132.2+0.1739*P45(i)-(1.148*10^-
4)*(P45(i)^2)+(3.723*10^-8)*(P45(i)^3);
h55(i)=h45(i);
P25(i)=451.9+15.81*T45(i)+0.215*(T45(i)^2)+(1.3*10^-
3)*(T45(i)^3);
T25(i)=-1.73+1.239*Tc5(i);
h25(i)=414+0.6649*Tc5(i);
T15(i)=10;
```

```
P15(i)=451.9+15.81*T15(i)+0.215*(T15(i)^2)+(1.3*10^-
3)*(T15(i)^3);
h15(i)=384.9+0.1001*P15(i)-(9.58*10^-
5)*(P15(i)^2)+(3.742*10^-8)*(P15(i)^3);
%Refrigeration capacity= 1kw
mfr15s(i)=1/(h15(i)-h55(i));
woc15s(i)=mfr15(i)*(h25(i)-h15(i));
hrr15s(i)=mfr15(i)*(h25(i)-h45(i));
COP15s(i)=(h15(i)-h55(i))/(h25(i)-h15(i));
Tcompout15s(i)=T25(i);


% Ideal cycle with superheating and sub-cooling

Tc5(i)=i+29;
T55(i)=Tc5(i);
T65(i)=T55(i)-dosc;
P65(i)=560.2+18.19*T65(i)+0.2247*(T65(i)^2)+(1.179*10^-
3)*(T65(i)^3);
h65(i)=132.2+0.1739*P65(i)-(1.148*10^-
4)*(P65(i)^2)+(3.723*10^-8)*(P65(i)^3);
h75(i)=h65(i);
T45(i)=Tc5(i);
P45(i)=451.9+15.81*T45(i)+0.215*(T45(i)^2)+(1.3*10^-
3)*(T45(i)^3);
T35(i)=1.372+1.386*Tc5(i);
h35(i)=416.5+0.8134*Tc5(i);
h3s5(i)=417.3+0.6934*Tc5(i);
T3s5(i)=0.2090+1.308*Tc5(i);
h25(i)=6.66*h3s5(i)-5.66*h35(i);
%Refrigeration capacity= 1kw
mfr15i(i)=1/(h25(i)-h75(i));
woc15i(i)=mfr15(i)*(h3s5(i)-h25(i));
hrr15i(i)=mfr15(i)*(h3s5(i)-h65(i));
```

```
COP15i(i)=(h25(i)-h75(i))/(h3s5(i)-h25(i));
Tcompout15i(i)=T3s5(i);
end;

[COP15s,COP15i]'
plot(Tc5,COP15s,'+',Tc5,COP15i,'*')

xlabel('Tc (°C)')
ylabel('COP')
```

(2)

```
%This program is designed to compare performance parameters
for standard cycle between R407c and R22at constant
condensing temperature Tc = 40 °C and variable evaporating
temperatures.

% R407c performance parameters

% Tc=40 °C;

dosh=5;
dosc=5;
Iseff=0.85;

for i=1:1:26;
   Te3(i)=i-11;
T13(i)=Te3(i);
P13(i)=451.9+15.81*(T13(i))+0.215*(T13(i))^2+(1.3*10^-
3)*(T13(i))^3;
h13(i)=384.9+0.1001*(P13(i))-(9.579*10^-
5)*(P13(i))^2+(3.742*10^-8)*(P13(i))^3;
```

```
T23(i)=51.32-0.3198*T13(i);
h23(i)=443.9-0.3223*T13(i);
T43(i)=40;
P43(i)=560.2+18.19*T43(i)+0.2247*(T43(i)^2)+(1.179*10^-
3)*(T43(i)^3);
h43(i)=132.2+0.1739*(P43(i))-(1.148*10^-
4)*(P43(i))^2+(3.723*10^-8)*(P43(i))^3;
h53(i)=h43(i);
%Refrigeration capacity = 1 KW
mfr13(i)=1/(h13(i)-h53(i));
woc13(i)=mfr13(i)*(h23(i)-h13(i));
hrr13(i)=mfr13(i)*(h23(i)-h43(i));
COP13(i)=(h13(i)-h53(i))/(h23(i)-h13(i));
Tcompout13(i)=T23(i);
end;
[T13;mfr13;woc13;hrr13;COP13;Tcompout13]';
plot(T13,COP13,'+')

hold on

% R22 performance parameters

% Tc=40 ºC;

dosh=5;
dosc=5;
Iseff=0.85;

for i=1:1:26;
   Te322(i)=i-11;
T1322(i)=Te322(i);
P1322(i)=497.7+16.21*(T1322(i))+0.1967*(T1322(i))^2+(1.135*
10^-3)*(T1322(i))^3;
```

```
h1322(i)=249.9+0.365*(T1322(i))-(1.448*10^-3)*(T1322(i))^2-
(1.695*10^-5)*(T1322(i))^3;
T2322(i)=58.64-0.5365*T1322(i);
h2322(i)=278.2-0.4754*T1322(i);
T4322(i)=40;
h4322(i)=44.6+1.172*(T4322(i))+(1.339*10^-
3)*(T4322(i))^2+(1.023*10^-5)*(T4322(i))^3;
h5322(i)=h4322(i);
%Refrigeration capacity = 1 KW
mfr1322(i)=1/(h1322(i)-h5322(i));
woc1322(i)=mfr1322(i)*(h2322(i)-h1322(i));
hrr1322(i)=mfr1322(i)*(h2322(i)-h4322(i));
COP1322(i)=(h1322(i)-h5322(i))/(h2322(i)-h1322(i));
Tcompout1322(i)=T2322(i);

end;

[T1322;mfr1322;woc1322;hrr1322;COP1322;Tcompout1322]';

plot(T1322,COP1322,'*')

hold off

xlabel('Te (°C)')
ylabel('COP')



%This program is designed to compare performance parameters
for ideal cycle between R407c and R22 at constant
condensing temperature Tc = 40 °C and variable evaporating
temperatures.
```

```
% R407c performance parameters

% Tc=40 ºC;

dosh=5;
dosc=5;
Iseff=0.85;

for i=1:1:26;
Te13(i)=i-11;
T13(i)=Te13(i);
T23(i)=T13(i)+dosh;
P23(i)=451.9+15.81*T13(i)+0.215*(T13(i)^2)+(1.3*10^-
3)*(T13(i)^3);
B03(i)=416.1-(1.25*10^-2)*P23(i);
B13(i)=0.8126+(2*10^-4)*P23(i);
h23(i)=B03(i)+B13(i)*T23(i);
h3s3(i)=448.6-(0.3185)*T13(i);
T3s3(i)=56.24-(0.3149)*T13(i);
h33(i)=h23(i)+((h3s3(i)-h23(i))/Iseff);
T33(i)=62.1-0.4979*T13(i);
T53(i)=40;
T63(i)=T53(i)-dosc;
P63(i)=560.2+18.19*T63(i)+0.2247*(T63(i)^2)+(1.179*10^-
3)*(T63(i)^3);
h63(i)=132.2+0.1739*P63(i)-(1.148*10^-
4)*(P63(i)^2)+(3.723*10^-8)*(P63(i)^3);
h73(i)=h63(i);
%Refrigeration capacity = 1 kw
mfr13(i)=1/(h23(i)-h73(i));
woc13(i)=mfr13(i)*(h3s3(i)-h23(i));
hrr13(i)=mfr13(i)*(h3s3(i)-h63(i));
COP13(i)=(h23(i)-h73(i))/(h3s3(i)-h23(i));
Tcompout13(i)=T3s3(i);
```

```
end;

[T13;mfr13;woc13;hrr13;COP13;Tcompout13]';

plot(T13,COP13,'+')

hold on

% R22 performance parameters

% Tc=40 ºC;

dosh=5;
dosc=5;
Iseff=0.85;

for i=1:1:26;
Te1322(i)=i-11;
T1322(i)=Te1322(i);
T2322(i)=T1322(i)+dosh;
P2322(i)=497.7+16.21*T1322(i)+0.1967*(T1322(i)^2)+(1.135*10
^-3)*(T1322(i)^3);
B0322(i)=252.9-(5.1*10^-3)*P2322(i);
B1322(i)=0.6889+(5.85*10^-5)*P2322(i);
h2322(i)=B0322(i)+B1322(i)*T2322(i);
h3s322(i)=283-(0.1634)*T1322(i);
T3s322(i)=64.17-(0.1855)*T1322(i);
h3322(i)=h2322(i)+((h3s322(i)-h2322(i))/Iseff);
T3322(i)=70.12-0.355*T1322(i);
T5322(i)=40;
T6322(i)=T5322(i)-dosc;
h6322(i)=44.6+1.172*T6322(i)+(1.339*10^-
3)*(T6322(i)^2)+(1.023*10^-5)*(T6322(i)^3);
h7322(i)=h6322(i);
```

```
%Refrigeration capacity = 1 kw
mfr1322(i)=1/(h2322(i)-h7322(i));
woc1322(i)=mfr1322(i)*(h3s322(i)-h2322(i));
hrr1322(i)=mfr1322(i)*(h3s322(i)-h6322(i));
COP1322(i)=(h2322(i)-h7322(i))/(h3s322(i)-h2322(i));
Tcompout1322(i)=T3s322(i);
end;

[T1322;mfr1322;woc1322;hrr1322;COP1322;Tcompout1322]';

plot(T1322,COP1322,'*')

hold off

xlabel('Te (°C)')
ylabel('COP')



%This program is designed to compare performance parameters
for standard cycle between R407c and R22 at constant
evaporating temperature Te = 10 °C and variable condensing
temperatures.

% R407c performance parameters

% Te=10 °C;

dosh=5;
dosc=5;
Iseff=0.85;

for i=1:1:21;
Tc5(i)=i+29;
```

```
T45(i)=Tc5(i);
P45(i)=560.2+18.19*T45(i)+0.2247*(T45(i)^2)+(1.179*10^-
3)*(T45(i)^3);
h45(i)=132.2+0.1739*P45(i)-(1.148*10^-
4)*(P45(i)^2)+(3.723*10^-8)*(P45(i)^3);
h55(i)=h45(i);
P25(i)=451.9+15.81*T45(i)+0.215*(T45(i)^2)+(1.3*10^-
3)*(T45(i)^3);
T25(i)=-1.73+1.239*Tc5(i);
h25(i)=414+0.6649*Tc5(i);
T15(i)=10;
P15(i)=451.9+15.81*T15(i)+0.215*(T15(i)^2)+(1.3*10^-
3)*(T15(i)^3);
h15(i)=384.9+0.1001*P15(i)-(9.58*10^-
5)*(P15(i)^2)+(3.742*10^-8)*(P15(i)^3);
%Refrigeration capacity= 1kw
mfr15(i)=1/(h15(i)-h55(i));
woc15(i)=mfr15(i)*(h25(i)-h15(i));
hrr15(i)=mfr15(i)*(h25(i)-h45(i));
COP15(i)=(h15(i)-h55(i))/(h25(i)-h15(i));
Tcompout15(i)=T25(i);
end;

[T45;mfr15;woc15;hrr15;COP15;Tcompout15]';

plot(T45,COP15,'+')

hold on


% R22 performance parameters

% Te=10 ºC;
```

```
dosh=5;
dosc=5;
Iseff=0.85;

for i=1:1:21;
Tc522(i)=i+29;
T4522(i)=Tc522(i);
P4522(i)=497.7+16.21*T4522(i)+0.1967*(T4522(i)^2)+(1.135*10
^-3)*(T4522(i)^3);
h4522(i)=44.6+1.172*T4522(i)+(1.339*10^-
3)*(T4522(i)^2)+(1.023*10^-5)*(T4522(i)^3);
h5522(i)=h4522(i);
P2522(i)=P4522(i);
T2522(i)=-2.606+1.395*Tc522(i);
h2522(i)=248.5+0.62*Tc522(i);
T1522(i)=10;
h1522(i)=249.9+0.365*T1522(i)-(1.448*10^-3)*(T1522(i)^2)-
(1.695*10^-5)*(T1522(i)^3);
%Refrigeration capacity= 1kw
mfr1522(i)=1/(h1522(i)-h5522(i));
woc1522(i)=mfr1522(i)*(h2522(i)-h1522(i));
hrr1522(i)=mfr1522(i)*(h2522(i)-h4522(i));
COP1522(i)=(h1522(i)-h5522(i))/(h2522(i)-h1522(i));
Tcompout1522(i)=T2522(i);
end;

[T4522;mfr1522;woc1522;hrr1522;COP1522;Tcompout1522]';

plot(T4522,COP1522,'*')

hold off

xlabel('Tc (c)')
ylabel('COP')
```

```
%This program is designed to compare performance parameters
for ideal cycle between R407c and R22 at constant
evaporating temperature Te = 10 °C and variable condensing
temperatures.

% R407c performance parameters

% Te=10 °C;

dosh=5;
dosc=5;
Iseff=0.85;

for i=1:1:21;
Tc5(i)=i+29;
T55(i)=Tc5(i);
T65(i)=T55(i)-dosc;
P65(i)=560.2+18.19*T65(i)+0.2247*(T65(i)^2)+(1.179*10^-
3)*(T65(i)^3);
h65(i)=132.2+0.1739*P65(i)-(1.148*10^-
4)*(P65(i)^2)+(3.723*10^-8)*(P65(i)^3);
h75(i)=h65(i);
T45(i)=Tc5(i);
P45(i)=451.9+15.81*T45(i)+0.215*(T45(i)^2)+(1.3*10^-
3)*(T45(i)^3);
T35(i)=1.372+1.386*Tc5(i);
h35(i)=416.5+0.8134*Tc5(i);
h3s5(i)=417.3+0.6934*Tc5(i);
T3s5(i)=0.2090+1.308*Tc5(i);
h25(i)=6.66*h3s5(i)-5.66*h35(i);
%Refrigeration capacity= 1kw
mfr15(i)=1/(h25(i)-h75(i));
```

```
woc15(i)=mfr15(i)*(h3s5(i)-h25(i));
hrr15(i)=mfr15(i)*(h3s5(i)-h65(i));
COP15(i)=(h25(i)-h75(i))/(h3s5(i)-h25(i));
Tcompout15(i)=T3s5(i);
end;

plot(Tc5,COP15,'+')

hold on

% R22 performance parameters

% Te=10 ℃;

dosh=5;
dosc=5;
Iseff=0.85;

for i=1:1:21;
Tc522(i)=i+29;
T5522(i)=Tc522(i);
T6522(i)=T5522(i)-dosc;
h6522(i)=44.6+1.172*T6522(i)+(1.339*10^-
3)*(T6522(i)^2)+(1.023*10^-5)*(T6522(i)^3);
h7522(i)=h6522(i);
T4522(i)=Tc522(i);
P4522(i)=497.7+16.21*T4522(i)+0.1967*(T4522(i)^2)+(1.135*10
^-3)*(T4522(i)^3);
T3522(i)=6.49+1.498*Tc522(i);
h3522(i)=254.3+0.7676*Tc522(i);
h3s522(i)=255.2+0.654*Tc522(i);
T3s522(i)=6.744+1.386*Tc522(i);
h2522(i)=6.66*h3s522(i)-5.66*h3522(i);
%Refrigeration capacity= 1kw
```

```
mfr1522(i)=1/(h2522(i)-h7522(i));
woc1522(i)=mfr1522(i)*(h3s522(i)-h2522(i));
hrr1522(i)=mfr1522(i)*(h3s522(i)-h6522(i));
COP1522(i)=(h2522(i)-h7522(i))/(h3s522(i)-h2522(i));
Tcompout1522(i)=T3s522(i);
end;

plot(Tc522,COP1522,'*')

hold off

xlabel(' Tc (c)')
ylabel('COP')
```

******** Specified Program ********

```
%This program is developed to calculate performance parameters for constant condensing temperature Tc = 40 °C and variable evaporating temperature for non isentropic practical cycle in order to compare it with experimental data for refrigerant R407c.


% Tc=40 °C;

dosh=5;
dosc=5;
Iseff=0.85;

for i=1:1:26;
Te13(i)=i-11;
T13(i)=Te13(i);
T23(i)=T13(i)+dosh;
P23(i)=451.9+15.81*T13(i)+0.215*(T13(i)^2)+(1.3*10^-
3)*(T13(i)^3);
B03(i)=416.1-(1.25*10^-2)*P23(i);
B13(i)=0.8126+(2*10^-4)*P23(i);
h23(i)=B03(i)+B13(i)*T23(i);
h3s3(i)=448.6-(0.3185)*T13(i);
T3s3(i)=56.24-(0.3149)*T13(i);
h33(i)=h23(i)+((h3s3(i)-h23(i))/Iseff);
T33(i)=62.1-0.4979*T13(i);
T53(i)=40;
T63(i)=T53(i)-dosc;
P63(i)=560.2+18.19*T63(i)+0.2247*(T63(i)^2)+(1.179*10^-
3)*(T63(i)^3);
h63(i)=132.2+0.1739*P63(i)-(1.148*10^-
4)*(P63(i)^2)+(3.723*10^-8)*(P63(i)^3);
h73(i)=h63(i);
%Refrigeration capacity = 1 kw
```

```
mfr13(i)=1/(h23(i)-h73(i));
woc13(i)=mfr13(i)*(h33(i)-h23(i));
hrr13(i)=mfr13(i)*(h33(i)-h63(i));
COP13(i)=(h23(i)-h73(i))/(h33(i)-h23(i));
Tcompout13(i)=T33(i);
end;

[Te13;mfr13;woc13;hrr13;COP13;Tcompout13]'

plot(T13,COP13)



% This program is developed calculate performance parameters for constant evaporating temperature Te =12 ºC and variable condensing temperature for non isentropic practical cycle in order to compare it with experimental data for R407c.

% Te=12 ºC;

dosh=5;
dosc=5;
Iseff=0.85;

for i=1:1:21;
Tc5(i)=i+29;
T55(i)=Tc5(i);
T65(i)=T55(i)-dosc;
P65(i)=560.2+18.19*T65(i)+0.2247*(T65(i)^2)+(1.179*10^-
3)*(T65(i)^3);
h65(i)=132.2+0.1739*P65(i)-(1.148*10^-
4)*(P65(i)^2)+(3.723*10^-8)*(P65(i)^3);
h75(i)=h65(i);
```

```
T45(i)=Tc5(i);
P45(i)=451.9+15.81*T45(i)+0.215*(T45(i)^2)+(1.3*10^-
3)*(T45(i)^3);
T35(i)=0.5464+1.3804*Tc5(i);
h35(i)=415.74+0.8062*Tc5(i);
h3s5(i)=416.9+0.6874*Tc5(i);
T3s5(i)=-0.4766+1.3092*Tc5(i);
h25(i)=6.66*h3s5(i)-5.66*h35(i);
%Refrigeration capacity= 1kw
mfr15(i)=1/(h25(i)-h75(i));
woc15(i)=mfr15(i)*(h35(i)-h25(i));
hrr15(i)=mfr15(i)*(h35(i)-h65(i));
COP15(i)=(h25(i)-h75(i))/(h35(i)-h25(i));
Tcompout15(i)=T35(i);
end;

[Tc5;mfr15;woc15;hrr15;COP15;Tcompout15]'

plot(T55,COP15)
```

APPENDIX B

TABLES OF RESULTS

Table (B.1) Mass flow rate (kg/s) for standard cycle for different values of T_c

T_e (^oC)	T_c = 30 ^oC	T_c = 35 ^oC	T_c = 40 ^oC	T_c = 45 ^oC	T_c = 50 ^oC
-10	0.0063	0.0069	0.0079	0.0101	0.0176

-9	0.0063	0.0068	0.0079	0.0101	0.0174
-8	0.0062	0.0068	0.0078	0.01	0.0172
-7	0.0062	0.0068	0.0078	0.01	0.017
-6	0.0062	0.0067	0.0077	0.0099	0.0169
-5	0.0062	0.0067	0.0077	0.0098	0.0167
-4	0.0061	0.0067	0.0077	0.0098	0.0165
-3	0.0061	0.0067	0.0076	0.0097	0.0164
-2	0.0061	0.0066	0.0076	0.0097	0.0162
-1	0.0061	0.0066	0.0076	0.0096	0.0161
0	0.006	0.0066	0.0075	0.0096	0.0159
1	0.006	0.0066	0.0075	0.0095	0.0158
2	0.006	0.0065	0.0075	0.0095	0.0156
3	0.006	0.0065	0.0074	0.0094	0.0155
4	0.006	0.0065	0.0074	0.0094	0.0154
5	0.0059	0.0065	0.0074	0.0093	0.0152
6	0.0059	0.0064	0.0074	0.0093	0.0151
7	0.0059	0.0064	0.0073	0.0092	0.015
8	0.0059	0.0064	0.0073	0.0092	0.0149
9	0.0059	0.0064	0.0073	0.0091	0.0148
10	0.0059	0.0064	0.0072	0.0091	0.0147
11	0.0058	0.0063	0.0072	0.0091	0.0146
12	0.0058	0.0063	0.0072	0.009	0.0145
13	0.0058	0.0063	0.0072	0.009	0.0144
14	0.0058	0.0063	0.0072	0.0089	0.0143
15	0.0058	0.0063	0.0071	0.0089	0.0142

Table (B.2) Mass flow rate (kg/s) for ideal cycle for different values of T_c

T_e (^oC)	T_c = 30 ^oC	T_c = 35 ^oC	T_c = 40 ^oC	T_c = 45 ^oC	T_c = 50 ^oC
-10	0.0059	0.0063	0.0069	0.0079	0.0102
-9	0.0059	0.0063	0.0068	0.0079	0.0101

-8	0.0059	0.0062	0.0068	0.0078	0.0100
-7	0.0058	0.0062	0.0068	0.0078	0.0100
-6	0.0058	0.0062	0.0067	0.0077	0.0099
-5	0.0058	0.0061	0.0067	0.0077	0.0098
-4	0.0058	0.0061	0.0067	0.0077	0.0097
-3	0.0057	0.0061	0.0066	0.0076	0.0097
-2	0.0057	0.0061	0.0066	0.0076	0.0096
-1	0.0057	0.0060	0.0066	0.0075	0.0095
0	0.0057	0.0060	0.0065	0.0075	0.0095
1	0.0056	0.0060	0.0065	0.0074	0.0094
2	0.0056	0.0060	0.0065	0.0074	0.0094
3	0.0056	0.0059	0.0065	0.0074	0.0093
4	0.0056	0.0059	0.0064	0.0073	0.0092
5	0.0055	0.0059	0.0064	0.0073	0.0092
6	0.0055	0.0059	0.0064	0.0073	0.0091
7	0.0055	0.0058	0.0063	0.0072	0.0090
8	0.0055	0.0058	0.0063	0.0072	0.0090
9	0.0055	0.0058	0.0063	0.0071	0.0089
10	0.0054	0.0058	0.0062	0.0071	0.0089
11	0.0054	0.0057	0.0062	0.0071	0.0088
12	0.0054	0.0057	0.0062	0.0070	0.0088
13	0.0054	0.0057	0.0062	0.0070	0.0087
14	0.0053	0.0057	0.0061	0.0070	0.0086
15	0.0053	0.0056	0.0061	0.0069	0.0086

Table (B.3) Mass flow rate (kg/s) for standard cycle for different values of T_e

T_c (^oC)	T_e = -10	T_e = -5	T_e = 0	T_e = 5	T_e = 10	T_e = 15

	°C	°C	°C	°C	°C	°C
30	0.0063	0.0062	0.0060	0.0059	0.0059	0.0058
31	0.0064	0.0062	0.0061	0.0060	0.0059	0.0059
32	0.0065	0.0064	0.0062	0.0061	0.0060	0.0059
33	0.0066	0.0065	0.0063	0.0062	0.0061	0.0060
34	0.0067	0.0066	0.0065	0.0063	0.0062	0.0062
35	0.0069	0.0067	0.0066	0.0065	0.0064	0.0063
36	0.0070	0.0069	0.0067	0.0066	0.0065	0.0064
37	0.0072	0.0070	0.0069	0.0068	0.0067	0.0066
38	0.0074	0.0072	0.0071	0.0069	0.0068	0.0067
39	0.0076	0.0075	0.0073	0.0072	0.0070	0.0069
40	0.0079	0.0077	0.0075	0.0074	0.0072	0.0071
41	0.0082	0.0080	0.0078	0.007	0.0075	0.0074
42	0.0086	0.0084	0.0082	0.0080	0.0078	0.0077
43	0.0090	0.0088	0.0085	0.0083	0.0082	0.0080
44	0.0095	0.0093	0.0090	0.0088	0.0086	0.0084
45	0.0101	0.0098	0.0096	0.0093	0.0091	0.0089
46	0.0109	0.0106	0.0103	0.0100	0.0097	0.0095
47	0.0119	0.0115	0.0111	0.0108	0.0105	0.0103
48	0.0132	0.0127	0.0123	0.0119	0.0115	0.0112
49	0.0150	0.0144	0.0138	0.0133	0.0128	0.0125
50	0.0176	0.0167	0.0159	0.0152	0.0147	0.0142

Table (B.4) Mass flow rate (kg/s) for ideal cycle for different values of T_e

T_c (°C)	T_e = -10	T_e = -5	T_e = 0	T_e = 5	T_e = 10	T_e = 15

	°C	°C	°C	°C	°C	°C
30	0.0059	0.0058	0.0057	0.0055	0.0054	0.0053
31	0.0060	0.0058	0.0057	0.0056	0.0055	0.0054
32	0.0060	0.0059	0.0058	0.0057	0.0056	0.0054
33	0.0061	0.0060	0.0059	0.0057	0.0056	0.0055
34	0.0062	0.0061	0.0059	0.0058	0.0057	0.0056
35	0.0063	0.0061	0.0060	0.0059	0.0058	0.0056
36	0.0064	0.0062	0.0061	0.0060	0.0058	0.0057
37	0.0065	0.0063	0.0062	0.0061	0.0059	0.0058
38	0.0066	0.0064	0.0063	0.0062	0.0060	0.0059
39	0.0067	0.0066	0.0064	0.0063	0.0061	0.0060
40	0.0069	0.0067	0.0066	0.0064	0.0062	0.0061
41	0.0070	0.0069	0.0067	0.0065	0.0064	0.0062
42	0.0072	0.0070	0.0069	0.0067	0.0065	0.0063
43	0.0074	0.0072	0.0070	0.0069	0.0067	0.0065
44	0.0076	0.0074	0.0073	0.0071	0.0069	0.0067
45	0.0079	0.0077	0.0075	0.0073	0.0071	0.0069
46	0.0082	0.0080	0.0078	0.0075	0.0073	0.0071
47	0.0086	0.0083	0.0081	0.0078	0.0076	0.0074
48	0.0090	0.0087	0.0085	0.0082	0.0080	0.0077
49	0.0095	0.0092	0.0089	0.0086	0.0084	0.0081
50	0.0101	0.0098	0.0095	0.0091	0.0088	0.0085

Table (B.5) Comparison between standard and ideal mass flow (kg/s) rate at T_c = 40 °C

T_e (^oC)	Standard	Ideal with superheating and sub-cooling
-10	0.0079	0.0069
-9	0.0079	0.0068
-8	0.0078	0.0068
-7	0.0078	0.0068
-6	0.0077	0.0067
-5	0.0077	0.0067
-4	0.0077	0.0067
-3	0.0076	0.0066
-2	0.0076	0.0066
-1	0.0076	0.0066
0	0.0075	0.0065
1	0.0075	0.0065
2	0.0075	0.0065
3	0.0074	0.0065
4	0.0074	0.0064
5	0.0074	0.0064
6	0.0074	0.0064
7	0.0073	0.0063
8	0.0073	0.0063
9	0.0073	0.0063
10	0.0072	0.0062
11	0.0072	0.0062
12	0.0072	0.0062
13	0.0072	0.0062
14	0.0072	0.0061
15	0.0071	0.0061

Table (B.6) Comparison between standard and ideal mass flow (kg/s) rate at $T_e = 10\ ^oC$

T_c (^oC)	Standard	Ideal with superheating and sub-cooling
30	0.0059	0.0054
31	0.0059	0.0055
32	0.0060	0.0056
33	0.0061	0.0056
34	0.0062	0.0057
35	0.0064	0.0058
36	0.0065	0.0058
37	0.0067	0.0059
38	0.0068	0.0060
39	0.0070	0.0061
40	0.0072	0.0062
41	0.0075	0.0064
42	0.0078	0.0065
43	0.0082	0.0067
44	0.0086	0.0069
45	0.0091	0.0071
46	0.0097	0.0073
47	0.0105	0.0076
48	0.0115	0.0080
49	0.0128	0.0084
50	0.0147	0.0088

Table (B.7) Compressor power (kW) for standard cycle for different values of T_c

T_e (^oC)	T_c = 30 ^oC	T_c = 35 ^oC	T_c = 40 ^oC	T_c = 45 ^oC	T_c = 50 ^oC
-10	0.2007	0.2444	0.3086	0.4309	0.8055
-9	0.1942	0.2371	0.2999	0.4188	0.7806
-8	0.1877	0.2298	0.2912	0.4069	0.7562
-7	0.1813	0.2226	0.2825	0.3951	0.7324
-6	0.1750	0.2155	0.2740	0.3834	0.7090
-5	0.1687	0.2084	0.2656	0.3720	0.6863
-4	0.1624	0.2014	0.2573	0.3607	0.6640
-3	0.1563	0.1945	0.2491	0.3496	0.6423
-2	0.1502	0.1877	0.2411	0.3387	0.6212
-1	0.1442	0.1810	0.2331	0.3279	0.6006
0	0.1383	0.1744	0.2253	0.3174	0.5805
1	0.1325	0.1679	0.2176	0.3071	0.5610
2	0.1268	0.1615	0.2100	0.2970	0.5420
3	0.1211	0.1552	0.2026	0.2871	0.5235
4	0.1156	0.1491	0.1953	0.2773	0.5055
5	0.1102	0.1430	0.1882	0.2678	0.4881
6	0.1048	0.1370	0.1812	0.2585	0.4711
7	0.0995	0.1312	0.1743	0.2494	0.4546
8	0.0944	0.1255	0.1676	0.2405	0.4386
9	0.0893	0.1198	0.1610	0.2318	0.4230
10	0.0843	0.1143	0.1545	0.2233	0.4078
11	0.0794	0.1088	0.1481	0.2149	0.3930
12	0.0746	0.1035	0.1419	0.2067	0.3786
13	0.0699	0.0982	0.1357	0.1987	0.3645
14	0.0652	0.0930	0.1296	0.1908	0.3507
15	0.0605	0.0879	0.1237	0.1829	0.3372

Table (B.8) Compressor power (kW) for ideal cycle for different values of T_c

T_e (^oC)	$T_c = 30\ ^oC$	$T_c = 35\ ^oC$	$T_c = 40\ ^oC$	$T_c = 45\ ^oC$	$T_c = 50\ ^oC$
-10	0.2117	0.2527	0.3022	0.3740	0.5113
-9	0.2048	0.2452	0.2937	0.3637	0.4970
-8	0.1980	0.2377	0.2852	0.3536	0.4829
-7	0.1912	0.2303	0.2769	0.3435	0.4690
-6	0.1845	0.2229	0.2686	0.3335	0.4553
-5	0.1778	0.2156	0.2603	0.3237	0.4418
-4	0.1712	0.2084	0.2522	0.3139	0.4285
-3	0.1646	0.2012	0.2441	0.3042	0.4153
-2	0.1581	0.1941	0.2361	0.2947	0.4023
-1	0.1516	0.1870	0.2281	0.2852	0.3895
0	0.1451	0.1800	0.2203	0.2758	0.3768
1	0.1388	0.1730	0.2124	0.2665	0.3643
2	0.1324	0.1661	0.2047	0.2573	0.3519
3	0.1261	0.1593	0.1970	0.2482	0.3397
4	0.1198	0.1524	0.1893	0.2392	0.3276
5	0.1136	0.1457	0.1818	0.2302	0.3157
6	0.1074	0.1389	0.1742	0.2213	0.3039
7	0.1012	0.1322	0.1667	0.2125	0.2922
8	0.0951	0.1256	0.1593	0.2037	0.2806
9	0.0890	0.1189	0.1519	0.1951	0.2692
10	0.0829	0.1124	0.1446	0.1864	0.2578
11	0.0769	0.1058	0.1373	0.1779	0.2466
12	0.0709	0.0993	0.1300	0.1694	0.2355
13	0.0649	0.0928	0.1228	0.1609	0.2245
14	0.0589	0.0864	0.1157	0.1526	0.2136
15	0.0530	0.0799	0.1085	0.1442	0.2028

Table (B.9) Compressor power (kW) for standard cycle for different values of T_e

T_c (^oC)	T_e = -10 ^oC	T_e = -5 ^oC	T_e = 0 ^oC	T_e = 5 ^oC	T_e = 10 ^oC	T_e = 15 ^oC
30	0.2022	0.1691	0.1381	0.1106	0.0854	0.0620
31	0.2096	0.1759	0.1443	0.1163	0.0906	0.0668
32	0.2175	0.1830	0.1508	0.1222	0.0960	0.0717
33	0.2259	0.1906	0.1577	0.1284	.1017	0.0769
34	0.2349	0.1987	0.1650	0.1350	0.1076	0.0823
35	0.2446	0.2074	0.1728	0.1420	0.1140	0.0881
36	0.2551	0.2167	0.1812	0.1496	0.1208	0.0942
37	0.2666	0.2269	0.1903	0.1577	0.1280	0.1007
38	0.2792	0.2381	0.2002	0.1665	0.1359	0.1077
39	0.2932	0.2504	0.2111	0.1762	0.1445	0.1153
40	0.3089	0.2642	0.2232	0.1869	0.1539	0.1237
41	0.3266	0.2797	0.2369	0.1989	0.1644	0.1329
42	0.3470	0.2974	0.2523	0.2124	0.1763	0.1433
43	0.3706	0.3179	0.2701	0.2279	0.1897	0.1550
44	0.3985	0.3419	0.2909	0.2458	0.2053	0.1684
45	0.4319	0.3706	0.3155	0.2670	0.2236	0.1841
46	0.4728	0.4055	0.3454	0.2926	0.2454	0.2028
47	0.5242	0.4491	0.3823	0.3240	0.2721	0.2255
48	0.5908	0.5051	0.4295	0.3638	0.3058	0.2539
49	0.6808	0.5799	0.4919	0.4160	0.3495	0.2905
50	0.8091	0.6852	0.5787	0.878	0.4090	0.3399

Table (B.10) Compressor power (kW) for ideal cycle for different values of T_e

T_c (^oC)	T_e = -10 ^oC	T_e = -5 ^oC	T_e = 0 ^oC	T_e = 5 ^oC	T_e = 10 ^oC	T_e = 15 ^oC
30	0.2165	0.1791	0.1480	0.1157	0.0862	0.0545
31	0.2231	0.1852	0.1536	0.1207	0.0908	0.0586
32	0.2299	0.1916	0.1594	0.1259	0.0955	0.0628
33	0.2370	0.1982	0.1655	0.1313	0.1005	0.0671
34	0.2444	0.2051	0.1717	0.1368	0.1055	0.0716
35	0.2522	0.2124	0.1783	0.1426	0.1108	0.0765
36	0.2605	0.2200	0.1852	0.1487	0.1163	0.0810
37	0.2692	0.2280	0.1924	0.1551	0.1221	0.0861
38	0.2786	0.2366	0.2001	0.1618	0.1282	0.0913
39	0.2886	0.2458	0.2083	0.1689	0.1346	0.0968
40	0.2994	0.2556	0.2171	0.1766	0.1414	0.1027
41	0.3112	0.2663	0.2266	0.1848	0.1487	0.1089
42	0.3240	0.2780	0.2369	0.1937	0.1565	0.1155
43	0.3383	0.2907	0.2482	0.2034	0.1650	0.1227
44	0.3541	0.3049	0.2607	0.2140	0.1743	0.1304
45	0.3719	0.3208	0.2746	0.2258	0.1846	0.1389
46	0.3921	0.3387	0.2902	0.2390	0.1960	0.1484
47	0.4153	0.3592	0.3080	0.2540	0.2089	0.1589
48	0.4423	0.3830	0.3286	0.2711	0.2236	0.1708
49	0.4743	0.4109	0.3526	0.2911	0.2405	0.1845
50	0.5126	0.4442	0.3811	0.3146	0.2604	0.2004

Table (B.11) Comparison between standard and ideal compressor power (kW) at $T_c = 40\ ^oC$

T_e (^oC)	Standard	Ideal with superheating and sub-cooling
-10	0.3086	0.3022
-9	0.2999	0.2937
-8	0.2912	0.2852
-7	0.2825	0.2769
-6	0.2740	0.2686
-5	0.2656	0.2603
-4	0.2573	0.2522
-3	0.2491	0.2441
-2	0.2411	0.2361
-1	0.2331	0.2281
0	0.2253	0.2203
1	0.2176	0.2124
2	0.2100	0.2047
3	0.2026	0.1970
4	0.1953	0.1893
5	0.1882	0.1818
6	0.1812	0.1742
7	0.1743	0.1667
8	0.1676	0.1593
9	0.1610	0.1519
10	0.1545	0.1446
11	0.1481	0.1373
12	0.1419	0.1300
13	0.1357	0.1228
14	0.1296	0.1157
15	0.1237	0.1085

Table (B.12) Comparison between standard and ideal compressor power (kW) at $T_e = 10\ ^oC$

T_c (^oC)	Standard	Ideal with superheating and sub-cooling
30	0.0854	0.0862
31	0.0906	0.0908
32	0.0960	0.0955
33	.1017	0.1005
34	0.1076	0.1055
35	0.1140	0.1108
36	0.1208	0.1163
37	0.1280	0.1221
38	0.1359	0.1282
39	0.1445	0.1346
40	0.1539	0.1414
41	0.1644	0.1487
42	0.1763	0.1565
43	0.1897	0.1650
44	0.2053	0.1743
45	0.2236	0.1846
46	0.2454	0.1960
47	0.2721	0.2089
48	0.3058	0.2236
49	0.3495	0.2405
50	0.4090	0.2604

Table (B.13) Heat rejection rate (kW) for standard cycle for different values of T_c

T_e (°C)	T_c = 30 °C	T_c = 35 °C	T_c = 40 °C	T_c = 45 °C	T_c = 50 °C
-10	1.2007	1.2444	1.3086	1.4309	1.8055
-9	1.1942	1.2371	1.2999	1.4188	1.7806
-8	1.1877	1.2298	1.2912	1.4069	1.7562
-7	1.1813	1.2226	1.2825	1.3951	1.7324
-6	1.1750	1.2155	1.2740	1.3834	1.7090
-5	1.1687	1.2084	1.2656	1.3720	1.6863
-4	1.1624	1.2014	1.2573	1.3607	1.6640
-3	1.1563	1.1945	1.2491	1.3496	1.6423
-2	1.1502	1.1877	1.2411	1.3387	1.6212
-1	1.1442	1.1810	1.2331	1.3279	1.6006
0	1.1383	1.1744	1.2253	1.3174	1.5805
1	1.1325	1.1679	1.2176	1.3071	1.5610
2	1.1268	1.1915	1.2100	1.2970	1.5420
3	1.1211	1.1552	1.2026	1.2871	1.5235
4	1.1156	1.1491	1.1953	1.2773	1.5055
5	1.1102	1.1430	1.1882	1.2678	1.4881
6	1.1048	1.1370	1.1812	1.2585	1.4711
7	1.0995	1.1312	1.1743	1.2494	1.4546
8	1.0944	1.1255	1.1676	1.2405	1.4386
9	1.0893	1.1198	1.1610	1.2318	1.4230
10	1.0843	1.1143	1.1545	1.2233	1.4078
11	1.0794	1.1088	1.1481	1.2149	1.3930
12	1.0746	1.1035	1.1419	1.2067	1.3786
13	1.0699	1.0982	1.1357	1.1987	1.3645
14	1.0652	1.0930	1.1296	1.1908	1.3507
15	1.0605	1.0879	1.1237	1.1829	1.3372

Table (B.14) Heat rejection rate (kW) for ideal cycle for different values of T_c

T_e (^oC)	T_c = 30 ^oC	T_c = 35 ^oC	T_c = 40 ^oC	T_c = 45 ^oC	T_c = 50 ^oC
-10	1.2117	1.2527	1.3022	1.3740	1.5113
-9	1.2048	1.2452	1.2937	1.3637	1.4970
-8	1.1980	1.2377	1.2852	1.3536	1.4829
-7	1.1912	1.2303	1.2769	1.3435	1.4690
-6	1.1845	1.2229	1.2686	1.3335	1.4553
-5	1.1778	1.2156	1.2603	1.3237	1.4418
-4	1.1712	1.2084	1.2522	1.3139	1.4285
-3	1.1646	1.2012	1.2441	1.3042	1.4153
-2	1.1581	1.1941	1.2361	1.2947	1.4023
-1	1.1516	1.1870	1.2281	1.2852	1.3895
0	1.1451	1.1800	1.2203	1.2758	1.3768
1	1.1388	1.1730	1.2124	1.2665	1.3643
2	1.1324	1.1661	1.2047	1.2573	1.3519
3	1.1261	1.1593	1.1970	1.2482	1.3397
4	1.1198	1.1524	1.1893	1.2392	1.3276
5	1.1136	1.1457	1.1818	1.2302	1.3157
6	1.1074	1.1389	1.1742	1.2213	1.3039
7	1.1012	1.1322	1.1667	1.2125	1.2922
8	1.0951	1.1256	1.1593	1.2037	1.2806
9	1.0890	1.1189	1.1519	1.1951	1.2692
10	1.0829	1.1124	1.1446	1.1864	1.2578
11	1.0769	1.1028	1.1373	1.1779	1.2466
12	1.0709	1.0993	1.1300	1.1694	1.2355
13	1.0649	1.0928	1.1228	1.1609	1.2245
14	1.0589	1.0864	1.1157	1.1526	1.2136
15	1.0530	1.0799	1.1085	1.1442	1.2028

Table (B.15) Heat rejection rate (kW) for standard cycle for different values of T_e

T_c (^oC)	T_e = -10 ^oC	T_e = -5 ^oC	T_e = 0 ^oC	T_e = 5 ^oC	T_e = 10 ^oC	T_e = 15 ^oC
30	1.2022	1.1691	1.1381	1.1106	1.0854	1.0620
31	1.2096	1.1759	1.1443	1.1163	1.0906	1.0668
32	1.2175	1.1830	1.1508	1.1222	1.0960	1.0717
33	1.2259	1.1906	1.1577	1.1284	1.1017	1.0769
34	1.2349	1.1987	1.1650	1.1350	1.1076	1.0823
35	1.2446	1.2074	1.1728	1.1420	1.1140	1.0881
36	1.2551	1.2167	1.1812	1.1496	1.1208	1.0942
37	1.2666	1.2269	1.1903	1.1577	1.1280	1.1007
38	1.2792	1.2381	1.2002	1.1665	1.1359	1.1077
39	1.2932	1.2504	1.2111	1.1762	1.1445	1.1153
40	1.3089	1.2642	1.2232	1.1869	1.1539	1.1237
41	1.3266	1.2797	1.2369	1.1989	1.1644	1.1329
42	1.3470	1.2974	1.2523	1.2124	1.1763	1.1433
43	1.3706	1.3179	1.2701	1.2279	1.1897	1.1550
44	1.3985	1.3419	1.2909	1.2458	1.2053	1.1684
45	1.4319	1.3706	1.3155	1.2670	1.2236	1.1841
46	1.4728	1.4055	1.3454	1.2926	1.2454	1.2028
47	1.5242	1.4491	1.3823	1.3240	1.2721	1.2255
48	1.5908	1.5051	1.4295	1.3638	1.3058	1.2539
49	1.6808	1.5799	1.4919	1.4160	1.3495	1.2905
50	1.8091	1.6852	1.5787	1.4878	1.4090	1.3399

Table (B.16) Heat rejection rate (kW) for ideal cycle for different values of T_e

T_c (^oC)	T_e = -10 ^oC	T_e = -5 ^oC	T_e = 0 ^oC	T_e = 5 ^oC	T_e = 10 ^oC	T_e = 15 ^oC
30	1.2165	1.1791	1.1480	1.1157	1.0862	1.0545
31	1.2231	1.1852	1.1536	1.1207	1.0908	1.0586
32	1.2299	1.1916	1.1594	1.1259	1.0955	1.0628
33	1.2370	1.1982	1.1655	1.1313	1.1005	1.0671
34	1.2444	1.2051	1.1717	1.1368	1.1055	1.0716
35	1.2522	1.2124	1.1783	1.1426	1.1108	1.0762
36	1.2605	1.2200	1.1852	1.1487	1.1163	1.0810
37	1.2692	1.2280	1.1924	1.1551	1.1221	1.0861
38	1.2786	1.2366	1.2001	1.1618	1.1282	1.0913
39	1.2886	1.2458	1.2083	1.1689	1.1346	1.0968
40	1.2994	1.2556	1.2171	1.1766	1.1414	1.1027
41	1.3112	1.2663	1.2266	1.1848	1.1487	1.1089
42	1.3240	1.2780	1.2369	1.1937	1.1565	1.1155
43	1.3383	1.2907	1.2482	1.2034	1.1650	1.1227
44	1.3541	1.3049	1.2607	1.2140	1.1743	1.1304
45	1.3719	1.3208	1.2746	1.2258	1.1846	1.1389
46	1.3921	1.3387	1.2902	1.2390	1.1960	1.1484
47	1.4153	1.3592	1.3080	1.2540	1.2089	1.1589
48	1.4423	1.3830	1.3286	1.2711	1.2236	1.1708
49	1.4743	1.4109	1.3526	1.2911	1.2405	1.1845
50	1.5126	1.4442	1.3811	1.3146	1.2604	1.2004

Table (B.17) Comparison between standard and ideal heat rejection rate (kW) at $T_c = 40\ ^oC$

T_e (^oC)	Standard	Ideal with superheating and sub-cooling
-10	1.3086	1.3022
-9	1.2999	1.2937
-8	1.2912	1.2852
-7	1.2825	1.2769
-6	1.2740	1.2686
-5	1.2656	1.2603
-4	1.2573	1.2522
-3	1.2491	1.2441
-2	1.2411	1.2361
-1	1.2331	1.2281
0	1.2253	1.2203
1	1.2176	1.2124
2	1.2100	1.2047
3	1.2026	1.1970
4	1.1953	1.1893
5	1.1882	1.1818
6	1.1812	1.1742
7	1.1743	1.1667
8	1.1676	1.1593
9	1.1610	1.1519
10	1.1545	1.1446
11	1.1481	1.1373
12	1.1419	1.1300
13	1.1357	1.1228
14	1.1296	1.1157
15	1.1237	1.1085

Table (B.18) Comparison between standard and ideal heat rejection rate (kW) at $T_e = 10\ ^oC$

T_c (^oC)	Standard	Ideal with superheating and sub-cooling
30	1.0854	1.0862
31	1.0906	1.0908
32	1.0960	1.0955
33	1.1017	1.1005
34	1.1076	1.1055
35	1.1140	1.1108
36	1.1208	1.1163
37	1.1280	1.1221
38	1.1359	1.1282
39	1.1445	1.1346
40	1.1539	1.1414
41	1.1644	1.1487
42	1.1763	1.1565
43	1.1897	1.1650
44	1.2053	1.1743
45	1.2236	1.1846
46	1.2454	1.1960
47	1.2721	1.2089
48	1.3058	1.2236
49	1.3495	1.2405
50	1.4090	1.2604

Table (B.19) Coefficient of performance for standard cycle for different values of T_c

T_e (^oC)	T_c = 30 ^oC	T_c = 35 ^oC	T_c = 40 ^oC	T_c = 45 ^oC	T_c = 50 ^oC
-10	4.9819	4.0915	3.2401	2.3207	1.2415
-9	5.1491	4.2180	3.3350	2.3877	1.2811
-8	5.3265	4.3515	3.4346	2.4579	1.3224
-7	5.5150	4.4924	3.5392	2.5312	1.3655
-6	5.7154	4.6412	3.6492	2.6080	1.4103
-5	5.9286	4.7984	3.7647	2.6884	1.4571
-4	6.1558	4.9646	3.8862	2.7726	1.5059
-3	6.3980	5.1404	4.0139	2.8606	1.5568
-2	6.6567	5.3265	4.1483	2.9528	1.6098
-1	6.9333	5.5238	4.2897	3.0494	1.6650
0	7.2294	5.7329	4.4386	3.1505	1.7226
1	7.5469	5.9548	4.5955	3.2564	1.7826
2	7.8879	6.1906	4.7608	3.3674	1.8451
3	8.2549	6.4413	4.9352	3.4837	1.9102
4	8.6507	6.7082	5.1192	3.6056	1.9781
5	9.0784	6.9929	5.3135	3.7336	2.0489
6	9.5419	7.2969	5.5191	3.8678	2.1227
7	10.0456	7.6221	5.7366	4.0089	2.1997
8	10.5950	7.9709	5.9673	4.1573	2.2801
9	11.1964	8.3458	6.2123	4.3136	2.3642
10	11.8579	8.7499	6.4730	4.4784	2.4522
11	12.5893	9.1871	6.7512	4.6526	2.5444
12	13.4027	9.6620	7.0489	4.8372	2.6413
13	14.3141	10.1802	7.3687	5.0333	2.7433
14	15.3439	10.7489	7.7135	5.2424	2.8511
15	16.5192	11.3771	8.0873	5.4662	2.9653

Table (B.20) Coefficient of performance for ideal cycle for different values of T_c

T_e (^oC)	T_c = 30 ^oC	T_c = 35 ^oC	T_c = 40 ^oC	T_c = 45 ^oC	T_c = 50 ^oC
-10	4.7231	3.9568	3.3087	2.6735	1.9559
-9	4.8821	4.0786	3.4049	2.7492	2.0121
-8	5.0507	4.2071	3.5059	2.8284	2.0708
-7	5.2299	4.3426	3.6120	2.9113	2.1322
-6	5.4207	4.4859	3.7237	2.9983	2.1963
-5	5.6242	4.6377	3.8414	3.0896	2.2635
-4	5.8419	4.7988	3.9656	3.1857	2.3340
-3	6.0754	4.9700	4.0969	3.2868	2.4080
-2	6.3263	5.1524	4.2359	3.3835	2.4857
-1	6.5969	5.3471	4.3834	3.5061	2.5676
0	6.8894	5.5555	4.5403	3.6253	2.6539
1	7.2069	5.7791	4.7073	3.7517	2.7451
2	7.5527	6.1198	4.8857	3.8859	2.8416
3	7.9308	6.2794	5.0766	4.0288	2.9438
4	8.3460	6.5604	5.2815	4.1811	3.0524
5	8.8041	6.8658	5.5019	4.3440	3.1679
6	9.3123	7.1987	5.7397	4.5185	3.2910
7	9.8794	7.5632	5.9972	4.7061	3.4227
8	10.5164	7.9641	6.2769	4.9083	3.5637
9	11.2371	8.4072	6.5819	5.1268	3.7153
10	12.0595	8.8996	6.9159	5.3538	3.8785
11	13.0068	9.4502	7.2833	5.6219	4.0550
12	14.1100	10.0701	7.6894	5.9039	4.2463
13	15.4115	10.7733	8.1408	6.2135	4.4545
14	16.9703	11.5780	8.6456	6.5549	4.6820
15	18.8714	12.5083	9.2140	6.9335	4.9315

Table (B.21) Coefficient of performance for standard cycle for different values of T_e

T_c (^oC)	T_e = -10 ^oC	T_e = -5 ^oC	T_e = 0 ^oC	T_e = 5 ^oC	T_e = 10 ^oC	T_e = 15 ^oC
30	4.9466	5.9128	7.2388	9.0405	11.7048	16.1201
31	4.7703	5.6853	6.9290	8.6017	11.0374	14.9741
32	4.5969	5.4635	6.6306	8.1853	10.4166	13.9419
33	4.4258	5.2464	6.3419	7.7881	9.8360	13.0045
34	4.2563	5.0331	6.0615	7.4075	9.2897	12.1463
35	4.0878	4.8227	5.7879	7.0410	8.7729	11.3549
36	3.9196	4.6145	5.5199	6.6866	8.2813	10.6197
37	3.7511	4.4074	5.2562	6.3422	7.8110	9.9320
38	3.5817	4.2008	4.9957	6.0059	7.3587	9.2844
39	3.4107	3.9938	4.7372	5.6759	6.9214	8.6706
40	3.2376	3.7855	4.4796	5.3507	6.4963	8.0851
41	3.0615	3.5753	4.2219	5.0288	6.0810	7.5230
42	2.8820	3.3623	3.9631	4.7086	5.6731	6.9801
43	2.6983	3.1457	3.7020	4.3887	5.2705	6.4527
44	2.5097	2.9246	3.4377	4.0679	4.8711	5.9374
45	2.3155	2.6984	3.1692	3.7447	4.4732	5.4310
46	2.1151	2.4661	2.8954	3.4180	4.0750	4.9309
47	1.9077	2.2269	2.6155	3.0864	3.6746	4.4343
48	1.6926	1.9800	2.3283	2.7487	3.2705	3.9388
49	1.4689	1.7245	2.0329	2.4037	2.8611	3.4421
50	1.2359	1.4594	1.7281	2.0501	2.4448	2.9422

Table (B.22) Coefficient of performance for ideal cycle for different values of T_e

T_c (^oC)	T_e = -10 ^oC	T_e = -5 ^oC	T_e = 0 ^oC	T_e = 5 ^oC	T_e = 10 ^oC	T_e = 15 ^oC
30	4.6182	5.5832	6.7551	8.3968	11.6034	18.3555
31	4.4826	5.3983	6.5086	8.2817	11.0137	17.0701
32	4.3500	5.2191	6.2717	7.9417	10.4659	15.9251
33	4.2197	5.0449	6.0435	7.6180	9.9547	14.8966
34	4.0915	4.8750	5.8227	7.3085	9.4754	13.9660
35	3.9648	4.7088	5.6085	7.0115	9.0240	13.1178
36	3.8393	4.5457	5.4000	6.7255	8.5968	12.3395
37	3.7145	4.3850	5.1963	6.4490	8.1909	11.6208
38	3.5900	4.2262	4.9964	6.1806	7.8032	10.9530
39	3.4654	4.0687	4.7997	5.9190	7.4314	10.3287
40	3.3401	3.9118	4.6053	5.6630	7.0732	9.7416
41	3.2138	3.7550	4.4124	5.4115	6.7263	9.1864
42	3.0860	3.5977	4.2204	5.1634	6.3890	8.6582
43	2.9563	3.4394	4.0284	4.9176	6.0594	8.1530
44	2.8241	3.2795	3.8357	4.6731	5.7359	7.6670
45	2.6889	3.1172	3.6416	4.4289	5.4170	7.1969
46	2.5503	2.9522	3.4454	4.1840	5.1010	6.7399
47	2.4078	2.7836	3.2463	3.9375	4.7867	6.2931
48	2.2607	2.6110	3.0435	3.6883	4.4727	5.8541
49	2.1086	2.4337	2.8364	3.4357	4.1576	5.4205
50	1.9508	2.2510	2.6242	3.1785	3.8402	4.9903

Table (B.23) Comparison between standard and ideal coefficient of performance at $T_c = 40\ ^oC$

T_e (^oC)	Standard	Ideal with superheating and sub-cooling
-10	3.2401	3.3087
-9	3.3350	3.4049
-8	3.4346	3.5059
-7	3.5392	3.6120
-6	3.6492	3.7237
-5	3.7647	3.8414
-4	3.8862	3.9656
-3	4.0139	4.0969
-2	4.1483	4.2359
-1	4.2897	4.3834
0	4.4386	4.5403
1	4.5955	4.7073
2	4.7608	4.8857
3	4.9352	5.0766
4	5.1192	5.2815
5	5.3135	5.5019
6	5.5191	5.7397
7	5.7366	5.9972
8	5.9673	6.2769
9	6.2123	6.5819
10	6.4730	6.9159
11	6.7512	7.2833
12	7.0489	7.6894
13	7.3687	8.1408
14	7.7135	8.6456
15	8.0873	9.2140

Table (B.24) Comparison between standard and ideal coefficient of performance at $T_e = 10\ ^oC$

T_c (^oC)	Standard	Ideal with superheating and sub-cooling
30	11.7048	11.6034
31	11.0374	11.0137
32	10.4166	10.4659
33	9.8360	9.9547
34	9.2897	9.4754
35	8.7729	9.0240
36	8.2813	8.5968
37	7.8110	8.1909
38	7.3587	7.8032
39	6.9214	7.4314
40	6.4963	7.0732
41	6.0810	6.7263
42	5.6731	6.3890
43	5.2705	6.0594
44	4.8711	5.7359
45	4.4732	5.4170
46	4.0750	5.1010
47	3.6746	4.7867
48	3.2705	4.4727
49	2.8611	4.1576
50	2.4448	3.8402

Table (B.25) Compressor discharge temperature (^{o}C) for standard cycle for different values of T_c

T_e (^{o}C)	T_c = 30 ^{o}C	T_c = 35 ^{o}C	T_c = 40 ^{o}C	T_c = 45 ^{o}C	T_c = 50 ^{o}C
-10	42.1020	47.7380	54.5180	60.6380	66.2690
-9	41.7748	47.4142	54.1982	60.3232	65.9571
-8	41.4476	47.0904	53.8784	60.0084	65.6452
-7	41.1204	46.7666	53.5586	59.6936	65.3333
-6	40.7932	46.4428	53.2388	59.3788	65.0214
-5	40.4660	46.1190	52.9190	59.0640	64.7095
-4	40.1388	45.7952	52.5992	58.7492	64.3976
-3	39.8116	45.4714	52.2794	58.4344	64.0857
-2	39.4844	45.1476	51.9596	58.1196	63.7738
-1	39.1572	44.8238	51.6398	57.8048	63.4619
0	38.8300	44.500	51.3200	57.4900	63.1500
1	38.5028	44.1762	51.0002	57.1752	62.8381
2	38.1756	43.8524	50.6804	56.8604	62.5262
3	37.8484	43.5286	50.3606	56.5456	62.2143
4	37.5212	43.2048	50.0408	56.2308	61.9024
5	37.1940	42.8810	49.7210	55.9160	61.5905
6	36.8668	42.5572	49.4012	55.6012	61.2786
7	36.5396	42.2334	49.0814	55.2864	60.9667
8	36.2124	41.9096	48.7616	54.9716	60.6548
9	35.8852	41.5858	48.4418	54.6568	60.3429
10	35.5580	41.2620	48.1220	54.3420	60.0310
11	35.2308	40.9382	47.8022	54.0272	59.7191
12	34.9036	40.6144	47.4824	53.7124	59.4072
13	34.5764	40.2906	47.1626	53.3976	59.0953
14	34.2492	39.9668	46.8428	53.0828	58.7834
15	33.9220	39.6430	46.5230	52.7680	58.4715

Table (B.26) Compressor discharge temperature (^{o}C) for ideal cycle for different values of T_c

T_e (^{o}C)	T_c = 30 ^{o}C	T_c = 35 ^{o}C	T_c = 40 ^{o}C	T_c = 45 ^{o}C	T_c = 50 ^{o}C
-10	45.1010	52.6890	59.3890	65.4690	71.0470
-9	44.7799	52.3711	59.0741	65.1571	70.7383
-8	44.4588	52.0532	58.7592	64.8452	70.4296
-7	44.1377	51.7353	58.4443	64.5333	70.1209
-6	43.8166	51.4174	58.1294	64.2214	69.8122
-5	43.4955	51.0995	57.8145	63.9095	69.5035
-4	43.1744	50.7816	57.4996	63.5976	69.1948
-3	42.8533	50.4637	57.1847	63.2857	68.8861
-2	42.5322	50.1458	56.8698	62.9738	68.5774
-1	42.2111	49.8279	56.5549	62.6619	68.2687
0	41.8900	49.5100	56.2400	62.3500	67.9600
1	41.5689	49.1921	55.9251	62.0381	67.6513
2	41.2478	48.8742	55.6102	61.7262	67.3426
3	40.9267	48.5563	55.2953	61.4143	67.0339
4	40.6056	48.2384	54.9804	61.1024	66.7252
5	40.2845	47.9205	54.6655	60.7905	66.4165
6	39.9634	47.6026	54.3506	60.4786	66.1078
7	39.6423	47.2847	54.0357	60.1667	65.7991
8	39.3212	46.9668	53.7208	59.8548	65.4904
9	39.0001	46.6489	53.4059	59.5429	65.1817
10	38.6790	46.3310	53.0910	59.2310	64.8730
11	38.3579	46.0131	52.7761	58.9191	64.5643
12	38.0368	45.6952	52.4612	58.6072	64.2556
13	37.7157	45.3773	52.1463	58.2953	63.9469
14	37.3946	45.0594	51.8314	57.9834	63.6382
15	37.0735	44.7415	51.5165	57.6715	63.3295

Table (B.27) Compressor discharge temperature (^oC) for standard cycle for different values of T_e

T_c (^oC)	T_e = -10 ^oC	T_e = -5 ^oC	T_e = 0 ^oC	T_e = 5 ^oC	T_e = 10 ^oC	T_e = 15 ^oC
30	42.1600	40.3280	38.6000	37.0080	35.4400	33.9460
31	43.3840	41.5560	39.8320	38.2450	36.6790	35.1900
32	44.6080	42.7840	41.0640	39.4820	37.9180	36.4340
33	45.8320	44.0120	42.2960	40.7190	39.1570	37.6780
34	47.0560	45.2400	43.5280	41.9560	40.3960	38.9220
35	48.2800	46.4680	44.7600	43.1930	41.6350	40.1660
36	49.5040	47.6960	45.9920	44.4300	42.8740	41.4100
37	50.7280	48.9240	47.2240	45.6670	44.1130	42.6540
38	51.9520	50.1520	48.4560	46.9040	45.3520	43.8980
39	53.1760	51.3800	49.6880	48.1410	46.5910	45.1420
40	54.4000	52.6080	50.9200	49.3780	47.8300	46.3860
41	55.6240	53.8360	52.1520	50.6150	49.0690	47.6300
42	56.8480	55.0640	53.3840	51.8520	50.3080	48.8740
43	58.0720	56.2920	54.6160	53.0890	51.5470	50.1180
44	59.2960	57.5200	55.8480	54.3260	52.7860	51.3620
45	60.5200	58.7480	57.0800	55.5630	54.0250	52.6060
46	61.7440	59.9760	58.3120	56.8000	55.2640	53.8500
47	62.9680	61.2040	59.5440	58.0370	56.5030	55.0940
48	64.1920	62.4320	60.7760	59.2740	57.7420	56.3380
49	65.4160	63.6600	62.0080	60.5110	58.9810	57.5820
50	66.6400	64.8880	63.2400	61.7480	60.2200	58.8260

Table (B.28) Compressor discharge temperature (^{o}C) for ideal cycle for different values of T_e

T_c (^{o}C)	T_e = -10 ^{o}C	T_e = -5 ^{o}C	T_e = 0 ^{o}C	T_e = 5 ^{o}C	T_e = 10 ^{o}C	T_e = 15 ^{o}C
30	45.9550	44.1420	42.4130	40.9680	39.4490	37.8250
31	47.2490	45.4400	43.7510	42.2630	40.7570	39.1360
32	48.5430	46.7380	45.0170	43.5580	42.0650	40.4470
33	49.8370	48.0360	46.3190	44.8530	43.3730	41.7580
34	51.1310	49.3340	47.6210	46.1480	44.6810	43.0690
35	52.4250	50.6320	48.9230	47.44430	45.9890	44.3800
36	53.7190	51.9300	50.2250	48.7380	47.2970	45.6910
37	55.0130	53.2280	51.5270	50.0330	48.6050	47.0020
38	56.3070	54.5260	52.8290	51.3280	49.9130	48.3130
39	57.6010	55.8240	54.1310	52.6230	51.2210	49.6240
40	58.8950	57.1220	55.4330	53.9180	52.5290	50.9350
41	60.1890	58.4200	56.7350	55.2130	53.8370	52.2460
42	61.4830	59.7180	58.0370	56.5080	55.1450	53.5570
43	62.7770	61.0160	59.3390	57.8030	56.4530	54.8680
44	64.0710	62.3140	60.6410	59.0980	57.7610	56.1790
45	65.3650	63.6120	61.9430	60.3930	59.0690	57.4900
46	66.6590	64.9100	63.2450	61.6880	60.3770	58.8010
47	67.9530	66.2080	64.5470	62.9830	61.6850	60.1120
48	69.2470	67.5060	65.8490	64.2780	62.9930	61.4230
49	70.5410	68.8040	67.1510	65.5730	64.3010	62.7340
50	71.8350	70.1020	68.4530	66.8680	65.6090	64.0450

Table (B.29) Comparison between standard and ideal compressor discharge temperature (^{o}C) atT_c = 40 ^{o}C

T_e (^{o}C)	Standard	Ideal with superheating and sub-cooling
-10	54.5180	59.3890
-9	54.1982	59.0741
-8	53.8784	58.7592
-7	53.5586	58.4443
-6	53.2388	58.1294
-5	52.9190	57.8145
-4	52.5992	57.4996
-3	52.2794	57.1847
-2	51.9596	56.8698
-1	51.6398	56.5549
0	51.3200	56.2400
1	51.0002	55.9251
2	50.6804	55.6102
3	50.3606	55.2953
4	50.0408	54.9804
5	49.7210	54.6655
6	49.4012	54.3506
7	49.0814	54.0357
8	48.7616	53.7208
9	48.4418	53.4059
10	48.1220	53.0910
11	47.8022	52.7761
12	47.4824	52.4612
13	47.1626	52.1463
14	46.8428	51.8314
15	46.5230	51.5165

Table (B.30) Comparison between standard and ideal compressor discharge temperature (^{o}C) atT_e = 10 ^{o}C

T_c (^{o}C)	Standard	Ideal with superheating and sub-cooling
30	35.4400	39.4490
31	36.6790	40.7570
32	37.9180	42.0650
33	39.1570	43.3730
34	40.3960	44.6810
35	41.6350	45.9890
36	42.8740	47.2970
37	44.1130	48.6050
38	45.3520	49.9130
39	46.5910	51.2210
40	47.8300	52.5290
41	49.0690	53.8370
42	50.3080	55.1450
43	51.5470	56.4530
44	52.7860	57.7610
45	54.0250	59.0690
46	55.2640	60.3770
47	56.5030	61.6850
48	57.7420	62.9930
49	58.9810	64.3010
50	60.2200	65.6090

Table (B.31) Comparison between standard mass flow rate (kg/s) for R407c and R22 at T_c=40 ^oC

T_e (^oC)	R407c	R22
-10	0.0079	0.0066
-9	0.0079	0.0066
-8	0.0078	0.0066
-7	0.0078	0.0065
-6	0.0077	0.0065
-5	0.0077	0.0065
-4	0.0077	0.0065
-3	0.0076	0.0065
-2	0.0076	0.0065
-1	0.0076	0.0064
0	0.0075	0.0064
1	0.0075	0.0064
2	0.0075	0.0064
3	0.0074	0.0064
4	0.0074	0.0064
5	0.0074	0.0064
6	0.0074	0.0063
7	0.0073	0.0063
8	0.0073	0.0063
9	0.0073	0.0063
10	0.0072	0.0063
11	0.0072	0.0063
12	0.0072	0.0063
13	0.0072	0.0062
14	0.0072	0.0062
15	0.0071	0.0062

Table (B.32) Comparison between ideal mass flow rate (kg/s) for R407c and R22 at T_c=40 ^oC

T_e (^oC)	R407c	R22
-10	0.0069	0.0063
-9	0.0068	0.0062
-8	0.0068	0.0062
-7	0.0068	0.0062
-6	0.0067	0.0062
-5	0.0067	0.0061
-4	0.0067	0.0061
-3	0.0066	0.0061
-2	0.0066	0.0061
-1	0.0066	0.0060
0	0.0065	0.0060
1	0.0065	0.0060
2	0.0065	0.0060
3	0.0065	0.0059
4	0.0064	0.0059
5	0.0064	0.0059
6	0.0064	0.0059
7	0.0063	0.0059
8	0.0063	0.0058
9	0.0063	0.0058
10	0.0062	0.0058
11	0.0062	0.0058
12	0.0062	0.0057
13	0.0062	0.0057
14	0.0061	0.0057
15	0.0061	0.0057

Table (B.33) Comparison between standard mass flow rate (kg/s) for R407c and R22 at T_e=10 ^oC

T_c (^oC)	R407c	R22
30	0.0059	0.0058
31	0.0059	0.0059
32	0.0060	0.0059
33	0.0061	0.0059
34	0.0062	0.0060
35	0.0064	0.0060
36	0.0065	0.0061
37	0.0067	0.0061
38	0.0068	0.0062
39	0.0070	0.0062
40	0.0072	0.0063
41	0.0075	0.0063
42	0.0078	0.0064
43	0.0082	0.0064
44	0.0086	0.0065
45	0.0091	0.0066
46	0.0097	0.0066
47	0.0105	0.0067
48	0.0115	0.0067
49	0.0128	0.0068
50	0.0147	0.0069

Table (B.34) Comparison between ideal mass flow rate (kg/s) for R407c and R22 at T_e=10 ^oC

T_c (^oC)	R407c	R22
30	0.0054	0.0054
31	0.0055	0.0054
32	0.0056	0.0055
33	0.0056	0.0055
34	0.0057	0.0055
35	0.0058	0.0056
36	0.0058	0.0056
37	0.0059	0.0057
38	0.0060	0.0057
39	0.0061	0.0057
40	0.0062	0.0058
41	0.0064	0.0058
42	0.0065	0.0059
43	0.0067	0.0059
44	0.0069	0.0060
45	0.0071	0.0060
46	0.0073	0.0061
47	0.0076	0.0061
48	0.0080	0.0062
49	0.0084	0.0062
50	0.0088	0.0063

Table (B.35) Comparison between standard coefficient of performance for R407c and R22 at T_c=40 ^oC

T_e (^oC)	R407c	R22
-10	3.2401	4.1227
-9	3.3350	4.2324
-8	3.4346	4.3472
-7	3.5392	4.4675
-6	3.6492	4.5936
-5	3.7647	4.7259
-4	3.8862	4.8650
-3	4.0139	5.0112
-2	4.1483	5.1652
-1	4.2897	5.3276
0	4.4386	5.4990
1	4.5955	5.6803
2	4.7608	5.8722
3	4.9352	6.0756
4	5.1192	6.2917
5	5.3135	6.5217
6	5.5191	6.7668
7	5.7366	7.0286
8	5.9673	7.3088
9	6.2123	7.6094
10	6.4730	7.9327
11	6.7512	8.2812
12	7.0489	8.6579
13	7.3687	9.0666
14	7.7135	9.5111
15	8.0873	9.9966

Table (B.36) Comparison between ideal coefficient of performance for R407c and R22 at T_c=40 ^oC

T_e (^oC)	R407c	R22
-10	3.3087	4.3099
-9	3.4049	4.4232
-8	3.5059	4.5416
-7	3.6120	4.6654
-6	3.7237	4.7951
-5	3.8414	4.9311
-4	3.9656	5.0738
-3	4.0969	5.2237
-2	4.2359	5.3816
-1	4.3834	5.5479
0	4.5403	5.7233
1	4.7073	5.9088
2	4.8857	6.1052
3	5.0766	6.3134
4	5.2815	6.5346
5	5.5019	6.7701
6	5.7397	7.0212
7	5.9972	7.2897
8	6.2769	7.5774
9	6.5819	7.8865
10	6.9159	8.2195
11	7.2833	8.5792
12	7.6894	8.9690
13	8.1408	9.3930
14	8.6456	9.8558
15	9.2140	10.3632

Table (B.37) Comparison between standard coefficient of performance for R407c and R22 at T_e=10 ^oC

T_c (^oC)	R407c	R22
30	11.7048	12.5547
31	11.0374	11.9221
32	10.4166	11.3417
33	9.8360	10.8072
34	9.2897	10.3133
35	8.7729	9.8556
36	8.2813	9.4301
37	7.8110	9.0336
38	7.3587	8.6632
39	6.9214	8.3163
40	6.4963	7.9908
41	6.0810	7.6847
42	5.6731	7.3963
43	5.2705	7.1241
44	4.8711	6.8667
45	4.4732	6.6229
46	4.0750	6.3917
47	3.6746	6.1721
48	3.2705	5.9632
49	2.8611	5.7643
50	2.4448	5.5746

Table (B.38) Comparison between ideal coefficient of performance for R407c and R22 at T_e=10 ^oC

T_c (^oC)	R407c	R22
30	11.6034	13.0838
31	11.0137	12.4326
32	10.4659	11.8353
33	9.9547	11.2854
34	9.4754	10.7773
35	9.0240	10.3065
36	8.5968	9.8691
37	8.1909	9.4614
38	7.8032	9.0806
39	7.4314	8.7241
40	7.0732	8.3896
41	6.7263	8.0751
42	6.3890	7.7788
43	6.0594	7.4992
44	5.7359	7.2349
45	5.4170	6.9846
46	5.1010	6.7473
47	4.7867	6.5219
48	4.4727	6.3075
49	4.1576	6.1034
50	3.8402	5.9088

Table (B.39) Comparison between practical cycle mass flow rate results (gram/s) and experimental data at $T_c = 40\ ^oC$

T_e (^oC)	Practical (gram/s) per 1 kW refrigeration capacity	Refrigeration capacity (kW)	Practical compared results (gram/s)	Experimental (Herz 2003) (gram/s)
5	6.4	3.3471	21.421	19.815
7	6.3	3.5891	22.611	21.026
10	6.2	3.9141	24.267	22.383
13	6.2	4.2830	26.554	24.310
15	6.1	4.9643	30.280	28.333

Table (B.40) Comparison between practical cycle mass flow rate results (gram/s) and experimental data at T_e = 12 ^oC

T_c (^oC)	Practical (gram/s) per 1 kW refrigeration capacity	Refrigeration capacity (kW)	Practical compared results (gram/s)	Experimental (Herz 2003) (gram/s)
37	5.9	5.4726	32.288	31.792
38	6.0	5.4699	32.819	32.48
40	6.2	4.8802	30.257	29.541
42	6.5	4.3901	28.535	26.863

Table (B.41) Comparison between practical cycle compressor power (kW) and experimental data at $T_c = 40\ ^oC$

T_e (^oC)	Practical (kW) per 1 kW refrigeration capacity	Refrigeration capacity (kW)	Practical compared results (kW)	Experimental (Herz 2003) (kW)
5	0.2138	3.3471	0.7156	1.1025
7	0.1962	3.5891	0.7040	1.0912
10	0.1701	3.9141	0.6658	1.0874
13	0.1445	4.2830	0.6189	1.0574
15	0.1277	4.9643	0.6340	1.0462

Table (B.42) Comparison between practical cycle compressor power (kW) and experimental data at T_e = 12 ^oC

T_c (^oC)	Practical (kW) per 1 kW refrigeration capacity	Refrigeration capacity (kW)	Practical compared results (kW)	Experimental (Herz 2003) (kW)
37	0.1264	5.4726	0.6917	0.99
38	0.1332	5.4699	0.7285	1.088
40	0.1478	4.8802	0.7213	1.080
42	0.1646	4.3901	0.7226	1.093

Table (B.43) Comparison between practical cycle heat rejection rate (kW) and experimental data at $T_c = 40\ ^oC$

T_e (^oC)	Practical (kW) per 1 kW refrigeration capacity	Refrigeration capacity (kW)	Practical compared results (kW)	Experimental (Herz 2003) (kW)
5	1.2138	3.3471	4.0627	4.4496
7	1.1962	3.5891	4.2932	4.6817
10	1.1701	3.9141	4.5798	5.0015
13	1.1445	4.2830	4.9019	5.3405
15	1.1277	4.9643	5.5982	6.0105

Table (B.44) Comparison between practical cycle heat rejection rate (kW) and experimental data at T_e = 12 ^oC

T_c (^oC)	Practical (kW) per 1 kW refrigeration capacity	Refrigeration capacity (kW)	Practical compared results (kW)	Experimental (Herz 2003) (kW)
37	1.1264	5.4726	6.1643	6.4627
38	1.1332	5.4699	6.1985	6.5579
40	1.1478	4.8802	5.6015	5.9605
42	1.1646	4.3901	5.1127	5.4838

Table (B.45) Comparison between practical cycle coefficient of performance and experimental data at $T_c = 40\ ^oC$

T_e (^oC)	Practical	Experimental (Herz 2003)
5	4.6766	3.0359
7	5.0976	3.2890
10	5.8785	3.5991
13	6.9197	4.0501
15	7.8319	4.7448

Table (B.46) Comparison between practical cycle coefficient of performance and experimental data at $T_e = 12\ ^oC$

T_c (^oC)	Practical	Experimental (Herz 2003)
37	7.9084	5.5279
38	7.5081	5.0277
40	6.7637	4.5171
42	6.0771	4.0143

دراسة أداء وحدة شباك لتكييف الهواء باستخدام غاز R-407c بدلا من غاز R-22 باستخدام الحاسوب.

إعداد

عبد الرزاق سليمان الشقيرات

أشراف

الأستاذ الدكتور محمد احمد السعد

ملخـــــــص

يهدف هذا البحث إلى تطوير برنامج محاكاة لدراسة أداء وحدة شباك لتكييف الهواء باستخدام غاز التبريد R-407c بدلا من غاز R-22 . حيث يقوم هذا البرنامج باحتساب معدل الجريان ، قدرة الضاغطة ، معدل انتقال الحرارة من المكثف، معامل الأداء ودرجة حرارة التدفق من الضاغطة وذلك لكل واحد كيلواط قدرة تبريد لـــدورات التبريـــد المعيارية، والمثالية مع وجود التسخين الفائق والتبريد الدوني.

تدل نتائج هذا البحث على إمكانية استخدام غاز R-407c كغاز بديل عن غاز R-22 في هـــذا النـــوع مـــن وحدات التكييف.

أشارت نتائج هذا البحث إلى أن معدل الجريان لغاز R-407c عند استخدامه كغاز تبريد بديلاً لغاز R-22 يرتفع بنسبة 14.3 % في الدورة المعيارية. ولكنه في الدورة المثالية يرتفع بنسبة 6.9 % عند درجة حرارة مبرد 10 ^{o}C ودرجة حرارة مكثف 40 ^{o}C .

من جهة أخرى فان معامل الأداء ينخفض من 7.9 الى 6.4 عند استخدام غاز R-407c بدلاً من غاز R-22 في الدورة المعيارية ، وكذلك فأنه ينخفض من 8.2 الى 6.9 في حالة الدورة المثالية مع وجود التسخين الفائق والتبريد الدوني عند نفس الظروف .